

Aus dem  
Comprehensive Pneumology Center (CPC)  
Helmholtz Center Munich



**Regulation of pro-lymphangiogenic factors in post-lung transplant settings**

Dissertation  
zum Erwerb des Doctor of Philosophy (Ph.D.) an der Medizinischen Fakultät der  
Ludwig-Maximilians-Universität München

vorgelegt von  
Sarah Schulte-Döinghaus

aus  
München

Jahr  
2024

---

Mit Genehmigung der Medizinischen Fakultät der  
Ludwig-Maximilians-Universität München

Erstes Gutachten: Prof. Dr. Sebastian Michel  
Zweites Gutachten: Prof. Dr. Ali Önder Yildirim  
Drittes Gutachten: Prof. Dr. Anne Hilgendorff  
Viertes Gutachten: Prof. Dr. Matthias Griese

Dekan: Prof. Dr. med. Thomas Gudermann

Tag der mündlichen Prüfung: 11.06.2024

---

## License

This work is licensed under [CC BY-SA 4.0](https://creativecommons.org/licenses/by-sa/4.0/) (<https://creativecommons.org/licenses/by-sa/4.0/>).

# Table of Content

<b>Table of Content</b> .....	<b>1</b>
<b>Abstract</b> .....	<b>3</b>
<b>List of Figures</b> .....	<b>5</b>
<b>List of Tables</b> .....	<b>6</b>
<b>List of Abbreviations</b> .....	<b>7</b>
<b>1. Introduction</b> .....	<b>12</b>
1.1 Lung Transplantation as Final Option for Terminal Lung Diseases.....	12
1.2 Post-Transplantation Complications .....	12
1.2.1 Ischemia Reperfusion Injury .....	13
1.2.2 Primary Graft Dysfunction.....	14
1.2.3 Acute Rejection .....	14
1.2.4 Chronic Rejection.....	15
1.3 Pulmonary Macrophages post Lung Transplantation .....	16
1.4 The Lymphatic System in Lung Transplantation.....	17
1.4.1 VEGFR-3 - VEGF-C - Signaling.....	18
1.4.2 Ccbe1.....	19
1.4.3 Adams3 .....	19
1.5 Aim of the Study.....	20
<b>2. Material and Methods</b> .....	<b>21</b>
2.1 Materials.....	21
2.1.1 Mice and Maintenance.....	21
2.1.2 Informed Consent Healthy PBMC Donors .....	21
2.1.3 Commercially Available Kits.....	21
2.1.4 Devices .....	21
2.1.5 Software .....	23
2.1.6 Reagents and Solutions.....	23
2.1.7 Buffers and Stock Solutions.....	25
2.1.8 Cell Culture Media .....	25
2.1.9 Other Consumables .....	26
2.1.10 Antibodies .....	27
2.1.11 Murine Primer.....	27
2.1.12 Enzymes .....	28
2.1.13 Stimulants and Inhibitors.....	28
2.1.14 Cell Lines .....	29
2.1.15 Tools for Data mining.....	29
2.2 Methods .....	29
2.2.1 Isolation of Murine Bone Marrow .....	29
2.2.2 Differentiation of Bone Marrow-Derived Macrophages.....	29
2.2.3 Isolation of Murine Monocytes .....	30
2.2.4 Isolation of Human Blood-Derived Monocytes.....	30
2.2.5 Cell Lines .....	31

2.2.6	Cell Culture .....	31
2.2.7	Inhibition of NF- $\kappa$ B .....	31
2.2.8	Inhibition of pSTAT1 .....	31
2.2.9	RNA Extraction .....	31
2.2.10	Determination of RNA Concentration .....	32
2.2.11	cDNA Synthesis .....	32
2.2.12	Quantitative Polymerase Chain Reaction (qPCR) .....	32
2.2.13	Flow Cytometry .....	32
2.2.14	Gating Strategy for FC Analysis.....	33
2.2.15	Immunofluorescence Staining.....	33
2.2.16	Protein Extraction.....	33
2.2.17	Bicinchoninic Acid Assay .....	33
2.2.18	SDS Polyacrylamide Gel Electrophoresis.....	34
2.2.19	Immunoblotting .....	34
2.2.20	Conditioned Medium Experiments .....	35
2.2.21	Analysis of Publicly Available ChIPSeq Data .....	35
2.2.22	Statistical Analysis .....	35
<b>3.</b>	<b>Results .....</b>	<b>36</b>
3.1	<i>Vegf-c</i> , <i>Ccbe1</i> and <i>Adamts3</i> Expression in Proinflammatory Macrophages and Monocytes.....	36
3.2	Positive Regulation of Pro-Lymphangiogenic Factors.....	43
3.3	Negative Regulation of Pro-Lymphangiogenic Factors .....	48
3.4	Treatment of SVEC4.10 Cells with Macrophage Conditioned Medium.....	51
<b>4.</b>	<b>Discussion .....</b>	<b>57</b>
4.1	<i>Vegf-c</i> , <i>Ccbe1</i> and <i>Adamts3</i> Expression is Upregulated In Pro-Inflammatory Macrophages and Monocytes.....	57
4.2	LPS Upregulates <i>Vegf-c</i> , <i>Ccbe1</i> and <i>Adamts3</i> via the NF- $\kappa$ B Subunit p65 .....	58
4.3	IFN $\gamma$ Induced Inhibition of <i>Vegf-C</i> and <i>Ccbe1</i> Expression Signals via a STAT1 Dependent Pathway.....	59
4.4	Macrophage Derived VEGF-C Activates VEGFR-3 Signaling in Lymphatic Endothelial Cells .....	60
<b>5.</b>	<b>Conclusions, Limitations, and Future Directions.....</b>	<b>63</b>
	<b>References .....</b>	<b>65</b>
	<b>Apendix A:: .....</b>	<b>77</b>
	<b>Acknowledgements.....</b>	<b>78</b>
	<b>Affidavit .....</b>	<b>79</b>
	<b>Confirmation of Congruency .....</b>	<b>80</b>
	<b>List of Publications .....</b>	<b>81</b>

## Abstract

Five and a half years after Lung Transplantation (LTx), Bronchiolitis Obliterans Syndrome (BOS) becomes the main leading cause of death. Main risk factors for BOS development include episodes of acute rejection, as well as Ischemia Reperfusion Injury (IRI). IRI is a complex inflammatory response, which involves activation of innate immunity transmitted by Toll-Like Receptor 4 (TLR4) signaling. An exogenous TLR4 ligand includes Lipopolysaccharide (LPS) from *Pseudomonas aeruginosa* infection, which is strongly associated with BOS development. Hallmarks of BOS entail inflammatory fibrosis and immune cell infiltration including T-cells and monocytes. Apoptotic donor-derived lung macrophages are then replaced by recruited monocytes as part of the innate immunity. However, classical recruited monocytes, as well as alveolar macrophages can contribute to alloimmunity. Further, macrophages were shown to be a potential source of Vascular endothelial growth factor c (Vegf-c) upon TLR4 engagement in experimental models of other inflammatory diseases. Vegf-c, a well-known growth factor, induces lymphangiogenesis. Increased lymphatic activation, caused by IRI or VEGF-C, was found to be detrimental to survival in rat heart allografts and molecular VEGF-C trapping significantly improved cardiac allograft survival. However, in a study of acute lung rejection led to a loss of lymphatic vessels and injection of recombinant human (rh)VEGF-C156s 20 days after developing acute rejection, improved drainage of harmful molecules in the lung and reduced inflammatory cell infiltration, including macrophages. Less profibrotic macrophages, as well as a faster recovery was observed in a bleomycin model of lung fibrosis, a long-term result in end stage BOS, by an expanded lymphatic network, induced by transgenic *Vegf-c* overexpression. Altogether, it remains unclear, whether *Vegf-c* is beneficial or detrimental after lung transplantation and how its expression may be regulated. Therefore, this thesis elaborates potential regulatory mechanisms of pro-lymphangiogenic gene expression. Cell line and primary macrophages of murine and human origin were stimulated with LPS, LPS + Interferon gamma (IFN $\gamma$ ), IFN $\gamma$  or Interleukin 4 (IL-4). After analysis of potentially regulating transcription factors by online Chromatin Immunoprecipitation sequencing (ChIPseq) data for *Vegf-c* expression in macrophages, combined treatment of LPS-stimulated cells with a p65 translocation inhibitor or combined treatment of LPS + IFN $\gamma$  with a Signal Transducer and Activator of Transcription 1 (STAT1) phosphorylation inhibitor was applied for several time periods. Expression levels of the pro-lymphangiogenic genes *Vegf-c*, Collagen and Calcium Binding EGF Domain 1 (*Ccbe1*), and A Disintegrin and Metalloprotease with Thrombospondin Motifs-3 (*Adamts3*) were determined by quantitative Polymerase Chain Reaction (qPCR). In addition, *Vegf-c* protein was measured by immunoblotting and Flow Cytometry (FC) in a murine macrophage cell line as well as in human blood-derived monocytes. Finally, conditioned medium of these stimulated macrophages was applied on top of a murine lymph node-derived cell line, followed by readout of p-p44/p42 levels by immunoblotting. This study found that TLR4 engagement leads to the upregulation of *Vegf-c*, *Ccbe1*, and *Adamts3* mRNA in macrophages. In addition, LPS treatment upregulates *Vegf-c* protein. While p65-dependent TLR4-signaling positively regulates all three lymphangiogenic factors, the STAT1-dependent IFN $\gamma$ -signaling pathway negatively affects their expression. Blockage of STAT1 phosphorylation rescues *Vegf-c* and *Ccbe1* mRNA in primary mouse macrophages and *Vegf-c* protein in a mouse macrophage cell line and human monocytes. The study also found that released and functionally cleaved VEGF-C of cell line and primary murine macrophages elevates p44/p42 phosphorylation downstream of the Vascular Endothelial Growth Factor Receptor 3 (VEGFR-3) receptor of a tested endothelial cell line of lymphatic identity. In summary, genetic regulation of pro-lymphangiogenic factors under conditions post-LTx was investigated. I ascertained that 1) *Vegf-c*, *Ccbe1*, and *Adamts3* are expressed in proin-

---

flammatory macrophages and monocytes, 2) their genetic upregulation is regulated through the TLR4 pathway, and p65 3) IFN $\gamma$  inhibiting the LPS-induced upregulation of Vegf-c, Ccbe1, and Adamts3 via STAT1, and 4) VEGF-C derived from LPS stimulated macrophages upregulated p-p44/p42 signaling in lymphatic endothelial cells.

## List of Figures

<b>Figure 1.4.1 Mechanism of Proteolytic VEGF-C Activation by CCBE1 and ADAMTS3 (Jeltsch et al., 2014)</b> .....	19
<b>Figure 3.1.1 <i>Vegf-c</i> Expression in RAW264.7 Cells</b> .....	36
<b>Figure 3.1.2 VEGF-C Determined by Immunoblotting</b> .....	36
<b>Figure 3.1.3 VEGF-C Determined by Flow Cytometry</b> .....	37
<b>Figure 3.1.4 <i>Ccbe1</i> Expression in RAW264.7 Cells</b> .....	37
<b>Figure 3.1.5 <i>Adamts3</i> Expression in RAW264.7 Cells</b> .....	38
<b>Figure 3.1.6 <i>Vegf-c</i> Expression in BMDMs</b> .....	39
<b>Figure 3.1.7 <i>Ccbe1</i> Expression in BMDMs</b> .....	40
<b>Figure 3.1.8 <i>Adamts3</i> Expression in BMDMs</b> .....	41
<b>Figure 3.1.9 <i>Vegf-c</i> mRNA and Protein Levels in Murine Monocytes</b> .....	42
<b>Figure 3.1.10 <i>Vegf-c</i> Protein in Human Monocytes Determined by Flow Cytometry</b> .....	42
<b>Figure 3.2.1 Regulatory Potential of p65 to Regulate MΦ <i>Vegf-c</i></b> .....	43
<b>Figure 3.2.2 ChIP-seq Peaks Aligned to <i>Vegf-c</i> Sequence</b> .....	44
<b>Figure 3.2.3 <i>Vegf-c</i> Expression in RAW264.7 Cells</b> .....	45
<b>Figure 3.2.4 <i>Ccbe1</i> Expression in RAW264.7 Cells</b> .....	45
<b>Figure 3.2.5 Expression of <i>Vegf-c</i>, <i>Ccbe1</i> and <i>Adamts3</i> in BMDMs</b> .....	46
<b>Figure 3.2.6 <i>Vegf-c</i> Expression in Murine Monocytes</b> .....	46
<b>Figure 3.2.7 <i>Ccbe1</i> Expression in Murine Monocytes</b> .....	47
<b>Figure 3.2.8 <i>Adamts3</i> Expression in Murine Monocytes</b> .....	47
<b>Figure 3.2.9 <i>Vegf-c</i> Protein Levels in Human Blood Derived Monocytes</b> .....	48
<b>Figure 3.3.1 Regulatory Potential of Stat1 to Regulate MΦ <i>Vegf-c</i></b> .....	48
<b>Figure 3.3.2 <i>Vegf-c</i> Protein Levels in RAW264.7 Cells Determined by Flow Cytometry</b> .....	49
<b>Figure 3.3.3 Pro-Lymphangiogenic Expression in BMDMs</b> .....	50
<b>Figure 3.3.4 VEGF-C Levels in Human Blood-Derived Monocytes Determined by Flow Cytometry</b> .....	50
<b>Figure 3.4.1 PODOPLANIN and VEGFR-3 Expression In SVEC4.10 Cells</b> .....	51
<b>Figure 3.4.2 p-p44/p42 Levels in rhVEGF-C156s Stimulated SVEC4.10 Cells</b> .....	52
<b>Figure 3.4.3 Experimental Setup with LPS-Stimulated Macrophage Conditioned Medium</b> .....	53
<b>Figure 3.4.4 p-p44/p42 Levels in SVEC4.10 Cells Treated by Macrophage Conditioned Medium</b> .....	54
<b>Figure 3.4.5 Experimental Setup with LPS + IFNγ-Stimulated Macrophage Conditioned Medium</b> .....	55
<b>Figure 3.4.6 SVEC4.10 Cells Treated with LPS/LPS +IFNγ-Macrophage Conditioned Medium</b> .....	55
<b>Figure 3.4.7 <i>Vegf-c</i> Expression of BMDMs and Respective p-p44 Levels Induced in SVEC4.10 Cells</b> .....	56

## List of Tables

Table 1.2.4.1 BOS Classification.....	15
Table 2.1.3.1 Commercially Available Kits.....	21
Table 2.1.4.1 Devices.....	21
Table 2.1.5.1 Software .....	23
Table 2.1.6.1 Reagents and Solutions .....	23
Table 2.1.7.1 Buffers and Stock Solutions .....	25
Table 2.1.8.1 Cell Culture Media.....	25
Table 2.1.9.1 Other Consumables .....	26
Table 2.1.10.1 Antibodies .....	27
Table 2.1.11.1 Murine Primer.....	27
Table 2.1.12.1 Enzymes .....	28
Table 2.1.13.1 Stimulants and Inhibitors.....	28
Table 2.1.14.1 Cell Lines .....	29
Table 2.1.15.1 Tools for Data Mining .....	29

## List of Abbreviations

Abbreviation	Full Term
<b>A</b>	
A1ATD	Alpha-1-Antitrypsin Deficiency
Adams3	A Disintegrin and Metalloproteinase with Thrombospondin Motifs 3
AF	Alexa Fluor
AM	Alveolar Macrophages
ANOVA	Analysis Of Variance
APC	Antigen-Presenting Cells
AR	Acute Rejection
<b>B</b>	
β-ME	Beta-Mercaptoethanol
B/S/P	Buffer with BSA, Saponin, PBS
BAL	Bronchoalveolar Lavage
BCA Assay	Bicinchoninic Acid Assay
BECs	Blood Endothelial Cells
BM	Bone Marrow
BMDM	Bone Marrow-Derived Macrophages
BO	Bronchiolitis Obliterans
BOS	Bronchiolitis Obliterans Syndrome
BSA	Bovine Serum Albumin
<b>C</b>	
Ccbe1	Collagen and Calcium Binding EGF Domain 1
CCL2	CC-Motif-Chemokine Ligand 2
cCREs	Candidate Cis-Regulatory Elements
CD	Cluster of Differentiation
ChIPseq	Chromatin Immunoprecipitation Sequencing
CLAD	Chronic Lung Allograft Dysfunction
CM	Macrophage-Conditioned Medium
CMV	Cytomegalovirus
Col2a1	Procollagen II
COPD	Chronic Obstructive Pulmonary Disease
CT	Computer Tomography
ctrl	Control
- ctrl	Negative Control
+ ctrl	Positive Control
<b>D</b>	
DAMP	Damage Associated Molecular Pattern
DC	Dendritic Cells
°C	Degree Celsius
DMEM	Dulbecco's Modified Eagle's Medium
DNA	Desoxyribonucleic Acid
dNK-CM	Conditioned Medium of Decidual Natural Killer Cells
<b>E</b>	
EDTA	Ethylenediaminetetraacetic Acid
ELISA	Enzyme-Linked Immunosorbent Assay
ENCODE	Encyclopedia of DNA Elements

enhD	Distal Enhancer-Like Signatures
enhP	Proximal Enhancer-Like Signatures
ERK 1/2	Extracellular Signal-Regulated Kinase 1 and 2

## F

FC	Flow Cytometry
FcR	Fc-Receptor
FCS	Fetal Calf Serum
FE	Forced Expiration
FEF	Forced Expiratory Flow
FEV1	Forced Expiratory Volume per One Second
Flu	Fludarabine
FVC	Forced Vital Capacity

## G

GAS	Gamma Interferon Activated Site
GERD	Gastroesophageal Reflux Disease
GFP	Green Fluorescent Protein
GM-CSF	Granulocyte/Macrophage-Colony-Stimulating Factor
GODT	Global Observatory on Donation and Transplantation
GVHD	Graft Versus Host Disease

## H

h	Hours
H3K27ac	Histone-3-Lysine-27 Acetylation
H3K4me3	Histone 3 Lysine 4 Trimethyl
HDLECs	Human Dermal Lymphatic Endothelial Cells
HLA	Human-Leucocyte-Antigen
HMGB1	High-Mobility-Group-Box-Protein B1
Hprt1	Hypoxanthine Phosphoribosyl Transferase 1
HRCT	High-Resolution Computer Tomography
HRP	Horse Radish Peroxidase
HSC	Hematopoietic Stem Cells
HSCT	Hematopoietic Stem Cell Transplantation

## I

IFN $\gamma$	Interferon Gamma
IFN $\gamma$ R	IFN $\gamma$ -Receptor
IKK $\alpha$	Inhibitor of Nuclear Factor Kappa-B Kinase Subunit Alpha
IKK $\beta$	Inhibitor of Nuclear Factor Kappa-B Kinase Subunit Beta
IL-4	Interleukin 4
ILD-not IIP	Interstitial Lung Disease – not Idiopathic Interstitial Pneumonia
IM	Interstitial Macrophages
iNKT	Invariant Natural Killer T Cells
Inos1	Inducible Nitric Oxide Synthase 1
IRF1	Interferon Response Factor 1
IRI	Ischemia Reperfusion Injury
ISG	Interferon Stimulated Genes
I $\kappa$ B	Inhibitor of NF- $\kappa$ B

## J

JAK1/2	Janus Kinase 1/2
--------	------------------

**K**

kb	Kilobase
kDA	Kilodalton
KEGG	Kyoto Encyclopedia of Genes and Genomes

**L**

LECs	Lymphatic Endothelial Cells
LHI	Institute of Lung Health and Immunity
LMW-HA	Low-Molecular-Weight Hyaluronic Acid
LPS	Lipopolysaccharide
LTx	Lung Transplantation
LV	Lymphatic Vessel
LVD	Lymphatic Vessel Density

**M**

M	Mol/Liter
MACS	Magnetic Activated Cell Sorting
M-CSF	Macrophage-Colony-Stimulating Factor
MHC	Major Histocompatibility Complex
µg	Microgram
µl	Microliter
µm	Micrometer
µM	Micromolar
min	Minutes
ml	Milliliter
mm	Millimeter
mM	Millimolar
Mrc1	Mannose Receptor C-Type 1
mRNA	Messenger Ribonucleic Acid
mTOR	Mammalian Target of Rapamycin
MΦ	Macrophages

**N**

NADPH	Nicotinamide Adenine Dinucleotide Phosphate
NF-κB	Nuclear Factor Kappa-Light-Chain-Enhancer of Activated B Cells
ng	Nanogram
nM	Nanomolar
nm	Nanometer
NOX2	NADPH Oxidase 2
ns.	Not Significant

**P**

p	Probability Value
p42	Erk 2
p44	Erk 1
PAMP	Pathogen Associated Molecular Pattern
PBMC	Peripheral Blood Mononuclear Cells
PBST	Phosphate Buffered Saline Tween 20
PDPN	Podoplanin
PEM	Peritoneal Exudate Macrophages
pERK 1/2	Phosphorylated Extracellular Signal-Regulated Kinase 1 And 2
PFA	Paraformaldehyde
PGD	Primary Graft Dysfunction

PMN	Polymorphonuclear Neutrophils
p-p44/p42	pErk 1/2
prom	Promoter-Like Signatures
pSTAT1	Phosphorylated STAT1
PVDF	Polyvinylidene Fluoride

## Q

qPCR	Quantitative Polymerase Chain Reaction
------	--

## R

RAF	Rapidly Accelerated Fibrosarcoma
RAS	Restrictive Allograft Syndrome
RAW264.7	Murine Macrophage Cell Line, created by Ralph, rAschke et Watson
ROS	Reactive Oxygen Species
RP	Regulatory Potential
RPMI medium	Roswell Park Memorial Institute Medium
RT	Room Temperature (20-25°)

## S

s	Seconds
SD	Standard Deviation
SDS	Sodium Dodecyl Sulfate
SDS-PAGE	SDS Polyacrylamide Gel Electrophoresis
SH2	Src Homology 2
SOT	Solid Organ Transplants
Stat1	Signal Transducer and Activator of Transcription 1
SVEC4.10	Simian Virus 40-Transformed Mouse Microvascular Endothelial Cell Line

## T

TBB	Transbronchial Biopsy
TCP45	T Cell Protein Tyrosine Phosphatase 45
TF	Transcription Factors
TH1	T-Helper Cell 1
TH2	T-Helper Cell 2
TLC	Total Lung Capacity
TLR4	Toll-Like Receptor 4
TNF $\alpha$	Tumor Necrosis Factor Alpha
TSS	Transcription Start Site

## V

V	Volt
VCL	Vinculin
Vegf-c	Vascular Endothelial Growth Factor C
Vegfr-3	Vascular Endothelial Growth Factor Receptor 3

## W

WB	Western Blot /Immunoblot
WHO-ONT	World Health Organization and the Spanish Transplant Organization, Organización Nacional De Trasplantes
WT	Wildtype

**Y**

Y440 Tyrosine Residue 440  
Y701 Tyrosine 701

# 1. Introduction

## 1.1 Lung Transplantation as Final Option for Terminal Lung Diseases

Lung transplantation (LTx) is the last option for end-stage respiratory failure. End-stage respiratory failure mainly occurs in terminal lung diseases like Chronic Obstructive Pulmonary Disease (COPD), Idiopathic Interstitial Pneumonia (IIP), Cystic Fibrosis (CF), Interstitial Lung Disease-not Idiopathic Interstitial Pneumonia (ILD-not IIP), Alpha-1-Antitrypsin Deficiency (A1ATD) and re-transplantation after allograft rejection (Chambers et al., 2019). In 2022, 6,784 lung transplants were registered worldwide, with 2,073 performed in the European Union and 254 in Germany (*Global Observatory on Donation and Transplantation*). Those 2022 data are based on the Global Observatory on Donation and Transplantation (GODT) data, produced by the WHO-ONT (World Health Organization and the Spanish Transplant Organization, Organización Nacional de Trasplantes (ONT)) collaboration. However, despite increasing numbers of transplantation (*Global Observatory on Donation and Transplantation*) and improving surgery technique and treatment, the median survival time of LTx patients with 6.8 years in 2017 remains significantly lower compared to other Solid Organ Transplants (SOT) due to the development of chronic allograft rejection (Barker et al., 2014; Chambers et al., 2019). Lung allografts are more susceptible to rejection as they face several specific challenges like a large overall surface area, including blood endothelium, mechanical ventilation with air contaminated by nosocomial pathogens, continued exposure to a plethora of particles in the environment, and the constant patrolling of the organ by immune cells and the existence of intra-organ lymphoid tissue. Thus, lung transplants are more prone to Ischemia-Reperfusion Injury (IRI), infection, as well as rapid innate and adaptive immune processes, which can trigger allograft rejection (Gelman et al., 2009; Kreisel et al., 2011; Krupnick et al., 2014; Witt et al., 2014). Chronic Lung Allograft Rejection (CLAD), displayed as Bronchiolitis Obliterans Syndrome (BOS), becomes the primary cause of death one-year post-LTx surgery (Chambers et al., 2019).

## 1.2 Post-Transplantation Complications

Besides surgery-related complications like vessel/bronchial anastomosis issues, edema, and IRI (Hanley & Welsh, 2003), infections and allograft immunity pose a significant risk to the transplant. Infections, promoted by impaired mucociliary clearance and cough reflex, intubation, and immunosuppression (Hanley & Welsh, 2003), frequently are caused by gram-negative bacteria like *Pseudomonas aeruginosa* (containing Lipopolysaccharide (LPS)), Cytomegalovirus (CMV) or fungi (*Aspergillus* spp., *Candida* spp.) (Hanley & Welsh, 2003) and treated by antibiotic, antiviral or antifungal medication respectively (Kennedy & Razonable, 2017).

Important alloimmune mechanisms for developing lung allograft rejection entail interactions of Antigen-Presenting Cells (APC) with T cells, whereby one originates from the donor and one from the recipient. In direct allorecognition allogeneic Major Histocompatibility Complexes (MHC) are directly presented by donor APCs to recipient T cells. In indirect allorecognition recipient APCs digest and present alloantigens as MHC-peptides to recipient T cells. In the semi-direct allorecognition, donor alloantigens are presented by recipient APC to recipient T cells (Martinu et al., 2009; Wood & Goto, 2012; Yoshiyasu & Sato, 2020). Therefore, past research and post-LTx treatment mainly focused on targeting the proliferation and activation of lymphocytes, especially T cells. Common treatment strategies are categorized into induction therapy

and maintenance therapy. Induction therapy is usually based on the depletion of T lymphocytes by antibodies (polyclonal anti-thymocyte globulins, monoclonal anti- Cluster of Differentiation 3 (CD3) or monoclonal anti-CD25) or IL-2-agonists (Basiliximab) to prevent proliferation and activation of T cells. Maintenance therapy often comprises a glucocorticoid (Prednisone), a calcineurin inhibitor (Tacrolimus), inhibiting T cell activation, and an antimetabolite, inhibiting de-novo purine synthesis of active lymphocytes (Mycophenolate-Mofetil) or mammalian Target of Rapamycin (mTOR) inhibitors, impairing antigen presentation by reduction of macrophage CD80 expression (Sirolimus) (Chambers et al., 2017; Chung & Dilling, 2020; Knoop et al., 2004; Salehi & Reed, 2015; Sweet, 2013). However, subsequent immune responses to infections and lung allograft rejection persist despite current treatment regimens. Therefore, further research on the immunopathological mechanism of lung allograft rejection is needed.

### 1.2.1 Ischemia Reperfusion Injury

The onset of Ischemia-Reperfusion Injury (IRI) is initiated by a sudden cessation of blood flow in the organ donor and involves a complex process. The organ then undergoes cold storage, followed by implantation and sudden reperfusion with the blood of the organ receiver. This process triggers a large cascade of immunological processes (de Perrot et al., 2003; den Hengst et al., 2010; Talaie et al., 2021; Weyker et al., 2013). In a nutshell, the changing levels of mechanical shear stress and sudden supply of oxygen without present antioxidants on Blood Endothelial Cells (BECs) results in the activation of Nicotinamide Adenine Dinucleotide Phosphate (NADPH) Oxidase 2 (NOX2) and generation of Reactive Oxygen Species (ROS) by BECs and Polymorphonuclear Neutrophils (PMNs) within 6 to 24 hours (Chatterjee et al., 2014). Furthermore, when NOX2 is activated in CD4<sup>+</sup> invariant Natural Killer T cells (iNKT), it leads to the expression of Interleukin-17 A (IL-17A). In addition, studies of IRI in dogs demonstrated a significant increase of IFN $\gamma$  in Bronchoalveolar Lavage (BAL) one and four hours after transplantation (Serrick et al., 1994) and a marked elevation of BAL fluid IFN $\gamma$  up to 14 days after LTx in grafted lungs compared to native lungs (Chang et al., 1991). IL-17A in turn, triggers the release of inflammatory cytokines and chemokines such as Tumor Necrosis Factor Alpha (TNF $\alpha$ ), CC-motif-Chemokine Ligand 2 (CCL2), CC-Chemokine Ligand 5 (CCL5), and Interleukin 6 (IL-6), leading to the infiltration and activation of neutrophils and monocytes, followed by pulmonary injury (Ferrari & Andrade, 2015; Laubach & Sharma, 2016; Sharma et al., 2016; Sharma et al., 2011). Monocytes are important mediators for neutrophil influx post IRI (Gelman et al., 2010; Maus et al., 2003) and depletion of monocytes dampens lung injury and inflammation. However, adoptive transfer of monocytes results in partial restoration of acute lung injury (Tatham et al., 2018). When ROS is released, it causes cell damage and apoptosis of alveolar epithelial cells, BECs, and alveolar macrophages. This damage results in the release of cell contents containing Damage-Associated Pattern (DAMP) molecules, which further lead to blood vessel damage and the disruption of the endothelial barrier, important hallmark characteristics of IRI (Laubach & Sharma, 2016; Yang & Tracey, 2010). Blood vessel damage causes edema, which is a buildup of fluid in the lungs, while Lymphatic Vessel (LV) damage results in insufficient drainage and immune reactions caused by DAMPs (Chatterjee et al., 2014). IRI also implies an inflammatory response, which involves the activation of innate immunity transmitted by Toll-Like Receptor 4 (TLR4) signaling (Kreisel & Goldstein, 2013; Merry et al., 2015; Shimamoto et al., 2006; Takahashi et al., 2016; Wu et al., 2007; Zanotti et al., 2009; Zhao et al., 2006). Endogenous TLR4 ligands include DAMP molecules like High-Mobility-Group-Box-Protein B1 (HMGB1) (Arslan et al., 2010; Yang & Tracey, 2010) (reviewed in (Chen et al., 2010; Hasenauer et al.,

2021)) and Low-Molecular-Weight Hyaluronic Acid (LMW-HA), which both are increasingly released by damaged, necrotic or apoptotic cells post-transplantation, can both bind to TLR4 (Andrade et al., 2006; Sharma et al., 2013; Todd et al., 2014; Yang et al., 2010), and are enhanced during IRI (Leventhal & Schroppe, 2012). Inflammatory mechanisms caused by DAMPS activating the innate immune system are also called sterile inflammation (Abraham et al., 2000; Chen & Nunez, 2010; Hasenauer et al., 2021). Merry and colleagues have demonstrated, that TLR4 in alveolar macrophages is a key receptor for sterile inflammation of the lung allograft (Merry et al., 2015; Zanotti et al., 2009). Furthermore, a study done by Wu et al. showed decreased IRI by HMGB1 blockage and increased injury by recombinant HMGB1. However, neither of these treatments had an impact in TLR4<sup>-/-</sup> mice, indicating the importance of TLR4 (Wu et al., 2010). An exogenous TLR4 ligand includes LPS from *Pseudomonas aeruginosa* infection, which is a Pathogen-Associated Molecular Pattern (PAMP) molecule frequently found in lung transplantation patients and strongly associated with BOS development (Botha et al., 2008).

### 1.2.2 Primary Graft Dysfunction

Primary Graft Dysfunction (PGD) is an early and rapid process after surgery and cannot be detected through lung function tests that are typically used to diagnose acute or chronic allograft rejection. PGD is caused mainly by IRI and has an incidence rate of approximately 30% within the first 72 hours of transplantation. PGD is a result of the innate immune system and allograft rejection was commonly believed to be solely associated with the adaptive immune system. However, PGD and chronic allograft rejection are strongly associated with each other (Bharat et al., 2008). PGD is associated with high early mortality rates, and if a patient survives, they face a significant risk of acute allograft rejection and chronic allograft rejection (Fiser et al., 2002; Kreisel et al., 2011; Porteous et al., 2015; Verleden et al., 2014).

### 1.2.3 Acute Rejection

Acute Rejection (AR) is a type of cellular immune response diagnosed between three months and one-year post-surgery by immune cell infiltrates visible on Transbronchial Biopsies (TBB) and increased amounts of eosinophils and lymphocytes present in BAL. AR is displayed by unspecific symptoms of tiredness, cough, dyspnea, fever, or hypoxemia. Further indicators of the disease are a 5-10% reduction of the Forced Expiratory Volume per One Second (FEV1) and visible cellular infiltrates on X-rays or Computer Tomography (CT) scans (Hanley & Welsh, 2003). The diagnosis of AR is classified into two subgroups, A and B, each containing grades of severity from 0 (no rejection) to 4 (severe rejection). Perivascular and interstitial mononuclear cell infiltrates define class A, while class B is defined by airway inflammation and is seen as a possible precursor of Bronchiolitis Obliterans (BO). For example, AR class A, grade 4 includes evident diffuse perivascular interstitial and alveolar infiltrations of mononuclear cells. Further, the destruction of alveolar pneumocytes in association with intra-alveolar necrotic cells, macrophages, hyaline membranes, hemorrhage, and neutrophil granulocytes besides parenchymal necrosis and necrotic vasculitis occur. In comparison, AR, class B, grade 4 is displayed by a dense band of activated mononuclear cells in the bronchi and bronchioles, detachment of the epithelium from the basal membrane epithelial ulceration, fibrous-purulent exudates consisting of neutrophils, and epithelial necrosis (Yousem et al., 1996). Besides that, early after LTx, immune cells including T cells massively infiltrate the lung allograft (Byrne et al., 2021). Recent

research has further focused on specific subsets of T cells in chronic lung allograft rejection (Bergantini et al., 2021; Tissot et al., 2019). Detection of BAL cell IFN $\gamma$  expression correlated significantly with acute rejection in human patients (Moudgil et al., 1999). Further, IFN $\gamma$  mRNA expression was associated with increased acute lung allograft dysfunction and to a greater decrement of FEV1. For IFN $\gamma$ , the sensitivity for acute cellular rejection was 78%, the specificity was 86%, the positive predictive value was 74% and the negative predictive value was 88% (Ross et al., 1999). In one study of murine lung transplant, CD4+ T cells isolated from allogeneic lung recipients lacking circulating classical monocytes were protected against allorecognition, but allografts still experienced acute rejection (Gelman et al., 2010). Treatment of AR is usually done by high dose steroids for three days (Hanley & Welsh, 2003).

### 1.2.4 Chronic Rejection

Chronic Lung Allograft Dysfunction (CLAD) is an umbrella term for different subtypes of chronic lung diseases, which are majorly diagnosed after lung transplantation (LTx). Subtypes of CLAD are BOS, which occurs in up to 70% of cases, Restrictive Allograft Syndrome (RAS), and a mixed type (Verleden et al., 2014). In contrast to BOS, RAS is defined by a restricted air flow pattern with the Total Lung Capacity (TLC) measuring  $\leq 90\%$  of stable baseline value. In addition, potential air trapping with infiltrates visible on High Resolution Computer Tomography (HRCT), parenchymal/pleural fibrosis with/without obliterated bronchioles detected in TBB and a strict progressive clinical course, comprise characteristics of RAS (Verleden et al., 2014). On the other hand, BOS is a diagnostic system for airway diseases after lung transplantation, based not on histopathological analysis but on specific examination techniques. Incidence of BOS diagnosis within five years post-surgery is up to 60% and after nine years up to 90% of LTx patients (Boehler et al., 1998; Estenne & Hertz, 2002; Neuringer et al., 1998). Despite BOS usually being observed in allograft recipients, it also can be found in patients of autoimmunity or graft-versus-host disease (Barker et al., 2014). BOS typically presents itself in patients with progressive dyspnea, non-productive cough over weeks or months, and an obstructive airflow pattern diagnosed by a decline of FEV1/Forced Vital Capacity (FVC) lower than 80% of baseline, air trapping visible on HRCT scans and a progressive clinical course (Sato, 2020; Verleden et al., 2014). The severity of BOS is classified by the decline of FEV1 as well as Forced Expiratory Flow (FEF) of the middle portion of a Forced Expiration (FE) (Table 1.2.4.1).

Table 1.2.4.1 BOS Classification

Classification of BOS severity according to (Estenne & Hertz, 2002). FEV1, Forced Expiratory Volume in 1 second. FEF 25–75, Forced Expiratory Flow (FEF) of the middle portion of a Forced Expiration (FE). Class 0p, potential BOS.

Severity	Spirometry values
BOS 0	FEV1 > 90% of baseline and FEF 25 - 75 > 75% of baseline
BOS 0p (potential)	FEV1 81% to 90% of baseline and/or FEF 25 - 75 $\leq$ 75% of baseline
BOS 1	FEV1 66% to 80% of baseline
BOS 2	FEV1 51% to 65% of baseline
BOS 3	50% or less of baseline

Once BOS is histologically proven by TBB, it is termed Bronchiolitis Obliterans (BO) (Estenne & Hertz, 2002). For histological analysis of BO, two subcategories exist. A is for BO without biopsy, and B is for histological evidence of BO (Estenne & Hertz, 2002). BO, category B is subdi-

vided into active BO and inactive BO, whereby active BO is defined as fibrosis with intrabronchial or peri-bronchial submucosal mononuclear cell infiltrates with progressive epithelial cell damage. Inactive BO on the other hand consists of a dense fibrotic scarring without cellular infiltrates (Yousem et al., 1996). While one mechanism of chronic rejection is indirect alloimmunity, the complete immunopathogenesis is not fully understood yet (Jaramillo et al., 2005). Well known risk factors for BOS development include donor-recipient mismatch for age, sex, Human-Leucocyte-Antigen (HLA) or CMV-status, and Gastroesophageal Reflux Disease (GERD). Further, IRI, AR, as well as alloimmune-induced autoimmunity and infections impose a significant risk to develop BOS. (Arjuna et al., 2021; Bando et al., 1995; Burton et al., 2009; Estenne & Hertz, 2002; Fiser et al., 2002; Sharples et al., 2002). Notably, certain factors repeatedly show association to development of BOS: Infection with *Pseudomonas aeruginosa* (Botha et al., 2008), enhanced levels of HMGB1 in mouse and human BAL (Takamori et al., 2019; Yoshiyasu & Sato, 2020), and increased levels of Interferon-gamma (IFN $\gamma$ )<sup>+</sup> T cells (Hodge et al., 2009; Hodge et al., 2012) have been published. Previous clinical research found significantly higher amounts of IFN $\gamma$ <sup>+</sup> T cells in induced sputum and BAL of BOS patients than in healthy allograft recipients or patients with stable lung transplants (Mamessier et al., 2007). Besides neutrophils and T cells, monocytes infiltrate the tissue in high amounts shortly after transplantation (Estenne & Hertz, 2002).

### 1.3 Pulmonary Macrophages post Lung Transplantation

About 95% of the alveolar space in the human lung consists of pulmonary macrophages, while less than 4% are lymphocytes, 1% Dendritic Cells (DC), and 1% neutrophils (Martin & Frevert, 2005). In addition to this astonishing fact, as mentioned before, macrophages (M $\Phi$ ) play a vital role in lung transplantation. Pulmonary macrophages are derived from Embryonic Hematopoietic Stem Cells (HSC), which constantly renew themselves by local proliferation (Epelman et al., 2014). In addition Bone Marrow (BM)-derived monocytes patrol the lung or are recruited to the lung via the bloodstream to react to tissue damage and inflammation (Geissmann et al., 2010). These recruited monocytes can potentially differentiate into Interstitial (IM) or Alveolar Macrophages (AM) by Macrophage-Colony-Stimulating Factor (M-CSF) or Granulocyte/Macrophage-Colony-Stimulating Factor (GM-CSF) in the lung respectively (Hamilton, 2002; Stanley et al., 1994). Further, pulmonary macrophages can polarize to different phenotypes, which were historically classified into M1 for pro-inflammatory macrophages by stimulation of the T-Helper Cell 1 (TH1)- cytokine IFN $\gamma$  or LPS and M2 for anti-inflammatory macrophages, typically stimulated by the TH2 cytokine Interleukin 4 (IL-4) (Hashimoto et al., 2013; Hussell & Bell, 2014; Mills et al., 2000). Two critical signaling pathways of pro-inflammatory macrophages entail TLR4-dependent and IFN $\gamma$ -dependent signaling. Once IFN $\gamma$  binds to IFN $\gamma$ -Receptor (IFN $\gamma$ R) on macrophages and monocytes, box 1 domains of the IFN $\gamma$ R1/2 move closer together to recruit Janus Kinase 1/2 (JAK1/JAK2) respectively (Blouin et al., 2016). JAK2 becomes autophosphorylated and activated before phosphorylating and activating JAK1. JAK1 phosphorylates the tyrosine residue 440 (Y440) of IFN $\gamma$ R1, followed by the formation of a docking site, which is specific for the Src Homology 2 (SH2) domain of Signal Transducer and Activator of Transcription 1 (STAT1) (Chapgier et al., 2006). STAT1 forms dimers and gets phosphorylated by JAK2 at tyrosine 701 (Y701). The phosphorylated STAT1 dimer (pSTAT1) is then translocated to the nucleus (Schroder et al., 2004), where it can bind to a promoter region to induce or inhibit transcription of various genes. Typical binding regions of pSTAT1 are Interferon Stimulated Genes (ISG)-regions or Gamma Interferon Activated Site (GAS) sequences (Decker et al., 1997). Many

genes induced by IFN $\gamma$  signaling transcribe transcription factors like Interferon Response Factor 1 (IRF1) (Bhat et al., 2018; Lehtonen et al., 1997). Finally nuclear pSTAT1 can be dephosphorylated by T Cell Protein Tyrosine Phosphatase 45 (TCP45) and transported back to the cytoplasm (Krämer et al., 2009). The innate immune system cells, containing macrophages and monocytes, react to pathogen-induced or sterile inflammation by binding the respective exogenous or endogenous TLR4-ligands (Medzhitov, 2001). Once TLR4 ligands bind, the signaling pathways are activated. One major downstream signaling pathway is the Nuclear Factor Kappa-Light-Chain-Enhancer of Activated B Cells (NF- $\kappa$ B)-pathway, consisting of the canonical and the non-canonical pathways, which can be modulated separately or combined. Bay 11-7082, a non-specific NF- $\kappa$ B inhibitor of both canonical and non-canonical NF- $\kappa$ B-signaling pathways, irreversibly inhibits Inhibitor of Nuclear Factor Kappa B Kinase Subunit Beta (IKK $\beta$ ) and Inhibitor of Nuclear Factor Kappa B Kinase Subunit Alpha (IKK $\alpha$ ). In the canonical pathway, inactive IKK $\beta$  cannot phosphorylate and degrade Inhibitor of NF- $\kappa$ B (I $\kappa$ B), which prohibits the release and translocation of Rel A (p65). In the non-canonical pathway, inactive IKK $\alpha$  cannot phosphorylate p100 and induce p100 processing, resulting in the p52-Rel B heterodimer translocating into the nucleus (Yu et al., 2020). JSH-23 specifically blocks p65 translocation to the nucleus without further disrupting the upstream signaling pathway (Shin et al., 2004).

Main functions of pulmonary macrophages entail phagocytosis, release of antimicrobial and pro-inflammatory agents (Xue et al., 2014) and surfactant clearance (Maus et al., 2002). Besides that, macrophages can function as APC to activate B and T-cells by presenting foreign antigen to them (Gaudino & Kumar, 2019; Mantovani et al., 2004) and therefore play an important role in alloimmunity and lung allograft rejection. Although monocytes and macrophages are increasingly seen as important in understanding immunopathology of allograft rejection, it is still not targeted in clinical therapy. However, understanding the role of monocytes and macrophages following lung transplantation could support in prevention and therapy of BOS (Schreurs et al., 2020). Donor lung macrophages induce an initial response in lung IRI, followed by recipient monocytes replacing the majority of apoptotic donor derived alveolar macrophages after transplantation (Bittmann et al., 2001; Byrne et al., 2020; Maus et al., 2006) and mediating downstream events (Kopecky et al., 2020) as contributing to the development of alloimmunity (Gelman et al., 2010). Further, an increasing amount of research shows accumulation of macrophages in settings of acute and chronic allograft injury (reviewed in Mannon, 2012). In a small clinical study absolute monocyte counts were decreased in LTx but slightly increased in BOS patients with shift towards classical monocytes and less nonclassical monocytes in both groups. But no significant differences between LTx and BOS patients due to a small number of total cells were detected (Schreurs et al., 2020). Notably, a study in epithelial ovarian cancer demonstrated increased Lymphatic Vessel Density (LVD) correlated with increased numbers of tumor associated macrophages alongside elevated expression of HMGB1 (W. Zhang et al., 2014). As HMGB1 is known as an endogenous TLR4 ligand and lymphangiogenesis being driven by vascular endothelial growth factors, this suggests macrophages expressing lymphatic vascular endothelial growth factors triggered by TLR4 signaling.

## 1.4 The Lymphatic System in Lung Transplantation

The lymphatic system consists of Lymphatic Endothelial Cells (LECs) lining up to LV, which play two major roles after LTx. First, LVs remove fluids and harmful molecules from the tissue and thus reduce edema and DAMP induced tissue damage (Ruggiero et al., 1994; Todd et al., 2014). Secondly, LVs transport immune cells toward lymph nodes, where immune cells get

activated by the presentation of alloantigens to trigger the alloimmune response (Alitalo, 2011; Zawieja, 2005). The lymphatic system and its signaling through the VEGFR-3 receptor and its ligand VEGF-C are discussed in several different inflammatory diseases. For example, blocking VEGFR-3 signaling in acute and Chronic Colitis aggravates intestinal inflammation by reducing lymphatic drainage, inducing edema, increasing inflammatory cell infiltration, and elevating pro-inflammatory cytokines (Wang et al., 2016). Similarly, Crohn's Disease and Ulcerative Colitis are chronic Inflammatory Bowel Diseases in which patients' colons presented increased levels of VEGF-C, and increased LVD and VEGF-C stimulation led to protection against Colitis and reduced inflammatory cell infiltrate. This study demonstrated clearance of the inflamed area by Evans blue, Green Fluorescent Protein (GFP)+ inflammatory cells, and fluorescent-coated LPS beads. All methods proved that lymphatic clearance towards the draining lymph node was increased by VEGF-C treatment. Further, migration of macrophages was especially observed, whereas migration of DCs did not occur (D'Alessio et al., 2014). In a study of mouse glioblastoma, adenoviral *Vegf-c* led to increased lymphatic drainage of tumors and, thus, to enhanced priming of anti-tumor CD8+ T cells in the draining deep cervical lymph nodes. Following CD8+ T cell priming, these cells migrate toward the tumor and induce rapid clearance of the glioblastoma (E. Song et al., 2020). This pictures the opposite mechanism of what is needed for lung allograft tolerance. However, the role of lymphangiogenesis and VEGF-C in lung transplantation is not understood in detail yet. Whereas some studies show detrimental effects of lymphangiogenesis on other solid organ transplants like heart or cornea (Claus Cursiefen et al., 2004; Dashkevich et al., 2016), research done in kidney allografts showed prolonged survival by VEGF-C induction (Pedersen et al., 2020; Todd et al., 2014). Further, one study in acute lung rejection has illustrated that activation of lymphatic endothelium via VEGFR-3 by external VEGF-C protects the allograft by facilitating the clearance of hazard molecules (Cui et al., 2015). Hence, more research is needed to understand the underlying molecular mechanisms of lung allograft immunity.

#### 1.4.1 VEGFR-3 - VEGF-C - Signaling

VEGFR-3-VEGF-C signaling is fundamental to lymphangiogenic proliferation and survival (Ma & Oliver, 2017; Vimalraj et al., 2023). VEGFR-3 is expressed in LECs, acting as a homodimer that responds to the extracellular ligands VEGF-C and VEGF-D. When bound to its primary ligand VEGF-C, VEGFR-3 homodimers activate the Rapidly Accelerated Fibrosarcoma (RAS) - Extracellular Signal-Regulated Kinase 1 and 2 (RAF-ERK1/2) pathway, which involves multiple cell activities, including proliferation, migration, and survival. Thus, a standard downstream readout of activated VEGFR-3 signaling is determining elevated levels of pERK (p-p44/p42) by Western Blot (WB) after a stimulation time between 5 and 60 minutes (Achen et al., 1998; Coso et al., 2011; Deng et al., 2015; Joukov et al., 1996; Koch et al., 2011; Mäkinen et al., 2001; Simons et al., 2016; Veikkola et al., 2001). *Vegf-c* expression is reported in Dendritic Cells (DC), CD4+ T cells and macrophages (Baluk et al., 2005; C. Cursiefen et al., 2004; Hamrah et al., 2003; Nykanen et al., 2010; Schoppmann et al., 2002). Secreted VEGF-C initially exists as a 58 kilodalton (kDA) precursor with limited VEGFR-3 activation potential. Some research suggests Collagen and Calcium-Binding EGF Domain-1 (CCBE1) and A Disintegrin and Metalloproteinase with Thrombospondin Motifs 3 (ADAMTS3) to process VEGF-C into its fully active form of 21 kDA (Jeltsch et al., 2014). Both have been shown to facilitate cleavage of VEGF-C sufficiently alone (Janssen et al., 2016; Jeltsch et al., 2014).

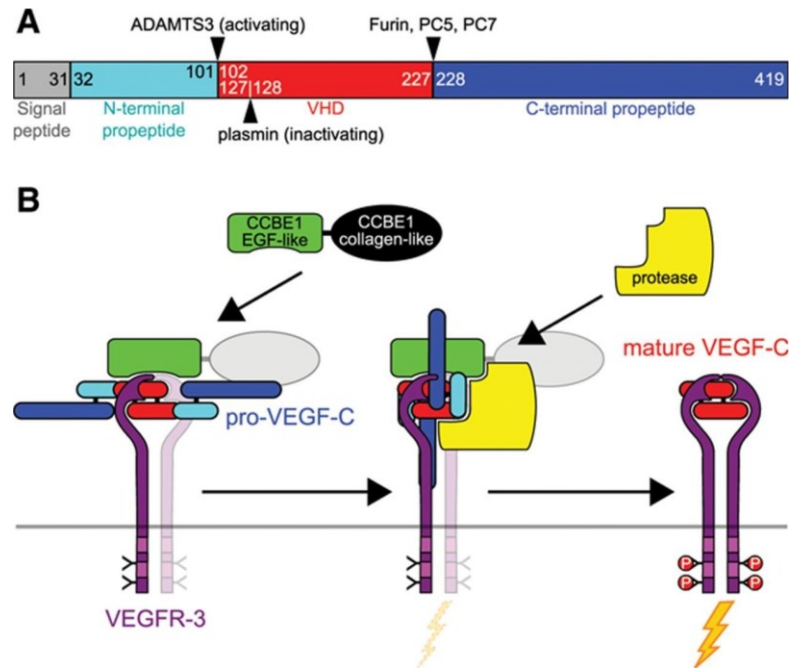


**Figure 1.4.1 Mechanism of Proteolytic VEGF-C Activation by CCBE1 and ADAMTS3 (Jeltsch et al., 2014)**

The binding of pro-VEGF-C to VEGFR-3 is facilitated by the N-terminal domain of CCBE1, followed by proteolytic processing of pro-VEGF-C to produce mature VEGF-C, which in turn activates VEGFR-3. However, the greyish elements of the figure are hypothetical, and the initial binding of VEGF-C to VEGFR-3 could involve either a monomeric or dimeric VEGFR-3. Additionally, it remains unknown whether the function of CCBE1 requires the removal of its C-terminal domain (**Figure 1.4.1**). Notably, experiments by Jeltsch et al. have shown that CCBE1 could potentially induce a high level of biologically active VEGF-C (Jeltsch et al., 2014)

### 1.4.2 Ccbe1

The co-enzyme CCBE1 is known to be expressed in fibroblasts (Jha et al., 2017; J. Song et al., 2020; Wang et al., 2020), smooth muscle cells, endothelial cells (Jha et al., 2017), and epithelial colorectal cancer cells (Zhao et al., 2018). Further, CCBE1 is associated with several human diseases, including Hennekam Lymphangiectasia-Lymphedema Syndrome Type 1 (Alders et al., 2009) and is involved in VEGF-C processing (Jeltsch et al., 2014). CCBE1 facilitates the assembly of a cleavage complex by recruiting pro-VEGF-C from the liquid phase to the cell surface. However, how this interaction occurs is still not fully determined as it may be too weak to detect (Künnapuu et al., 2021), even though predictions as depicted in **Figure 1.4.1** exist (Bui et al., 2016; Jeltsch et al., 2014).

### 1.4.3 Adamts3

ADAMTS3 is expressed in various cell types, such as trophoblastic cells, mesenchymal cells around blood vessels (Janssen et al., 2016), the mouse central nervous system and cartilage (Le Goff et al., 2006). It has been found to cleave pro-VEGF-C exclusively (Janssen et al., 2016) and inactivate reelin, a brain glycoprotein (Ogino et al., 2017). Moreover, it also processes Procollagen II (Col2a1), which is a type of cartilage collagen (Fernandes et al., 2001). In

*Adamts3*<sup>-/-</sup> mice, there is an absence of lymphatics and Hennekam Lymphangiectasia-Lymphedema Syndrome Type 3 is a human disease associated with *Adamts3*. However, *Adamts3* remains much less characterized compared to other *Adamts* (Dupont et al., 2022; Le Goff et al., 2006).

## 1.5 Aim of the Study

Although lung transplantation (LTx) remains the only option for end-stage respiratory failure, it achieves a significantly lower survival time than any other solid organ transplant due to the development of Bronchiolitis Obliterans Syndrome (BOS). BOS is defined by inflammatory fibrosis and infiltration of immune cells like monocytes into the airway lumen (Barker et al., 2014). Monocytes can replace the majority of apoptotic donor-derived alveolar macrophages after transplantation (Byrne et al., 2020) and could act as Antigen-Presenting Cells (APC) to T cells. Vascular Endothelial Growth Factor C (VEGF-C), released by macrophages in other inflammatory diseases, binds to the lymphatic Vascular Endothelial Growth Receptor 3 (VEGFR-3), activating lymphatic endothelial cells. Activated lymphatic endothelium proliferates and thus increases lymphatic drainage of fluids, harmful molecules, and immune cells towards lymph nodes, initiating the alloimmune response. On the one hand, VEGFR-3 signaling block was reported to reduce antigen-presenting cell traffic and alloimmune response, improving the chronic rejection rate in experimental rat heart transplantation (Dashkevich et al., 2016). On the other hand, an expanded lymphatic network by transgenic *Vegf-c* overexpression decreased pro-fibrotic macrophage influx and accelerated recovery from bleomycin-induced lung injury in a mouse lung fibrosis model (Baluk et al., 2020). Further, additional VEGF-C increased lymphatic drainage and reduced acute rejection in a mouse model of acute lung rejection (Cui et al., 2015).

However, unknown remains:

- I) Whether post-LTx lymphangiogenesis is beneficial,
- II) how the temporal and spatial expression pattern of post-LTx *Vegf-c* looks like, and
- III) how *Vegf-c* expression could be regulated by macrophages in the setting of LTx.

Therefore, the main aim of this doctoral thesis was to determine the molecular mechanisms underlying the genetic regulation of pro-lymphangiogenic factors under conditions mimicking the stimulatory environment post-LTx.

In more detail, I intended to

1. Investigate gene expression patterns of pro-lymphangiogenic *Vegf-c*, *Ccbe1*, and *Adamts3* in different subsets of myeloid cells.
2. Identify signaling pathways in positive regulation of pro-lymphangiogenic gene expression in myeloid cells.
3. Identify signaling pathways in negative regulation of pro-lymphangiogenic gene expression in myeloid cells.
4. Ascertain the effect of modified gene expression in macrophages on lymphatic endothelium.

## 2. Material and Methods

### 2.1 Materials

#### 2.1.1 Mice and Maintenance

The experimental mice were maintained in the Institute of Lung Health and Immunity (LHI), Helmholtz Zentrum München. Wildtype (WT) mice of the C57BL/6N strain were bought from Charles River Deutschland (Sulzfeld, Germany). Animals were kept under the national and institutional guidelines, providing room temperature, humidity, 12 hours of light daily, food, and water ad libitum. The used mice were male and 7-25 weeks old. All experiments were approved by the local government for the administrative region of Upper Bavaria, Germany.

#### 2.1.2 Informed Consent Healthy PBMC Donors

Blood donors for Peripheral Blood Mononuclear Cells (PBMC) isolation were healthy and between 29 and 48 years old, two male and one female. All donors donated blood upon informed consent.

#### 2.1.3 Commercially Available Kits

Table 2.1.3.1 Commercially Available Kits

Name	Source
Amersham ECL Prime Western Blotting Detection Reagent	GE Healthcare
cDNA kit	Thermo Fisher Scientific GmbH
Endothelial Cell Growth Medium MV 2 KIT	Promocell
human Pan-Monocyte Isolation Kit	Miltenyi Biotec GmbH, USA
Monocyte Isolation Kit (BM), mouse	Miltenyi Biotec GmbH, USA
peqGOLD Total RNA Kit	PEQLAB Biotechnologie GmbH, Erlangen, Germany
Pierce BCA Protein Assay Kit	Thermo Fisher Scientific GmbH
Pierce ECL Western Blotting Substrate	Thermo Fisher Scientific GmbH
PowerUp SYBR Green Master Mix	Life Technologies GmbH
RNeasy Plus Mini Kit	Qiagen
SuperSignal West Femto Substrate	Thermo Fisher Scientific GmbH

#### 2.1.4 Devices

Table 2.1.4.1 Devices

Name	Source
-20°C freezer MediLine LGex 410	Liebherr, GNP
-80°C freezer U725	Innova, Vacuum insulation Panel Tech
Autoclave	WTC, binder

Axio Observer.Z1 microscope	Carl Zeiss Microscope GmbH, Jena, Germany
Axiomager with an M2 microscope	Carl Zeiss Microscope GmbH, Jena, Germany
Cell freezing container	CoolCell (Biocision)
Centrifuge 5430	Eppendorf AG, Hamburg, Germany
Centrifuge Galaxy 16 DH	VWR International GmbH, Darmstadt, Germany
ChemiDoc™ XRS + Molecular Imager®	Life Science Research Bio-Rad
Cool centrifuge, Mikro 220R	Andreas Hettich GmbH & Co.KG, Tuttlingen, Germany
Cool centrifuge, Rotina 35R	Andreas Hettich GmbH & Co.KG, Tuttlingen, Germany
Corning LSE™ Mini Microcentrifuge, 120V	Corning
FACS Canto II flow cytometer	BD Biosciences
Haemocytometer Neubauer	Karl Knecht Assistant, Sondheim, Germany
Heatblock HBT 130	DITABIS, Digital Biomedical Imaging Systems AG, Pforzheim, Germany
Heatblock Thermomixer Compact	Eppendorf AG, Hamburg, Germany
Heating-blocks	Haep Labor Consult
Incubator MCO-18AC	SANYO Component Europe GmbH, München, Germany
Lamina airflow	Laborgeräte, Pfaffenhofen, Germany
Liquid nitrogen cell tank BioSafe 420SC	Cryotherm
Magnetic fields separator	Miltenyi Biotech GmbH, USA
Magnetic Steerer IKAMAG REO	IKA Werke
Microscope	Carl Zeiss Microscope GmbH, Jena, Germany
Multiplate Reader Infinite 200 Pro	Tecan Trading AG
NanoDrop® ND-1000 spectrophotometer	Thermo Scientific, Wilmington, USA
PCR Thermocycler (Nexus Eco, Nexus Gradient)	Eppendorf AG, Hamburg, Germany
pH meter	pH-Meter inoLab pH 720 (W TW)
Pipetboy	INTEGRA Biosciences GmbH, Fernwald, Germany
Pipettes	Eppendorf AG, Hamburg, Germany
QuantStudio 5	Life Technologies
Racks for 1.5 ml tubes	Stratagene
Roll mixer	VWR International GmbH, Darmstadt, Germany
qPCR Thermocycler StepOne™	Applied Biosystems, Darmstadt, Germany
Scale, Precisa XT 6200C-FR	Pesa Waagen AG
SDS PAGE Chamber Bio-Rad	Bio – Rad Laboratories
Sub Aqua Pro Waterbath	Grant
Thermal Cycler PTC 200	Bio – Rad Laboratories
Thermomixer	Eppendorf AG, Hamburg, Germany
Vacuum pump	BVC basic, Vacuumbrand
Voltage device Bio-Rad	Bio – Rad Laboratories
Vortexer, VM3	Ingenieurbüro CAT M. Zipperer GmbH, Staufen, Germany

Vortexer, Vortex Genie 2	Scientific Industries, NY, USA
Western Blot Chamber, Bio-Rad	Bio – Rad Laboratories

## 2.1.5 Software

Table 2.1.5.1 Software

name	source
Axiovision 4.8 software	Carl Zeiss Microscope GmbH, Jena, Germany
BD FACSDIVA	BD Biosciences
FlowJo Software, Version 9.6.4	TreeStar Inc
GraphPad Prism 9.1	GraphPad Software
ImageJ 2.9.0/1.53t	Wayne Ranband and contributors National Institutes of Health, USA
ImageLab™ 5.2.1 Software	Life Science Research Bio-Rad
Light Cycler 480 software release 1.5.1	Roche Diagnostics
Magellan™	Tecan Life Sciences
Max Quant software package	University of Minnesota, USA
Microsoft Excel	Microsoft
Microsoft Powerpoint	Microsoft
Microsoft Word	Microsoft
Nucleic Acids - nd	Thermo Scientific, Wilmington, USA
PDF XChange Editor Version 9.3, build 361.0	PDF-X-Change Co Ltd.
QuantStudio™ Design & Analysis Software v1.5.2	Life Technologies, Applied Biosystems, Darmstadt, Germany
StepOne™ Software - Version 2.3	Life Technologies, Applied Biosystems, Darmstadt, Germany
ZEN 2010-Digital Imaging for Light-microscopy Software	Carl Zeiss Microscope GmbH, Jena, Germany

## 2.1.6 Reagents and Solutions

Table 2.1.6.1 Reagents and Solutions

name	source
Acrylamide: N,N'- Methylene- Bisacrylamide 40% (29:1)	Carl Roth
Ammonium Persulfate (APS)	ZYTOMED Systems
Antibody Diluent	ZYTOMED Systems
Blot Stripping Buffer	Thermo Scientific
Bovine Serum Albumin (BSA)	Sigma-Aldrich
Complete® Mini Without EDTA (Protease-Inhibitor)	Roche Diagnostics
Dakopen	Dako
Dimethyl Sulfoxide (DMSO)	Sigma Life Science, Carl Roth

Distilled water	ZYTOMED Systems
DNase/RNase free water	Promega
dNTP Solution 10mM (per dNTP) (contains dATP, dTTP, dGTP, dCTP)	Carl Roth
Dulbecco's Phosphate Buffered Saline (DPBS)	Biochrom GmbH
EDTA Buffer Ph 9	Roche Diagnostics
Ethanol (p.a.)	Sigma-Aldrich
Fetal Bovine Serum (FBS)	Bio and Sell
Fluorescent Mounting Medium	Dako
HEPES, 1M	Gibco by Life Technologies
HIER Citrate Buffer, pH 6	ZYTOMED Systems
Hoechst 33342, 20 mM Solution in Water	Anaspec Inc.
Isopropanol	Carl Roth
Laemmli Sample Buffer, 4x	Bio – Rad Laboratories
Lymphoprep	Stemcell Technologies Inc.
Methanol	Sigma-Aldrich, Merck-Millipore
Mgcl2 (25 mM)	Life Technologies GmbH
MuLV Reverse Transcriptase	Carl Roth
Non-Essential Amino Acids, 100x	Merck Millipore, Biochrom
Non-Fat Dried Milk Powder	AppliChem
Paraformaldehyde (PFA)	AppliChem
PCR Buffer II + MgCl <sub>2</sub>	New England Biolabs
Penicillin/Streptomycin	Gibco, Thermo Fisher Scientific GmbH
Phosphate Buffered Saline (PBS)	Applied Biosystems, Darmstadt, Germany
Platinum® SYBR® Green qPCR Supermix-UDG	Thermo Fisher Scientific GmbH
PowerUp™ SYBR™ Green Master Mix	Thermo Fisher Scientific GmbH
Precision Plus Protein™ Standards –Dual Color	Bio – Rad Laboratories
Random Hexamers 50 µM	Thermo Fisher Scientific GmbH
RNase Inhibitor 20 U/µl	Bela-pharm
Roswell Park Memorial (RPMI) Medium 1640	Gibco, Thermo Fisher Scientific GmbH
Sodium Dodecyl Sulfate (SDS)	AppliChem
Sodium Pyruvate, 100 mM	Gibco by Life Technologies
Temed	Bio – Rad Laboratories
Tris	Carl Roth
Trypsin (0.25%) -EDTA solution	Sigma-Aldrich
Tween 20	Sigma-Aldrich
Ultrapure™ Distilled Water DNase/RNase free	Invitrogen by Life Technologies
Xylene	Carl Roth
Xylol	Sigma-Aldrich
β-Mercaptoethanol (β-ME)	Sigma Life Science
β-Mercaptoethanol, 50 mM	Gibco by Life Technologies

## 2.1.7 Buffers and Stock Solutions

Table 2.1.7.1 Buffers and Stock Solutions

Buffer Name	Ingredients
B/S/P Permeabilization Buffer	1 % BSA 0.5% Saponin PBS
Laemmli Sample Buffer 1x	10 µl of β-Mercaptoethanol and 90µl of 4X Laemmli buffer
MACS (Magnetic Activated Cell Sorting) - Buffer	0.5% FBS 2 mM EDTA
PBS-T / Washing Buffer	1x PBS 1% Tween 20
Paraformaldehyde (PFA) 4%	4 g of PFA and 100 ml of PBS
PBS, 10x	25.6 g Na <sub>2</sub> HPO <sub>4</sub> 2g KH <sub>2</sub> PO <sub>4</sub> 80 g NaCl 2 g KCl 900 ml dH <sub>2</sub> O
Running Buffer	1,5 M Tris – HCl pH 8,8 5% v/v 10% SDS
RIPA	NaCl 150 mM Tris pH 7,2 10 mM SDS 0,1% Triton x 100 1% Deoxycholate 1% EDTA 5 mM
Transfer Buffer	150 mM Glycine 20 mM Tris 20% Methanol
TBS buffer 1x	20X TBS- 50 ml, dH <sub>2</sub> O-950 ml

## 2.1.8 Cell Culture Media

Table 2.1.8.1 Cell Culture Media

Cell Type	Media Ingredients
RAW264.7 Cell Culture Medium	DMEM (Dulbecco's Modified Eagle's Medium) F12 10% v/v FCS 1% v/v Penicilin/Streptomycin
SVEC4.10 (Simian Virus 40-Transformed Mouse Microvascular Endothelial Cell Line)	DMEM 10% v/v FCS 1% v/v Penicilin/Streptomycin
Svec4.10	G MV-2 kit (Promocell) without VEGF-A

Bone Marrow-Derived Macrophages (BMDM)/Monocytes	RPMI (Roswell Park Memorial Institute)1640 medium 10% v/v FCS 1% v/v Penicilin/Streptomycin 0.1% v/v 50 mM $\beta$ -Mercaptoethanol + 10/20/40ng/ml M-CSF/GM-CSF-...
Starve Medium for Each One	0.1% or 1% FCS (0.5-5ml FCS in 500ml)

### 2.1.9 Other Consumables

Table 2.1.9.1 Other Consumables

Name	Company
1.5 ml, 2 ml Eppendorf Tubes	Eppendorf AG, Hamburg, Germany
15 ml, 50 ml Falcons	Falcon
96 Wells qPCR Plate	Thermo Scientific, Wilmington, USA
96-Well Imaging Plates, Falcon®	Corning, Thermo Fisher Scientific GmbH
Absolute TM qPCR Seal (AB1170)	Thermo Scientific, Wilmington, USA
Cell Culture Dishes	Corning, Thermo Fisher Scientific GmbH
Cell Culture Flasks 75cm <sup>2</sup> (T75)	Greiner Bio-One
Cell Culture Plates	Greiner Bio-One, Cellstar
Cell Scraper	Corning, Thermo Fisher Scientific GmbH
Combitips Advanced®	Eppendorf AG, Hamburg, Germany
Coverslips Thickness 1.5H Round, Ø: 12 mm	Carl Roth ®
Cryovials 1.5 ml	Greiner Bio- One
Disposable Pipetting Reservoirs	Greiner Bio-One
Extra Thick Blot Paper - Filter Paper	Bio – Rad Laboratories
FACS Tubes	BD Bioscience
Glas Pasteur Pipettes	VWR International GmbH, Darmstadt, Germany
Gloves	Kimtech Sterling Nitrile Gloves
Immun - Blot PVDF Membranes for Protein Blotting	Bio – Rad Laboratories, Merck-Millipore
LS Columns	Miltenyi Biotech GmbH, USA
MACS Smart Filters (30 + 70 $\mu$ m)	Miltenyi Biotech GmbH, USA
Microscope Slides	Thermo Fisher Scientific GmbH
Miltenyi CT Tubes	Miltenyi Biotech GmbH, USA
Pipette Tips	Eppendorf AG, Hamburg, Germany
Polystyrene Round-Bottom Tube with Cell Strainer Cap	Falcon Corning
SepMate Tubes 50ml	Stemcell Technologies Inc.
Sterile Measuring Pipettes	VWR International GmbH, Darmstadt, Germany
Syringes And Needles	B.Braun
1.5 ml, 2 ml Eppendorf Tubes	Eppendorf AG, Hamburg, Germany

### 2.1.10 Antibodies

Table 2.1.10.1 Antibodies

Name	Host	Conjugate	Dilution	Company
Vegf-C (PA5-29772)	Rabbit	none	1:500/1:1000 for WB, 1:200 FC	Invitrogen
Anti-Rabbit IgG (7074S)	Goat	HRP	1:3000	Cell Signaling Technology
Actin (A3854)	Mouse mAb	HRP	1:50,000	Sigma-Aldrich
Anti-Rabbit AF 488 (A-11008)	Goat IgG	Alexa Fluor (AF) 488	1:200	Invitrogen
Podoplanin (TA336668)	Syrian Hamster mAb	none	1:200	Origene
Anti-Syrian Hamster AF 488 (ab180063)	Goat IgG	Alexa Fluor 488	1:800	abcam
Podoplanin (25-5381-82)	Syrian Hamster IgG	PE-Cy7	1:40	eBioscience
Vegfr-3 (130-112-772)	REA834 Human IgG1	PE	1:50	Miltenyi Biotec
p-p44/42 MAPK (T202-Y204) (4370S)	Rabbit	none	1:2000	Cell Signaling Technology
p44/42 MAPK (4695S)	Rabbit	none	1:1000	Cell Signaling Technology
Vinculin (42H89L44/700062)	Rabbit IgG	none	1:5000	Invitrogen
Vinculin-HRP (18799S)	Rabbit mAb	Horse-Radish-Peroxidase (HRP)	1:5000	Cell Signaling

### 2.1.11 Murine Primer

Table 2.1.11.1 Murine Primer

Gene Name	Source/mRNA Genebank Accession #/Primer Bank ID	Forward Primer (5' To 3')	Reverse Primer (5' To 5')
<i>Adamts3</i> (Harvard)	PrimerBank ID: 294345396c3 GeneBank Accession: NM_001081401	ACAGCCATCTACAC-GGAAGTG	ATGTCAC-CAACATAGGCACAG
<i>Ccbe1</i> (Harvard)	PrimerBank ID: 124378017c3 GeneBank Accession: NM_001081401	ACTGGCCTCAAAC-GCCTAC	CGGCCTTGCTTAA-TATGAGACAG
<i>Hprt1</i>		CCTAAGATGAGCG-	CCACAGGACTA-

1+2		CAAGTTGAA	GAACACCTGCTAA
<i>Hprt1</i> 3+4		AGCTACTG- TAATGATCAGTCAACG	AGAGGTCCTTTTCAC- CAGCA
<i>Inos1</i>		CGG- CAAACATGACTTCAGG C	GCACATCAAA- GCGGCCATAG
<i>Tnfa</i>		CACCAC- GCTCTTCTGTCT	GGCTAC- GCTCTTCTGACTC
<i>Vegf-c</i>	(Osawa et al., 2013)	CCAGCACAGGTTAC- CTCAGCAA	TAGACATGCACCGG- CAGGAA
<i>Stat1</i>		TACGAAAAGCAAGCG- TAATCT	TGCACATGACTT- GATCCTTCAC
<i>Irf1</i>		ATGCCAATCAC- TCGAATGCG	CCTGCTTT- GTATCGGCCTGT
<i>Mrc1</i> (CD206)		ACCTGGGGAC- CTGTTGTAT	AAAAATT- GCCTCGCGTCCAA

## 2.1.12 Enzymes

Table 2.1.12.1 Enzymes

Name	Function	Company
Vanadate	Inhibits Proteases	New England Biolabs Inc
Complete Mini, EDTA (11836170001)	Inhibits Proteases	Roche Diagnostics

## 2.1.13 Stimulants and Inhibitors

Table 2.1.13.1 Stimulants and Inhibitors

Name	Function	Company
Bay 11-7082 (B5556)	Canonical & non-canonical NF- $\kappa$ B Inhibitor	Sigma Aldrich-Merck
JSH-23 (J4455)	Canonical NF- $\kappa$ B Inhibitor	Sigma-Aldrich-Merck
Fludarabine	pSTAT1 Inhibitor	SelleckChem S1491
LPS (E-coli O55:B5)	TLR4-Binding	Sigma-Aldrich
rm (recombinant murine) M-CSF	drives Recruited Macrophage Differentiation	Immunotools
rm GM-CSF	Drives Alveolar Like Macrophage and DC Differentiation	Immunotools
m IFN- $\gamma$ (12343536)	Binding IFN Receptor	Immunotools
m IL-4 (12340043)	Binding IL-4 Receptor	Immunotools
rh (recombinant human) IFN- $\gamma$ (130-096-484)	Binding IFN Receptor	Miltenyi Biotec GmbH, USA
rh VEGF-C156s (752-VC)	Binding the VEGFR-3 Receptor	R&D systems

### 2.1.14 Cell Lines

Table 2.1.14.1 Cell Lines

Name	Cell Type	Company
RAW264.7	Murine Macrophages Cell Line	ATCC TIB-71
SVEC4.10	Simian Virus 40-Transformed Mouse Micro-Vascular Endothelial Cell Line	ATCC CRL-2181

### 2.1.15 Tools for Data mining

Table 2.1.15.1 Tools for Data Mining

Name	URL	Data Type	Type Analysis	Version
UCSC Genome Browser	<a href="http://genome.ucsc.edu">http://genome.ucsc.edu</a>	ChIPseq Data Sets	Chromatin Accessibility and TF Binding	Mouse genome mm10, 03/2023
Cistrome Data Browser	<a href="http://cistrome.org/db/#/">http://cistrome.org/db/#/</a>	ChIPseq Data Sets	Chromatin Accessibility and TF Binding	Mouse genome mm10, 03/2023
Cistrome Toolkit to Predict TF Binding	<a href="http://dbtoolkit.cistrome.org/">http://dbtoolkit.cistrome.org/</a>	ChIPseq Data Sets	RP Scores of TF	Mouse genome mm10, 03/2023

## 2.2 Methods

### 2.2.1 Isolation of Murine Bone Marrow

Male C57BL/6J were sacrificed by cervical dislocation. The femur and tibia of the hind legs were collected, muscle tissue was removed, and bones were cut open. Afterward, bone marrow was flushed out with RPMI medium with the help of an 18-gauge needle on a syringe. After centrifugation for 10 minutes at 410g, cells were re-suspended in RPMI, filtered through a 70µm nylon mesh, counted in a Neubauer counting chamber, supplemented with 10% FCS, 1% penicillin-streptomycin and 0.1% β-Mercaptoethanol and seeded 1.5ml suspension per 6 well at a concentration of  $1.7 \times 10^6$  cells/ml. Finally, it was topped up with 1.5ml of the above medium, supplemented with 40ng/ml M-CSF for recruited, monocyte-derived like macrophages or GM-CSF for alveolar-like macrophages, respectively.

### 2.2.2 Differentiation of Bone Marrow-Derived Macrophages

Isolated and seeded bone marrow cells are kept in culture for seven days with replacement of 1.5ml medium with 1.5ml fresh medium, supplemented with 20ng/ml M-CSF on days 2,4 and 6 and 10ng/ml M-CSF on day 7 before being washed thoroughly to remove undifferentiated cells. Then, cells were ready for polarization and stimulation. For polarization of macrophages towards a classical phenotype or a non-classical phenotype, differentiated cells were fetal calf serum (FCS)-starved for 12-18 hours with 0.1-1% FCS and then incubated with 1µg/ml LPS and 20ng/ml IFNγ or 20ng/ml IL-4 for 6-24 hours, respectively. Further, stimulation with 1µg/ml LPS or 20ng/ml IFNγ alone was also done. Successful stimulation was tested by quantitative Polymerase Chain Reaction (qPCR) of either the Inducible Nitric Oxide Synthase 1 (*Inos*) gene or

Tumor Necrosis Factor Alpha (*TNF $\alpha$* ) gene being upregulated by LPS or IFN $\gamma$  and Mannose Receptor C type 1 (*Mrc1*) by IL-4 stimulation, respectively.

### 2.2.3 Isolation of Murine Monocytes

For the isolation of monocytes from murine bone marrow, the isolated bone marrow suspension was processed with the monocyte isolation kit from Miltenyi. Negative selection by magnetically labeling non-target cells like T cells, B cells, Natural Killer (NK) cells, dendritic cells, erythroid cells, and granulocytes significantly increased the percentage of monocytes. The isolated bone marrow suspension was centrifuged and resuspended in 175 $\mu$ l of Magnetic Activated Cell Sorting (MACS) buffer (PBS with 2% FCS, 2mM EDTA) per  $5 \times 10^7$  cells and mixed with 25 $\mu$ l Fc-Receptor (FcR) blocking reagent as well as 50 $\mu$ l biotin-antibody cocktail per  $5 \times 10^7$  cells before incubation for 5 minutes at 2-8°C. After that, cells were washed with 10ml of MACS buffer per  $5 \times 10^7$  cells, centrifuged for 10 minutes at 300g, and resuspended in 400 $\mu$ l MACS buffer and 100 $\mu$ l of anti-biotin microbeads per  $5 \times 10^7$  cells. After a further 10 minutes of incubation at 2-8°C, the suspension was applied onto rinsed MACS LS columns clipped to a magnetic field. While magnetically labeled non-target cells were kept in the column, the flow-through representing the enriched monocyte fraction was collected together with three extra washes of the column with 3ml of MACS buffer. The monocyte-enriched suspension was centrifuged for 7 minutes at 300g and resuspended in RPMI medium supplemented with 10% FCS, 1% penicillin-streptomycin, and 0.1%  $\beta$ -Mercaptoethanol. Afterward, a medium supplemented with the listed stimulants for classical or non-classical polarization, respectively, was added on top. Successful polarization was assessed by qPCR as described for the macrophages before.

### 2.2.4 Isolation of Human Blood-Derived Monocytes

150 – 200 ml of fresh Ethylenediaminetetraacetic Acid (EDTA) blood was drawn from the donors and cooled on ice. First, all blood was filled into falcon tubes and centrifuged at 2300rpm for 10 min to separate serum from the rest. The serum was taken off, and the remaining blood was mixed in the following ratio: 15 ml of blood with 15 ml of PBS was mixed and gently pipetted on top of 15 ml of Lymphoprep at the wall of a 50 ml SepMate tube. This mixture was centrifuged for 10 minutes at 1200g with brakes on and as much clear supernatant as possible taken off until a whitish cloud of PBMCs was reached. The remaining transparent layer, including the cells, was quickly (< 2 sec) poured into a fresh falcon tube and centrifuged for another 10 minutes at 1200g to separate cells from platelets. The supernatant was removed, and the cell pellet consisting of PBMCs was washed two times with cold PBS. Next, monocytes were isolated from PBMCs using the Pan monocyte isolation kit from Miltenyi. Therefore, the cell number was determined by counting in a Neubauer counting chamber and  $1 \times 10^7$  cells resuspended in 40 $\mu$ l of MACS buffer. MACS buffer consisted of PBS with 2 mM EDTA and 0.5% FCS. 10 $\mu$ l of FcR blocking reagent as well as 10 $\mu$ l of biotin-antibody cocktail of the kit were added to each 40 $\mu$ l of cell suspension, mixed well, and incubated for 5 minutes at 2-8°C. 30 $\mu$ l of buffer was added per  $10^7$  cells and topped with 20 $\mu$ l of anti-biotin microbeads per  $10^7$  cells for 10 minutes at 2-8°C. Finishing that last incubation step, the whole cell suspension was applied on Miltenyi LS columns clipped to a magnetic field separator, which was washed with 2ml of MACS buffer before. The flow through of the cell suspension was collected containing the monocytes enriched cell population. Finally, the column was rewashed with MACS buffer to collect any resid-

ual monocytes, and the flow through was combined with the cell suspension for further cell culture.

### 2.2.5 Cell Lines

RAW264.7 cells were purchased from ATCC (ATCC TIB-71™) and cultured in DMEM-F12 medium supplemented with 10% FCS and 1% penicillin-streptomycin. Cells were used between passages 9 and 26. Successful polarization was tested by qPCR as described for the primary macrophages before. SVEC4.10 cells were purchased from ATCC (ATCC CRL-2181™) and cultured in DMEM medium supplemented in 10% FCS and 1% penicillin-streptomycin.

### 2.2.6 Cell Culture

All cells were cultured in T75 cell culture flasks or round cell culture dishes at 37°C with 5% CO<sub>2</sub> and 90% humidity.

### 2.2.7 Inhibition of NF-κB

To inhibit the canonical as well as the non-canonical NF-κB pathways, the chemical Bay 11-7082 was dissolved in dimethyl sulfoxide (DMSO) up to concentrations of 1, 2, or 5mM respectively and used in a 1:1000 dilution in medium to reach a final concentration of 1, 2 or 5 μM with a maximum final DMSO concentration of 0,1%. To specifically inhibit the canonical NF-κB pathway, the translocation of the subunit p65 (RelA) was inhibited with the chemical JSH-23, diluted in DMSO up to concentrations of 15, 30 and 40mM and used in a 1:1000 dilution in medium to reach a final concentration of 15, 30 or 40 μM with a maximum final DMSO concentration of 0,1%. Successful inhibition was tested by qPCR of the *Inos* gene being downregulated with NF-κB inhibition.

### 2.2.8 Inhibition of pSTAT1

To inhibit the signaling through pSTAT1, Fludarabine, a chemical for the depletion of Stat1 protein and its phosphorylation, was dissolved in DMSO up to concentrations of 5, 20, and 40 mM and used in a 1:1000 dilution in a medium to reach a final concentration of 5, 20 or 40 μM with a maximum final DMSO concentration of 0,1%. Successful inhibition was tested by qPCR of the *Irf1* gene being downregulated with STAT1 phosphorylation inhibition.

### 2.2.9 RNA Extraction

For the isolation of cytosolic RNA, either the PeqGOLD total RNA isolation kit or the Qiagen RNA plus mini kit was used. 500μl or 350μl RNA lysis buffer was added before loading the cell lysate onto DNA removing columns and centrifuging for 1 minute or 30 seconds at 12,000 or 8,000 x g, respectively. The flow-through was mixed with the same volume of 70% ethanol and added to RNA binding columns. These were centrifuged for 1 minute or 30 seconds at 10,000 or 8,000 x g, respectively. After washing with 500 or 700μl of wash buffer 1 and centrifuging for 40 seconds or 30 seconds at 10,000 or 8,000 x g, two more washing steps were done with 600μl or 500μl of wash buffer 2 at the same velocity. Between each washing step, the flow

through was discarded. Finally, an extra centrifugation step removed residual buffers. The dried RNA binding columns were loaded with 20-50 $\mu$ l of 70°C warm RNase-free water and left for incubation at room temperature or 70°C for 5 minutes. Centrifugation at 5,000 x g or 8,000 x g was done for 1 minute to elute the RNA, and the elute was immediately stored on ice.

### 2.2.10 Determination of RNA Concentration

To measure the concentration and purity of isolated RNA, 1 $\mu$ l of the elution was applied to a nanodrop machine and measured with the nucleic acid and RNA-40 setting before starting a two-step quantitative PCR (qPCR). The elution was considered pure when the A260/A280 nm ratio was around 2.

### 2.2.11 cDNA Synthesis

Preparing the first step of qPCR, volumes for equal amounts of RNA were calculated across all samples of the same experiment and filled up to 9 $\mu$ l with RNase-free water. Up to 1 $\mu$ g of RNA was then incubated at 70°C for 10 minutes and then cooled on ice for another 5 minutes. According to the protocol, the following volumes were mixed per sample: 10 $\mu$ l 2x RT buffer mix, 1 $\mu$ l of 20x RT enzyme mix, and 9 $\mu$ l of RNA. RNA elutions were then mixed with 11 $\mu$ l master mix, and reverse transcription started at a thermocycler with the following program: 60 minutes at 37°C, 5 minutes at 95°C and then cooled down to 4°C until samples were either used for qPCR or frozen at -20°C for storage. cDNA samples were filled up with up to 80 $\mu$ l H<sub>2</sub>O depending on the initial input of RNA before the cDNA transcription.

### 2.2.12 Quantitative Polymerase Chain Reaction (qPCR)

As the second step of qPCR, a master mix was prepared to contain 2.4 $\mu$ l H<sub>2</sub>O, 0.6 $\mu$ l gene-specific primer (listed in materials), and 5 $\mu$ l SYBR green Master Mix per 2  $\mu$ l RNA sample in a well of a 96-well plate. The PCR reaction was performed by the use of a Thermocycler StepOne™ following the scheme of 5 minutes at 95°C, 5 seconds at 95°C, 5 seconds at 59°C and 30 seconds at 72°C. After 45 cycles with this scheme, the reaction ended after 15 seconds at 95°C, followed by automated production of a melt curve. qPCR was done, including technical duplicates for each biological duplicate, and were normalized to the housekeeping gene Hypoxanthine Phosphoribosyl Transferase 1 (*Hprt1*). SYBR green is a fluorescent dye binding to double-stranded Desoxyribonucleic Acid (DNA). Therefore, by amplification during the PCR reaction, the intensity of the fluorescent signal increases equally to the amount of double-stranded DNA. For analysis, mean Ct values of technical duplicates were taken to calculate the relative expression levels of the tested genes. For calculation, the following equation was applied to all samples: relative expression =  $2^{-\Delta Ct}$  with  $\Delta Ct = Ct$  (gene of interest) – Ct (housekeeping gene).

### 2.2.13 Flow Cytometry

For Flow Cytometry (FC), harvested cells were counted, and a minimum of  $1 \times 10^5$  cells were aliquoted into each tube. After centrifugation at 300 x g for 7 minutes, the medium was removed by inverting the tube. To block unspecific antibody binding, 50 $\mu$ l of FcR block solution containing CD16/CD32 antibody (1:50 in PBS with 2% FCS) was added and incubated for 20 minutes,

followed by the addition of 50µl surface antibody staining master mix and a fixation specific live/dead cell stain if needed, for further 30 minutes. Surface staining was followed by washing with FACS buffer (PBS, 2% FCS). For intracellular staining, a fixation step for 10 minutes with 200µl 4% PFA at RT is done before washing with FACS buffer and permeabilizing with 1ml B/S/P buffer (1% BSA, 0.5% Saponin in PBS) for 10 minutes at RT. Subsequently, to permeabilization, cells are rewashed and resuspended in 50µl FcR Block as before for 10 minutes, followed by intracellular staining in B/S/P buffer for 30 minutes. The staining procedure was finished by washing twice with B/S/P buffer and once with FACS buffer before resuspending in 200µl FACS buffer for analysis.

### **2.2.14 Gating Strategy for FC Analysis**

Macrophage VEGF-C analysis was done by gating the live/dead stain-negative population and the VEGF-C positive population. Voltage adjustment and gate setting were based on a mixture of 50% positively stained and 50% unstained cells, separating positive and negative populations.

### **2.2.15 Immunofluorescence Staining**

20,000 SVEC4.10 cells were seeded on round-shaped microscopy coverslips inside a 12-well overnight. The next day, the medium was gently washed away with PBS before covering the cells with 4% PFA for 10 minutes at room temperature, followed by washing with a wash buffer consisting of PBS and 0.2% tween20. A solution with 10% goat serum, 1% BSA, 0.3% glycine, and 1% tween20 in PBS was applied to the PFA-fixed SVEC4.10 cells for 1 hour to block unspecific antibody binding. The blocking solution was removed gently and replaced by antibody solution, including a 1:50 PODOPLANIN antibody, 5% goat serum, and 0.2% tween20 in PBS. After two days of incubation, later coverslips were washed three times for 5 minutes with wash buffer as before and incubated in a secondary antibody solution including anti-syrian hamster AF488 1:800 as well as Hoechst-dye 1:800 for marking chromatin in nuclei. The stained cells were washed thrice for 5 minutes after 1 hour of secondary antibody incubation. Finally, dried coverslips were mounted upside down on microscope slides with a few microliters of fluorescent mounting medium and left to dry in the dark until images were taken.

### **2.2.16 Protein Extraction**

For isolation of proteins, lysis buffer prepared from RIPA buffer supplemented with the proteinase inhibitors vanadate (1:100) and complete (1:20) was prepared. 25 to 100 µl of this lysis buffer was used to resuspend the thawed cells. The suspension was transferred to fresh Eppendorf tubes, snap-frozen in liquid nitrogen for 5 seconds, and thawed on ice again. Lysates were then centrifuged at 13000 x g for 15 minutes at 4°C, and their supernatants were transferred into new Eppendorf tubes and stored at -80°C.

### **2.2.17 Bicinchoninic Acid Assay**

For measurement of total protein concentration, the Pierce BCA protein assay was used. Peptide bonds of proteins reduce copper ions, which then can form complexes with Bicinchoninic Acid (BCA). This reaction leads to violet coloration with the absorbance of light of 562 nm wave-

length (Walker, 1994). A standard curve with triplicates of different Bovine Serum Albumin (BSA) concentrations was prepared, and 10  $\mu$ l of each sample was mixed with 200  $\mu$ l working reagent containing copper and BCA added to 96-well plate wells. After 30 minutes of incubation at 37°C, the absorbance was measured in the Tecan Plate Reader. Following the protein concentration, the needed volume for 7.5-20 $\mu$ g of protein was calculated using the standard curve.

### 2.2.18 SDS Polyacrylamide Gel Electrophoresis

For size-dependent separation of proteins, proteins are denatured by heat and Sodium Dodecyl Sulfate (SDS), and thiol bonds are reduced by  $\beta$ -Mercaptoethanol ( $\beta$ -ME). Protein suspensions were thawed on ice, and 7.5-20 $\mu$ g of protein was mixed in a 1:4 ratio with freshly prepared loading buffer containing 1 ninth  $\beta$ -ME and 9 parts Laemmli buffer and heated to 95°C for 10 minutes before cooling on ice. SDS polyacrylamide gels were prepared by pouring a 10, 12, or 15% acrylamide separating gel solution into a cast of the company BioRad covered by isopropanol to smoothen the top surface. After polymerization, isopropanol was removed, a 5% acrylamide stacking gel solution was poured on top, and a 10/15-well comb was placed inside. After complete polymerization, the gel cassette was placed into a running module in a mini tank. The comb was removed after filling the running chamber and a mini tank with 1 x SDS- Polyacrylamide Gel Electrophoresis (PAGE) running buffer. Samples and marker were loaded into the wells before running the machine at 100 Volt (V) for approximately 15 minutes and another hour at 120 V (Laemmli, 1970; McLellan, 1982; Ornstein, 1964).

### 2.2.19 Immunoblotting

After running gel electrophoresis, separated proteins were transferred to a Polyvinylidene Fluoride (PVDF) membrane. For the transfer, a sandwich with one layer of sponge, filter paper, PVDF membrane, gel, filter paper, and sponge inside a gel holder cassette was prepared after soaking filter paper with 1 x transfer buffer and activating the membrane in 100% methanol for 1 minute. The sandwich was placed into a mini trans-blot module inside a mini tank filled with ice-cold 1 x transfer buffer and a cooling aid, and the transfer was done for 70 – 90 minutes at 100 V. In cases where VINCULIN was used as a loading control, the membrane was cut horizontally, one ladder band below the expected band of VINCULIN. Afterward, the membrane was washed three times for 15 minutes with 1 x Phosphate Buffered Saline Tween20 (PBST) buffer and blocked for 1 hour in 5% non-fat dry milk dissolved in 1 x PBST buffer. Following that step, the membrane was incubated with 5 – 7 ml 1% milk primary antibody solution at room temperature for 20 – 30 minutes and then at 4°C overnight. The next day, the membrane was rewashed six times for 5 minutes in 1 x PBST buffer before incubating for 1 hour in 5 – 7 ml 1% milk secondary antibody (Horse Radish Peroxidase (HRP)-conjugated) solution at room temperature. After incubation, the membrane was washed six times for 5 minutes in PBST. For detection, access PBST was gently removed with tissue, and 1.2 ml of mixed ECL detection reagent was applied on top of the membrane and incubated for 4 minutes. The chemiluminescent reaction was visualized on immunolabelled proteins using ChemiDoc Imager and Image Lab 5.1 software. For quantification, densitometry was done on single bands and normalized to bands of total p44/p42 (in case of p-p42/44) and then to  $\beta$ -ACTIN or VINCULIN (VCL), respectively.  $\beta$ -ACTIN was detected after washing the membrane three times with 1 x PBST, incubating in stripping buffer for 15 minutes, washing three times for 5 minutes in 1 x PBST, and repeating

immunodetection with an HRP-conjugated  $\beta$ -ACTIN antibody diluted 1:50,000 in 1% milk solution.

### 2.2.20 Conditioned Medium Experiments

For macrophage-Conditioned Medium (CM) experiments, macrophages were stimulated with 0.1 or 1% FCS starve medium supplemented with 1 $\mu$ g/ml LPS or 1 $\mu$ g/ml LPS+ 20ng/ml IFN $\gamma$  for 24 hours. Then, the conditioned medium (CM) was either directly transferred to starved SVEC4.10 cells or stored at -80°C until usage. Since higher percentages of FCS are known to induce p44/p42 phosphorylation, FCS starvation with 0.1% or 1% FCS was used as a negative control, whereas 10% FCS served as a positive control in p44/p42 phosphorylation.

### 2.2.21 Analysis of Publicly Available ChIPSeq Data

For analyzing publicly available Chromatin Immunoprecipitation sequencing (ChIPseq) datasets, three different tools were used. First, the online tool cistrome data browser (db) toolkit (Zheng et al., 2019) (see also "<http://dbtoolkit.cistrome.org/>") was utilized to predict transcription factor (TF) binding and chromatin regulation within 10,000 bases of the Transcription Start Site (TSS) of the gene *Vegf-c* in the mouse mm10 genome. The cistrome db toolkit calculates a Regulatory Potential (RP) score for available TFs in the dataset. The BETA algorithm (Wang et al., 2013) behind the tool assesses the RP score by a distance-weighted measure of all binding sites of the TFs within the selected distance of 10 kilobase (kb) of the selected target gene *Vegf-c*. Thus, the RP score quantifies the likelihood of a TF to regulate the target gene.

In addition, the cistrome data browser (Mei et al., 2017) (see also: "<http://cistrome.org/db/#/>") was employed with a selection of murine macrophages and the TF RelA (p65) or the histone activation mark Histone 3 Lysine 4 trimethyl (H3K4me3) respectively. The selection of displayed results was narrowed down to samples that only passed all quality controls. Only data sets on wild-type mice were chosen to ensure comparability of unstimulated versus LPS stimulated conditions, and control and LPS conditions were always selected from the same experimental setup uploaded by the same research group. The selected datasets were loaded into the batch view list and visualized in the UCSC genome browser (see also: "<http://genome.ucsc.edu/>"). The data view scaling was adjusted to even values, and the most recent NCBI reference sequence NM\_009506.2 of murine *Vegf-c* was displayed below the ChIPSeq peaks. Furthermore, Encyclopedia of DNA Elements (ENCODE) Candidate Cis-Regulatory Elements (cCREs) were shown with their abbreviated accession label and the short UCSC labels for their function. Besides proximal enhancer-like signatures (enhP) and distal enhancer-like signatures (enhD), promoter-like signatures (prom) are exhibited below the *Vegf-c* reference mRNA.

### 2.2.22 Statistical Analysis

All statistical testing was done using the GraphPad Prism software. For comparison between the two groups, non-parametric unpaired two-tailed Student's t-test and 1-way Analysis of Variance (ANOVA) following Bonferroni post-test were performed for multiple comparisons testing between groups. Error bars in bar graphs represent the Standard Deviation (SD) from the mean value, and a probability (p) value below 0.05 was considered significant.

### 3. Results

#### 3.1 *Vegf-c*, *Ccbe1* and *Adamts3* Expression in Proinflammatory Macrophages and Monocytes

To investigate *Vegf-c* expression patterns in pro- and anti-inflammatory macrophages, RAW264.7 cells were stimulated with 1 $\mu$ g/ml LPS, 20ng/ml IFN $\gamma$ , or 20ng/ml of IL-4 for 6, 12, and 24 hours. *Vegf-c* expression was detectable under all conditions, and stimulation with LPS alone strongly increased *Vegf-c* expression after 6 (**Figure 3.1.1 A**) and 12 hours (**Figure 3.1.1 B**) and peaked at 24 hours (**Figure 3.1.1 C**). In comparison, stimulation with LPS and IFN $\gamma$  together also led to a distinct elevation of the *Vegf-c* expression level but was clearly lower than with LPS alone (**Figure 3.1.1 A-C**). IFN $\gamma$  alone did not induce any change in expression at all, as IL-4 stimulation.

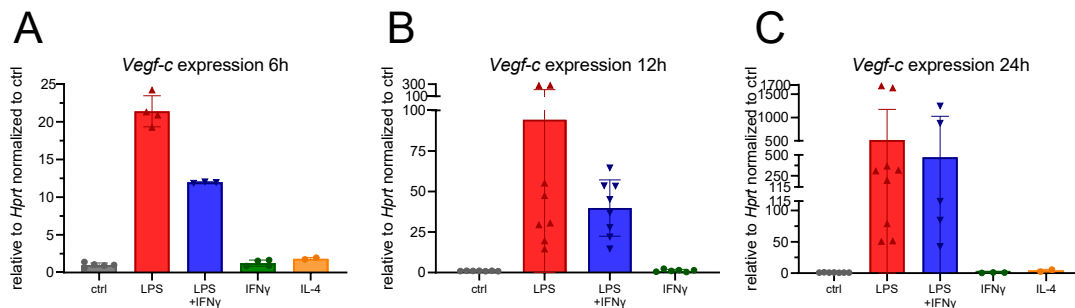


**Figure 3.1.1 *Vegf-c* Expression in RAW264.7 Cells.**

mRNA levels were determined by qPCR, including technical duplicates, and normalized to *Hprt1* as well as to untreated controls. Experiments, including two biological duplicates and two technical duplicates each, were repeated 3-6 (3x Fig. A; 4x Fig. B; 6x Fig. C) independent times, leading to n=1-9 per condition and timepoint in total (mean  $\pm$ SD). (**A**) Relative mRNA levels of *Vegf-c* in RAW264.7 cells after 6h of stimulation with 1 $\mu$ g/ml LPS, 1 $\mu$ g/ml LPS + 20ng/ml IFN $\gamma$ , 20ng/ml IFN $\gamma$  or 20ng/ml IL-4. (**B**) Relative mRNA levels of *Vegf-c* in RAW264.7 cells after 12h of stimulation with 1 $\mu$ g/ml LPS, 1 $\mu$ g/ml LPS + 20ng/ml IFN $\gamma$ , or 20ng/ml IFN $\gamma$ . (**C**) Relative mRNA levels of *Vegf-c* in RAW264.7 cells after 24h of stimulation with 1 $\mu$ g/ml LPS, 1 $\mu$ g/ml LPS + 20ng/ml IFN $\gamma$ , 20ng/ml IFN $\gamma$  or 20ng/ml IL-4.

To check *Vegf-c* protein levels, immunoblotting of RAW264.7 cell lysate was undertaken after 12 and 18 hours of LPS stimulation. This confirmed a visible increase of unprocessed VEGF-C at the size of 58kDa (**Figure 3.1.2**).

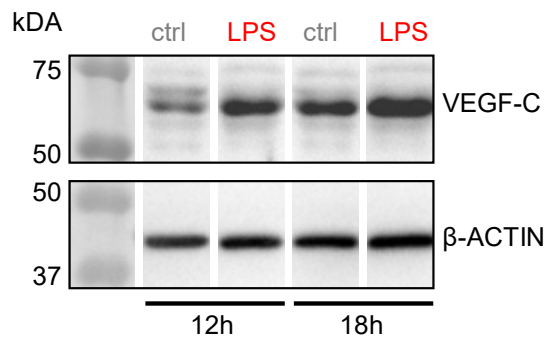


**Figure 3.1.2 VEGF-C Determined by Immunoblotting.**

Protein levels were determined by immunoblotting with anti-VEGF-C and  $\beta$ -ACTIN antibodies after 12 and 18 hours of stimulation with 1 $\mu$ g/ml LPS, including 6 hours with brefeldin A. Experiments, including two biological duplicates each, were repeated three independent times, leading to n=3 per condition in total.

For validation, VEGF-C levels of RAW264.7 cells were analyzed by Flow Cytometry (FC) after 24 hours of LPS, LPS+ IFN $\gamma$ , IFN $\gamma$ , or IL-4 stimulation (**Figure 3.1.3 A**). Analysis of the mean Fluorescence Intensity (FI) of all cells consolidated a visible rise of intracellular VEGF-C with LPS stimulation. In addition, the combination of LPS and IFN $\gamma$  resulted in almost no increase at all, similar to IFN $\gamma$  and IL-4 alone (**Figure 3.1.3 B**).

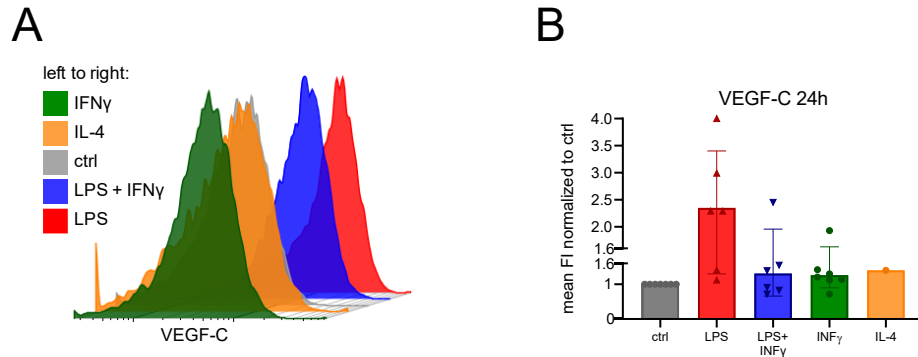


### Figure 3.1.3 VEGF-C Determined by Flow Cytometry

Vegf-c protein levels of RAW264.7 cells were determined by flow cytometry with anti-VEGF-C antibody after 24 hours of stimulation with 1 $\mu$ g/ml LPS, 1 $\mu$ g/ml LPS + 20ng/ml IFN $\gamma$ , 20ng/ml IFN $\gamma$  or 20ng/ml IL-4. Experiments, including two biological duplicates each, were repeated three independent times, leading to n=6 per condition in total (mean  $\pm$ SD). **(A)** Histogram of representative samples. **(B)** Quantification of Vegf-c protein in flow cytometry by mean fluorescent intensity (FI) values.

Applying the same experimental setup of stimulation as before, *Ccbe1* (**Figure 3.1.4 A-C**) and *Adamts3* (**Figure 3.1.5 A, B**) expressions were successfully detected in RAW264.7 macrophages. LPS treatment led to a considerably high rise in *Ccbe1* expression after 6 hours (**Figure 3.1.4 A**), which got further enhanced after 12 (**Figure 3.1.4 B**) and 24 hours (**Figure 3.1.4 C**). Whereas combined treatment with IFN $\gamma$  decreased the response after 6 hours (**Figure 3.1.4 A**), the addition of IFN $\gamma$  did not affect *Ccbe1* expression at 12 and 24-hour timepoints (**Figure 3.1.4 B, C**).

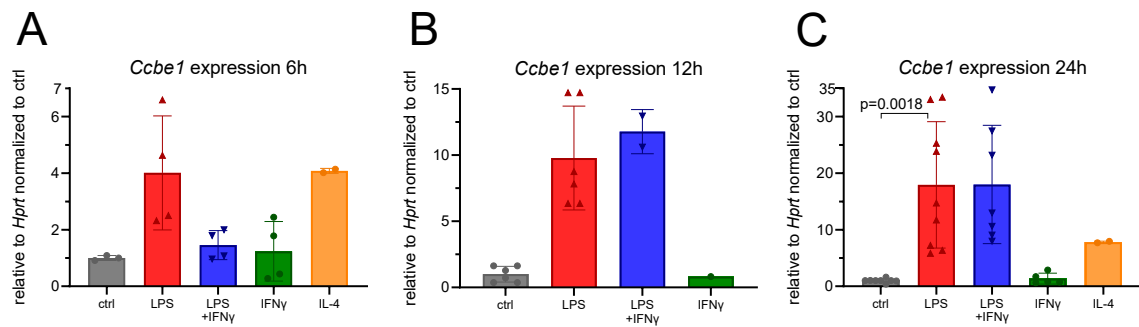


### Figure 3.1.4 *Ccbe1* Expression in RAW264.7 Cells

mRNA levels were determined by qPCR, including technical duplicates, and normalized to *Hprt1* as well as to untreated controls. Experiments, including two biological duplicates and two technical duplicates each, were repeated 2-6 (2x Fig. A; 3x Fig. B; 4; 6x Fig. C) independent times (mean  $\pm$ SD, 1-way ANOVA following Bonferroni post-test; ns = not significant, \* $p$  < 0.05, \*\* $p$  < 0.01, \*\*\* $p$  < 0.001, \*\*\*\* $p$  < 0.0001), leading to n=1-9 per condition and timepoint in total. **(A)** Relative mRNA levels of *Ccbe1* in RAW264.7 cells after 6h of stimulation with 1 $\mu$ g/ml LPS, 1 $\mu$ g/ml LPS + 20ng/ml IFN $\gamma$ , 20ng/ml IFN $\gamma$  or 20ng/ml IL-4. **(B)** Relative mRNA levels of *Ccbe1* in RAW264.7 cells after 12h of stimulation with 1 $\mu$ g/ml LPS, 1 $\mu$ g/ml LPS + 20ng/ml IFN $\gamma$ , or 20ng/ml IFN $\gamma$ . **(C)** Relative mRNA levels of *Ccbe1* in RAW264.7 cells after 24h of stimulation with 1 $\mu$ g/ml LPS, 1 $\mu$ g/ml LPS + 20ng/ml IFN $\gamma$ , 20ng/ml IFN $\gamma$  or 20ng/ml IL-4.

Measuring mRNA levels of *Adamts3*, RAW264.7 macrophages clearly expressed *Adamts3* in both six-hour and 24-hour time points (**Figure 3.1.5 A, B**). However, neither LPS nor IFN $\gamma$  increased or decreased *Adamts3* expression in this cell line (**Figure 3.1.5 A, B**).

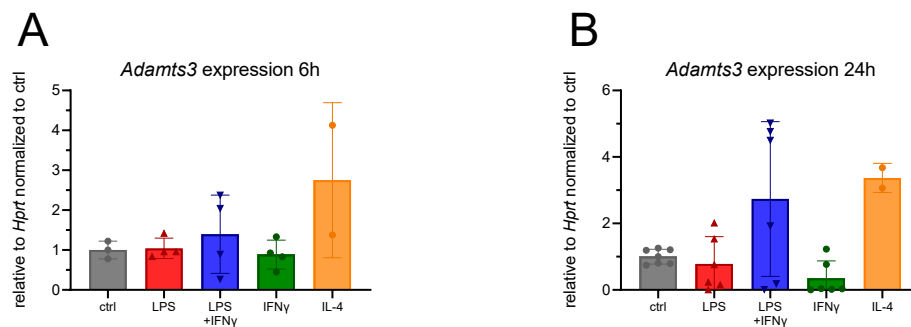


**Figure 3.1.5 *Adamts3* Expression in RAW264.7 Cells**

mRNA levels were determined by qPCR, including technical duplicates, and normalized to *Hprt1* as well as to untreated controls. Experiments, including two biological duplicates and two technical duplicates each, were repeated 2-4 (2x Fig. A; 4x Fig. B) independent times (mean  $\pm$ SD), leading to n=2-7 per condition and timepoint in total. **(A)** Relative mRNA levels of *Adamts3* in RAW264.7 cells after 6h of stimulation with 1 $\mu$ g/ml LPS, 1 $\mu$ g/ml LPS + 20ng/ml IFN $\gamma$ , 20ng/ml IFN $\gamma$  or 20ng/ml IL-4. **(B)** Relative mRNA levels of *Adamts3* in RAW264.7 cells after 24h of stimulation with 1 $\mu$ g/ml LPS, 1 $\mu$ g/ml LPS + 20ng/ml IFN $\gamma$ , 20ng/ml IFN $\gamma$  or 20ng/ml IL-4.

To confirm RAW264.7 data in primary cells, M-CSF treated murine bone marrow cells (**Figure 3.1.6 A, B, D**), which resemble recruited monocyte-derived macrophages, underwent the same treatment as RAW264.7 cells before.

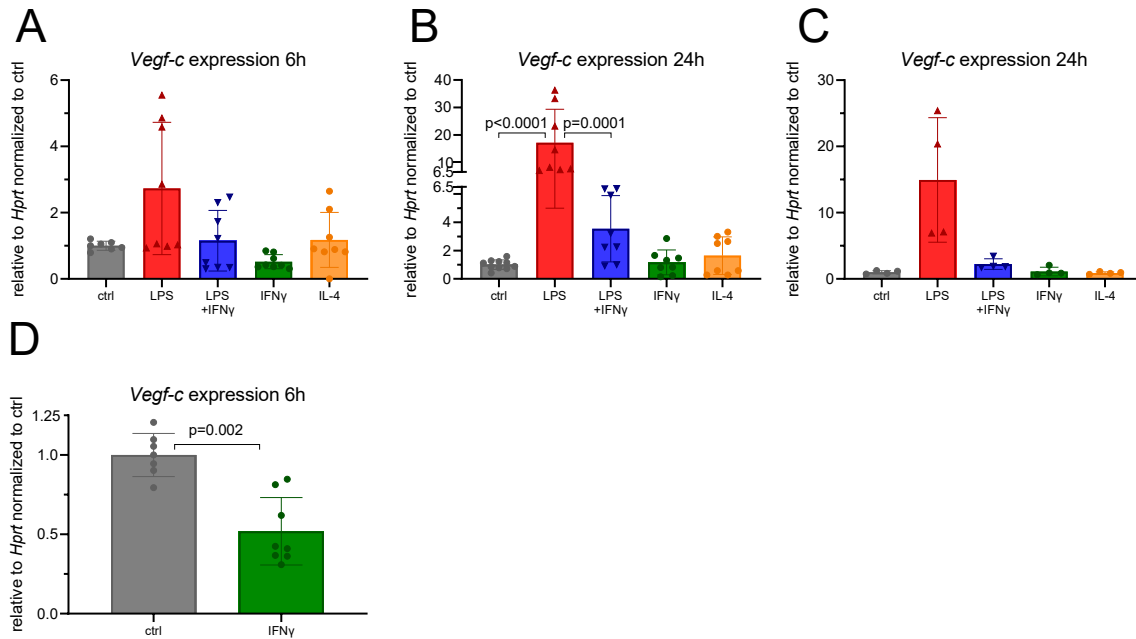


### Figure 3.1.6 *Vegf-c* Expression in BMDMs

mRNA levels were determined by qPCR, including technical duplicates, and normalized to *Hprt1* as well as to untreated controls. Experiments, including two biological, as well as two technical duplicates each, were repeated 1-3 (1x Fig. C, 2x Fig. A, 3x Fig. B, D) independent times with 1-2 mice each (mean  $\pm$ SD, 1-way ANOVA following Bonferroni post-test (Fig. B), non-parametric unpaired 2-tailed t-test (Fig. D); ns = not significant, \* $p < 0.05$ , \*\* $p < 0.01$ , \*\*\* $p < 0.001$ , \*\*\*\* $p < 0.0001$ ). **(A)** Relative mRNA levels of *Vegf-c* in BMDMs, differentiated with M-CSF and stimulated with 1 $\mu$ g/ml LPS, 1 $\mu$ g/ml LPS + 20ng/ml IFN $\gamma$ , 20ng/ml IFN $\gamma$  or 20ng/ml IL-4 for 6 hours. **(B)** Relative mRNA levels of *Vegf-c* in BMDMs, differentiated with M-CSF and stimulated with 1 $\mu$ g/ml LPS, 1 $\mu$ g/ml LPS + 20ng/ml IFN $\gamma$ , 20ng/ml IFN $\gamma$  or 20ng/ml IL-4 for 24 hours.  $p < 0.0001$ ,  $p = 0.0001$  **(C)** Relative mRNA levels of *Vegf-c* in BMDMs, differentiated with GM-CSF and stimulated with 1 $\mu$ g/ml LPS, 1 $\mu$ g/ml LPS + 20ng/ml IFN $\gamma$ , 20ng/ml IFN $\gamma$  or 20ng/ml IL-4 for 24 hours. **(D)** Relative mRNA levels of *Vegf-c* in BMDMs differentiated with M-CSF and stimulated with 20ng/ml IFN $\gamma$  for 6 hours.  $p = 0.002$ .

Levels of *Vegf-c* expression increased visibly after 6 hours ( **Figure 3.1.6 A**) and were highly significant ( $p < 0.0001$ ) after 24 hours (**Figure 3.1.6 B**) of LPS stimulation. Combined treatment with LPS and IFN $\gamma$  led to an evident shrinkage of *Vegf-c* expression levels after 6 hours (**Figure 3.1.6 A**). It was reduced to a highly significant ( $p = 0.0001$ ) level after 24 hours compared to LPS alone (**Figure 3.1.6 B**). Furthermore, after 6 hours of IFN $\gamma$  treatment, the expression of *Vegf-c* was dampened highly significantly ( $p = 0.0002$ ) compared to the untreated control (**Figure 3.1.6 D**), whereas 24 hours of IFN $\gamma$  treatment did not induce a change in expression level like IL-4 treatment (**Figure 3.1.6 B**). Since M-CSF-treated BMDMs resemble interstitial macrophages, the same treatment setup of 24 hours was repeated with GM-CSF-treated BMDMs as they resemble alveolar macrophages (**Figure 3.1.6 C**). Interestingly, alveolar-like BMDMs showed a substantial rise in *Vegf-c* expression, but the response to LPS + IFN $\gamma$  was close to the untreated control (**Figure 3.1.6 C**).

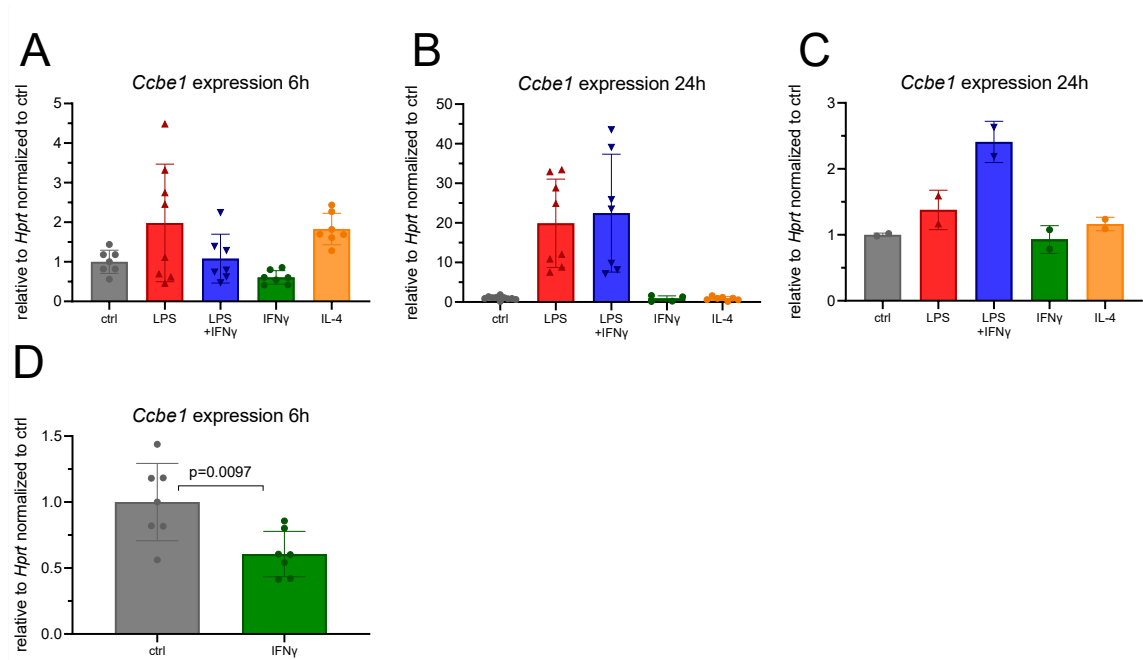


### Figure 3.1.7 *Ccbe1* Expression in BMDMs

mRNA levels were determined by qPCR, including technical duplicates, and normalized to *Hprt1* as well as to untreated controls. Experiments, including two biological, as well as two technical duplicates each, were repeated 1-3 (1x Fig. C; 2x Fig. A, D; 3x Fig. B) independent times with 1-2 mice each (mean  $\pm$ SD, non-parametric unpaired 2-tailed t-test (Fig. D); ns = not significant, \* $p < 0.05$ , \*\* $p < 0.01$ , \*\*\* $p < 0.001$ , \*\*\*\* $p < 0.0001$ ). **(A)** Relative mRNA levels of *Ccbe1* in BMDMs, differentiated with M-CSF and stimulated with 1 $\mu$ g/ml LPS, 1 $\mu$ g/ml LPS + 20ng/ml IFN $\gamma$ , 20ng/ml IFN $\gamma$  or 20ng/ml IL-4 for 6 hours. **(B)** Relative mRNA levels of *Ccbe1* in BMDMs, differentiated with M-CSF and stimulated with 1 $\mu$ g/ml LPS, 1 $\mu$ g/ml LPS + 20ng/ml IFN $\gamma$ , 20ng/ml IFN $\gamma$  or 20ng/ml IL-4 for 24 hours. **(C)** Relative mRNA levels of *Ccbe1* in BMDMs, differentiated with GM-CSF and stimulated with 1 $\mu$ g/ml LPS, 1 $\mu$ g/ml LPS + 20ng/ml IFN $\gamma$ , 20ng/ml IFN $\gamma$  or 20ng/ml IL-4 for 24 hours. **(D)** Relative mRNA levels of *Ccbe1* in BMDMs differentiated with M-CSF and stimulated with 20ng/ml IFN $\gamma$  for 6 hours.  $p = 0.0097$ .

Six hours of LPS treatment of M-CSF treated BMDMs led to a slight increase in *Ccbe1* expression (**Figure 3.1.7 A**), but to a significant ( $p = 0.0097$ ) decline upon IFN $\gamma$  alone (**Figure 3.1.7 D**). Like before, 24 hours of LPS treatment strongly induced *Ccbe1* expression. However, the combined treatment with LPS and IFN $\gamma$  had similar levels of *Ccbe1* expression (**Figure 3.1.7 B**). When analyzing alveolar-like BMDMs, *Ccbe1* expression only responded to treatment by LPS combined with IFN $\gamma$  (**Figure 3.1.7 C**).

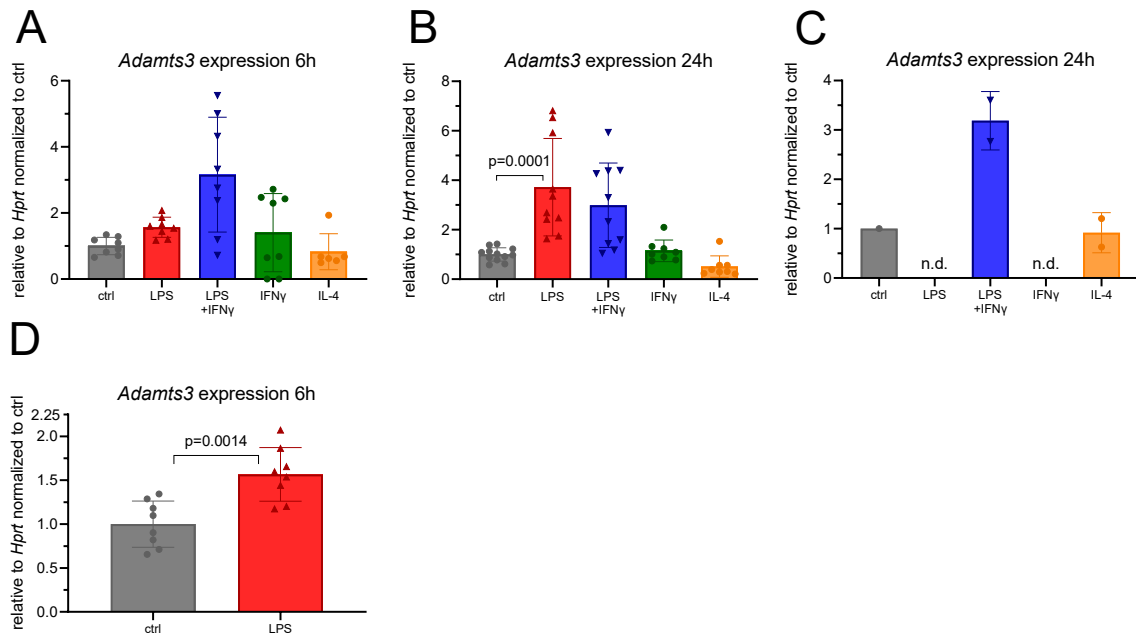


**Figure 3.1.8 Adamts3 Expression in BMDMs**

mRNA levels were determined by qPCR, including technical duplicates, and normalized to *Hprt1* as well as to untreated controls. Experiments, including two biological, as well as two technical duplicates each, were repeated 1-3 (1x Fig. C; 2x Fig. A, D; 3x Fig. B) independent times with 1-2 mice each (n.d. = not detectable, mean  $\pm$ SD, non-parametric unpaired 2-tailed t-test (Fig. D); ns = not significant, \* $p < 0.05$ , \*\* $p < 0.01$ , \*\*\* $p < 0.001$ , \*\*\*\* $p < 0.0001$ ). **(A)** Relative mRNA levels of *Adamts3* in BMDMs, differentiated with M-CSF and stimulated with 1 $\mu$ g/ml LPS, 1 $\mu$ g/ml LPS + 20ng/ml IFN $\gamma$ , 20ng/ml IFN $\gamma$  or 20ng/ml IL-4 for 6 hours. **(B)** Relative mRNA levels of *Adamts3* in BMDMs, differentiated with M-CSF and stimulated with 1 $\mu$ g/ml LPS, 1 $\mu$ g/ml LPS + 20ng/ml IFN $\gamma$ , 20ng/ml IFN $\gamma$  or 20ng/ml IL-4 for 24 hours.  $p = 0.0001$ . **(C)** Relative mRNA levels of *Adamts3* in BMDMs, differentiated with GM-CSF and stimulated with 1 $\mu$ g/ml LPS, 1 $\mu$ g/ml LPS + 20ng/ml IFN $\gamma$ , 20ng/ml IFN $\gamma$  or 20ng/ml IL-4 for 24 hours. **(D)** Relative mRNA levels of *Adamts3* in BMDMs, differentiated with M-CSF and stimulated with 1 $\mu$ g/ml LPS, 1 $\mu$ g/ml LPS + 20ng/ml IFN $\gamma$ , 20ng/ml IFN $\gamma$  or 20ng/ml IL-4 for 6 hours.  $p = 0.0014$ .

Analysis of *Adamts3* expression in M-CSF- treated BMDMs displayed a significant ( $p=0.0014$ ) increase of expression by six hours of LPS treatment (**Figure 3.1.8 D**), but a more robust increase by LPS and IFN $\gamma$  together (**Figure 3.1.8 A**). LPS treatment for 24 hours showed a highly significant ( $p=0.0001$ ) increase in *Adamts3* expression, and the addition of IFN $\gamma$  led to a similar level of *Adamts3* expression (**Figure 3.1.8 B**). Unexpectedly, the mRNA of *Adamts3* was barely detectable in alveolar-like BMDMs after 24 hours of treatment and not detectable (n.d.) in LPS or IFN $\gamma$  stimulated samples (**Figure 3.1.8 C**).

To ascertain whether myeloid cells start expressing pro-lymphatic factors by differentiating into macrophages or whether monocytes already exhibit expression, monocytes were isolated from murine bone marrow, and levels of *Vegf-c* mRNA and protein were measured by qPCR (**Figure 3.1.9 A**) as well as immunoblotting (**Figure 3.1.9 B**). After 24 hours of LPS stimulation, murine monocytes had a clearly elevated level of *Vegf-c* expression compared to untreated control. However, the combination of LPS and IFN $\gamma$  led to an even increased expression compared to LPS treatment alone. IFN $\gamma$  or IL-4 treatment showed similar expression to untreated control samples (**Figure 3.1.9 A**). Analyzing *Vegf-c* protein levels of pro-inflammatory (LPS) versus anti-inflammatory (IL-4) conditions by immunoblotting, murine monocytes displayed an enormously increased amount of *Vegf-c* protein after 24 hours of LPS, whereas IL-4 treatment did not affect levels of *Vegf-c* protein compared to untreated control (**Figure 3.1.9 B**).

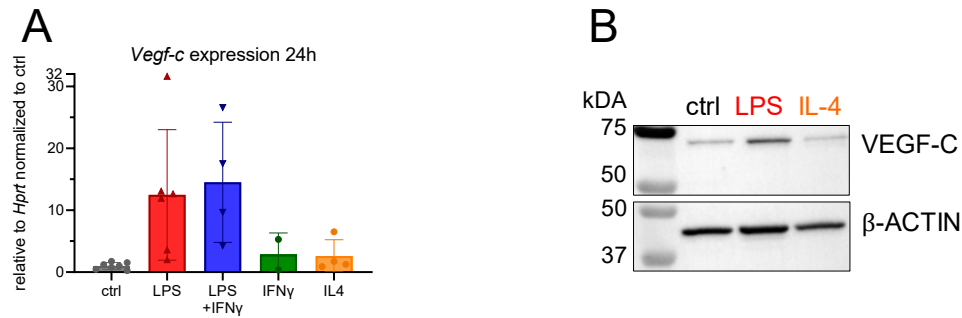


**Figure 3.1.9 Vegf-c mRNA and Protein Levels in Murine Monocytes.**

mRNA levels were determined by qPCR, including technical duplicates, and normalized to *Hprt1* as well as to untreated controls. Protein levels were determined by immunoblotting and with anti-VEGF-C and  $\beta$ -ACTIN antibodies. Experiments, including 2 biological duplicates (and two technical duplicates for qPCR) each, were repeated 1-4 (Fig 3 A: 2x IFN $\gamma$ , LPS+ IFN $\gamma$ , IL-4, 3x LPS, 4x ctrl; Fig 3 B: 1x) independent times, leading to n=1-4 per condition in total. **(A)** Relative mRNA levels of Vegf-c in murine bone marrow-derived monocytes after 24h of stimulation with 1 $\mu$ g/ml LPS, 1 $\mu$ g/ml LPS + 20ng/ml IFN $\gamma$ , 20ng/ml IFN $\gamma$  or 20ng/ml IL-4. **(B)** VEGF-C and  $\beta$ -ACTIN were determined by immunoblotting after 24 hours of stimulation with 1 $\mu$ g/ml LPS or 20ng/ml IL-4.

Finally, the same treatment protocol was applied to human monocytes isolated from fresh Peripheral Blood Mononuclear Cells (PBMCs). Vegf-c protein was determined by flow cytometry and analyzed by median Fluorescent Intensity (FI) (**Figure 3.1.10**). Lipopolysaccharide stimulation resulted in clearly elevated VEGF-C. In contrast to murine macrophages, the addition of IFN $\gamma$  clearly reduced that strong response and thus mirrored the expression pattern seen in murine BMDMs. Further, IL-4-treated human monocytes had similar VEGF-C levels to untreated baseline levels, with a tendency to be even slightly lower (**Figure 3.1.10**).

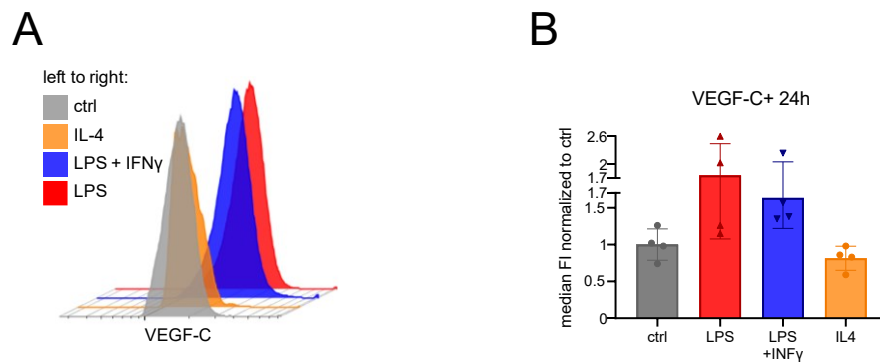


**Figure 3.1.10 Vegf-c Protein in Human Monocytes Determined by Flow Cytometry.**

Protein levels were determined by flow cytometry with anti-VEGF-C antibody. Experiments, including two biological duplicates each, were repeated 2-3 independent times, leading to n = 4 per condition in total. **(A)** Histogram of representative samples of Vegf-c protein levels determined in human blood-derived monocytes after 24 hours of stimulation with 1 $\mu$ g/ml LPS, 1 $\mu$ g/ml LPS + 20ng/ml IFN $\gamma$  or 20ng/ml IL-4. **(B)** Quantification of Vegf-c protein in flow cytometry by median Fluorescent Intensity (FI) values of VEGF-C positive human blood-derived monocytes after 24 hours of stimulation with 1 $\mu$ g/ml LPS, 1 $\mu$ g/ml LPS + 20ng/ml IFN $\gamma$  or 20ng/ml IL-4.

## 3.2 Positive Regulation of Pro-Lymphangiogenic Factors

As expression of lymphangiogenic factors increased consistently by LPS in macrophages and monocytes, the question arises which signaling pathways and transcription factors are engaged to regulate their gene expression. Thus, the online tool "Cistrome data browser toolkit" was used to predict the regulatory potential of common transcription factors to regulate *Vegf-c* expression.

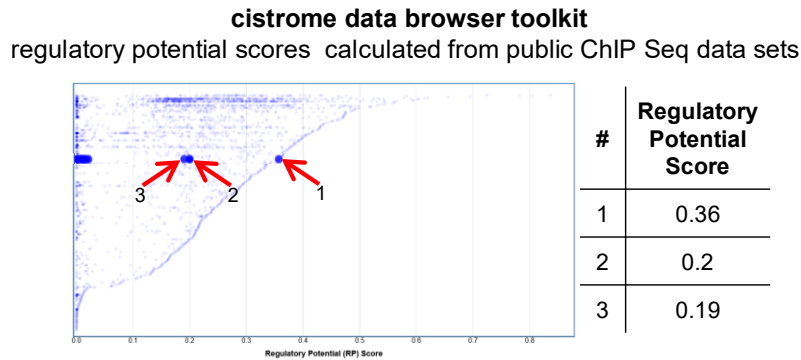
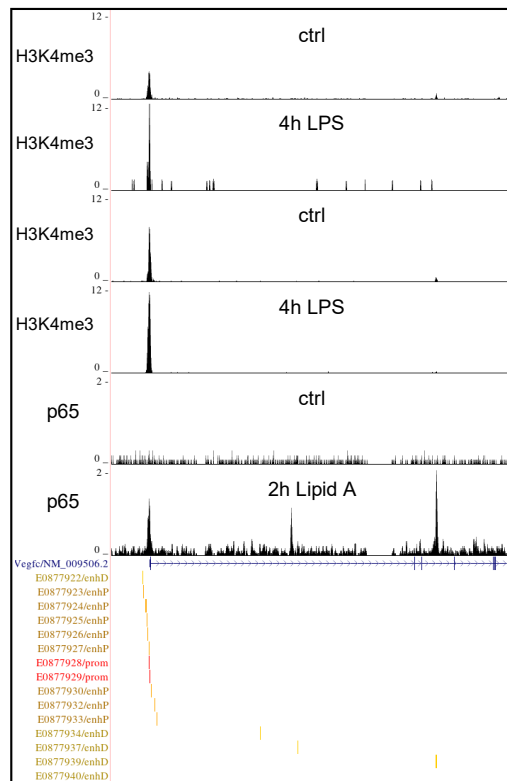


**Figure 3.2.1 Regulatory Potential of p65 to Regulate M $\Phi$  *Vegf-c*.**

The graphic depicting the dataset was downloaded from cistrome.org after adapting the settings according to the reference gene, biological source, and transcription factor. Dynamic plot display of RP scores of p65 in macrophage samples.

When viewing the data points stemming from macrophage samples, regulatory potential scores of 0.36, 0.2, and 0.19 were calculated, respectively (**Figure 3.2.1**). These indicate potential regulation of the *Vegf-c* gene by the TF p65. Further, publicly available histone ChIP-seq data in the cistrome data browser were used to ascertain the accessibility of chromatin in the promoter region of *Vegf-c*. Peaks of Histone-3-Lysine-4 trimethylation (H3K4me3), a so-called "activation mark," exhibit higher DNA accessibility for transcription factors to bind. Analyzing peaks of H3K4me3 in controls as well as LPS-treated samples of two independent datasets, higher amounts of H3K4 trimethylation can be found in the promoter region of the *Vegf-c* gene in LPS-treated samples, indicating higher DNA accessibility for TF to bind. Furthermore, ChIPseq peaks of p65 in macrophages treated with lipid A, a functional component of LPS, were compared to an untreated control. After two hours of lipid A treatment, a distinct peak of p65 binding to the promoter region of *Vegf-c* is visible. In contrast, untreated macrophages did not show any p65 binding in this experiment (**Figure 3.2.2**). In summary, p65 had high regulatory potential scores for regulating *Vegf-c* expression in macrophages. In addition, these scores were supported by higher chromatin accessibility and increased p65 binding upon LPS treatment.

**cistrome data browser**  
peaks of public ChIP-seq data sets displayed in UCSC genome browser



ChIP-seq data of H3K4me3 or p65 binding at the *Vegf-c* gene region

**Figure 3.2.2 ChIP-seq Peaks Aligned to *Vegf-c* Sequence.**

Peaks of H3K4me3 or p65 in public ChIPseq data sets of macrophage samples aligned to the murine *Vegf-c* reference sequence and ENCODE Candidate Cis-Regulatory Elements (cCREs), including promoter structures (prom, red) and proximal/distal enhancer structures (enhP/enhD, brown/yellow) displayed in the UCSC genome browser.

As analysis of public ChIPseq datasets indicated a high likelihood of p65/NF- $\kappa$ B to regulate *Vegf-c* upon LPS treatment in macrophages, I aimed to validate this by chemically inhibiting the NF- $\kappa$ B pathway. Bay 11-7082, a non-specific NF- $\kappa$ B inhibitor of both canonical and non-canonical NF- $\kappa$ B -signaling pathways, irreversibly inhibits IKK $\beta$  and IKK $\alpha$ . First, Bay 11-7082 was applied to macrophages one hour before the actual treatment and kept at a stable concentration of 5 $\mu$ M throughout the following LPS stimulation.

This treatment resulted in a clear dampening of the LPS-induced expression of *Vegf-c* (**Figure 3.2.3 A**) and *Ccbe1* (**Figure 3.2.4 A**) after 12 hours and a significant ( $p = 0.0012$ ) abrogation after 24 hours (**Figure 3.2.3**, **Figure 3.2.4**). To specify, whether the non-canonical or – as data of **Figure 3.2.1** and **Figure 3.2.2** indicate – the canonical NF- $\kappa$ B pathway is responsible for LPS-induced gene expression, JSH-23 was used. JSH-23 specifically blocks p65 translocation to the nucleus.

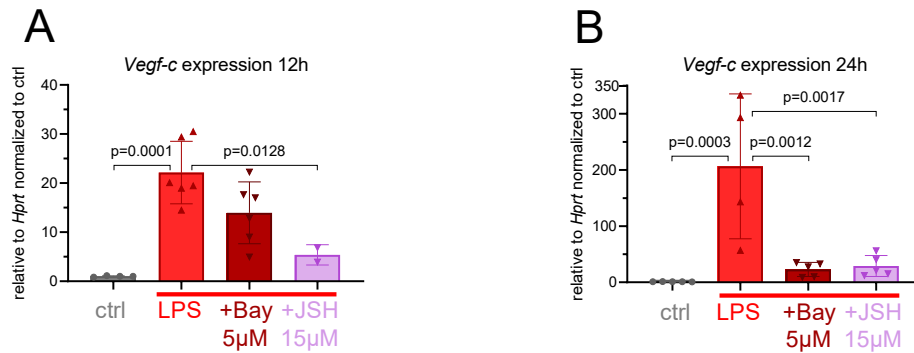


### Figure 3.2.3 *Vegf-c* Expression in RAW264.7 Cells

mRNA levels were determined by qPCR, including technical duplicates, and normalized to *Hprt1* as well as to untreated controls. Experiments, including two biological and two technical duplicates each, were repeated three independent times (mean  $\pm$ SD, 1-way ANOVA following Bonferroni post-test; ns not significant, \* $p < 0.05$ , \*\* $p < 0.01$ , \*\*\* $p < 0.001$ , \*\*\*\* $p < 0.0001$ ). **(A)** Relative mRNA levels of *Vegf-c* in RAW264.7 cells after 12h of stimulation with 1 $\mu$ g/ml LPS, 1 $\mu$ g/ml LPS + 5 $\mu$ M Bay 11-7082 or 1 $\mu$ g/ml LPS + 15 $\mu$ M JSH-23.  $p = 0.0001$ ,  $p = 0.0128$  **(B)** Relative mRNA levels of *Vegf-c* in RAW264.7 cells after 24h of stimulation with 1 $\mu$ g/ml LPS, 1 $\mu$ g/ml LPS + 5 $\mu$ M Bay 11-7082 or 1 $\mu$ g/ml LPS + 15 $\mu$ M JSH-23.  $p = 0.0003$ ,  $p = 0.0012$ ,  $p = 0.0017$

Application of JSH-23 kept at a stable concentration of 15 $\mu$ M throughout the experiment decreased the expression of *Ccbe1* (**Figure 3.2.4**) visibly, and the expression of *Vegf-c* (**Figure 3.2.3**) significantly ( $p = 0.0128$ ) after 12 hours of treatment. The JSH-23 mediated suppression of LPS-induced *Vegf-c* and *Ccbe1* expression became even more significant ( $p = 0.0003$  in **Figure 3.2.3 B** and  $p = .0086$  in **Figure 3.2.4 B**) after 24 hours.

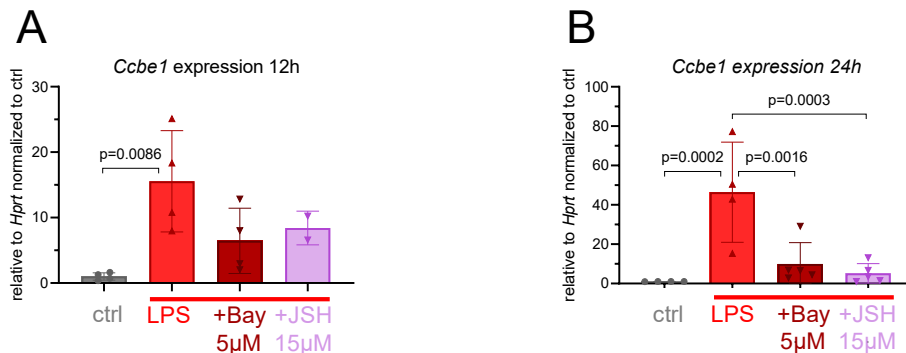


### Figure 3.2.4 *Ccbe1* Expression in RAW264.7 Cells

mRNA levels were determined by qPCR, including technical duplicates, and normalized to *Hprt1* as well as to untreated controls. Experiments, including two biological and two technical duplicates each, were repeated 2-3 independent times (mean  $\pm$ SD, 1-way ANOVA following Bonferroni post-test; ns not significant, \* $p < 0.05$ , \*\* $p < 0.01$ , \*\*\* $p < 0.001$ , \*\*\*\* $p < 0.0001$ ). **(A)** Relative mRNA levels of *Ccbe1* in RAW264.7 cells after 12h of stimulation with 1 $\mu$ g/ml LPS, 1 $\mu$ g/ml LPS + 5 $\mu$ M Bay 11-7082 or 1 $\mu$ g/ml LPS + 15 $\mu$ M JSH-23.  $p = 0.0086$  **(B)** Relative mRNA levels of *Ccbe1* in RAW264.7 cells after 12h of stimulation with 1 $\mu$ g/ml LPS, 1 $\mu$ g/ml LPS + 5 $\mu$ M Bay 11-7082 or 1 $\mu$ g/ml LPS + 15 $\mu$ M JSH-23.  $p = 0.0002$ ,  $p = 0.0016$ ,  $p = 0.0003$ .

This experiment validated the specific positive regulatory effect of p65 on mRNA levels of *Vegf-c* and *Ccbe1* by inhibiting p65 translocation in RAW264.7 cells.

To support these findings in primary cells, murine BMDMs were treated with LPS in combination with JSH-23 for 24 hours. As seen before in RAW264.7 cells, blockage of p65 translocation led to an apparent, concentration-dependent reduction of expression levels of *Vegf-c*, *Ccbe1*, and even *Adamts3* compared to LPS stimulation alone (**Figure 3.2.5 A-C**).

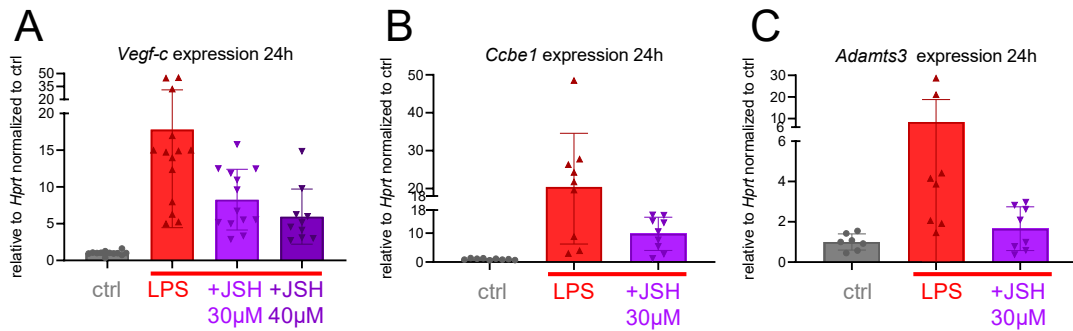


**Figure 3.2.5 Expression of *Vegf-c*, *Ccbe1* and *Adamts3* in BMDMs**

mRNA levels were determined by qPCR, including technical duplicates, and normalized to *Hprt1* as well as to untreated controls. Experiments were repeated 3-4 independent times with 1-2 mice, including two biological duplicates per mouse each. **(A)** Relative mRNA levels of *Vegf-c* in BMDMs, differentiated with M-CSF and stimulated with 1µg/ml LPS, 1µg/ml LPS + 30µM JSH-23 or 1µg/ml LPS + 40µM JSH-23 for 24 hours. **(B)** Relative mRNA levels of *Ccbe1* in BMDMs, differentiated with M-CSF and stimulated with 1µg/ml LPS, 1µg/ml LPS + 30µM JSH-23 or 1µg/ml LPS + 40µM JSH-23 for 24 hours. **(C)** Relative mRNA levels of *Adamts3* in BMDMs, differentiated with M-CSF and stimulated with 1µg/ml LPS, 1µg/ml LPS + 30µM JSH-23 or 1µg/ml LPS + 40µM JSH-23 for 24 hours.

With online data analysis indicating a regulatory role of p65 in *Vegf-c* expression and qPCR of RAW264.7 cells and murine BMDMs confirming these results as well as extending them to *Ccbe1* and *Adamts3*, as the next step, the very same setup in monocytes was tested.

As seen in murine macrophages, inhibition of either both NF-κB pathways or just inhibition of the canonical pathway in murine monocytes both had the same effect on repressing LPS-induced expression of all three pro-lymphangiogenic factors (**Figure 3.2.6**, **Figure 3.2.7**, **Figure 3.2.8**).

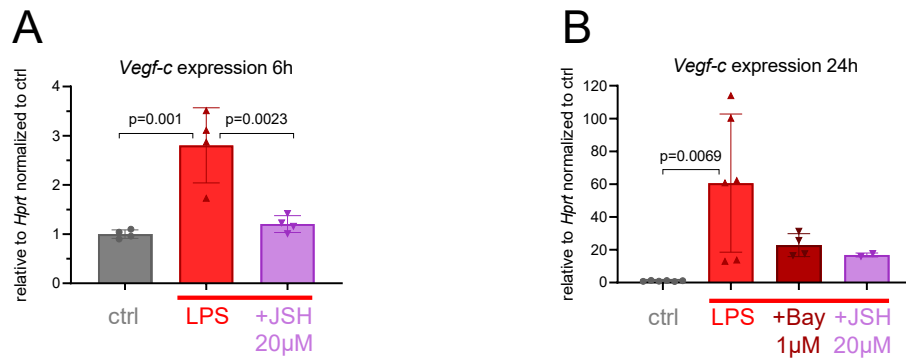


**Figure 3.2.6 *Vegf-c* Expression in Murine Monocytes.**

mRNA levels were determined by qPCR, including technical duplicates, and normalized to *Hprt1* as well as to untreated controls. Experiments, including two biological duplicates and two technical duplicates each, were repeated 1-3 independent times (mean ±SD, 1-way ANOVA following Bonferroni post-test; ns = not significant, \* $p < 0.05$ , \*\* $p < 0.01$ , \*\*\* $p < 0.001$ , \*\*\*\* $p < 0.0001$ ). **(A)** Relative mRNA levels of *Vegf-c* in primary murine bone marrow-derived monocytes stimulated with 1µg/ml LPS or 1µg/ml LPS + 20µM JSH-23 for 6 hours.  $p = 0.001$ ,  $p = 0.0023$  **(B)** Relative mRNA levels of *Vegf-c* in primary murine bone marrow-derived monocytes stimulated with 1µg/ml LPS or 1µg/ml LPS + 20µM JSH-23 for 24 hours.  $p = 0.0069$ .

A significant repression of expression levels was detected after six hours of stimulation in *Vegf-c* expression (**Figure 3.2.6 A**) ( $p = 0.0023$ ) and *Ccbe1* expression (**Figure 3.2.7 A**) ( $p = 0.033$ ).

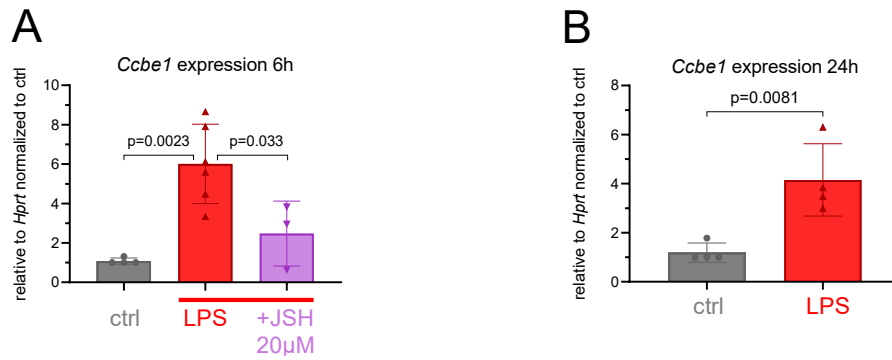


**Figure 3.2.7 *Ccbe1* Expression in Murine Monocytes**

mRNA levels were determined by qPCR, including technical duplicates, and normalized to *Hprt1* as well as to untreated controls. Experiments, including two biological duplicates and two technical duplicates each, were repeated 1-3 independent times (mean  $\pm$ SD, 1-way ANOVA following Bonferroni post-test (A), non-parametric unpaired 2-tailed t-test (B); ns = not significant, \* $p < 0.05$ , \*\* $p < 0.01$ , \*\*\* $p < 0.001$ , \*\*\*\* $p < 0.0001$ ). **(A)** Relative mRNA levels of *Ccbe1* in primary murine bone marrow-derived monocytes stimulated with 1µg/ml LPS or 1µg/ml LPS + 20µM JSH-23 for 6 hours.  $p = 0.0023$ ,  $p = 0.033$  **(B)** Relative mRNA levels of *Ccbe1* in primary murine bone marrow derived-monocytes stimulated with 1µg/ml LPS or 1µg/ml LPS + 20µM JSH-23 for 24 hours.  $p = 0.0081$

In addition, inhibition of both NF- $\kappa$ B pathways for 24 hours of LPS stimulation halved expression of *Adams3* (**Figure 3.2.8**) compared to untreated controls and significantly ( $p = 0.042$ ) reduced compared to LPS stimulation alone (**Figure 3.2.8**).

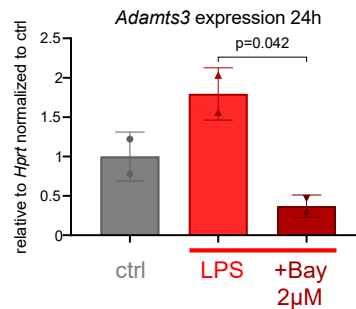


**Figure 3.2.8 *Adams3* Expression in Murine Monocytes**

mRNA levels were determined by qPCR, including technical duplicates, and normalized to *Hprt1* as well as to untreated controls. Experiments, including two biological duplicates and two technical duplicates each, were repeated 1-3 independent times (mean  $\pm$ SD, 1-way ANOVA following Bonferroni post-test; ns = not significant, \* $p < 0.05$ , \*\* $p < 0.01$ , \*\*\* $p < 0.001$ , \*\*\*\* $p < 0.0001$ ). Relative mRNA levels of *Adams3* in primary murine bone marrow derived-monocytes stimulated with 1µg/ml LPS or 1µg/ml LPS + 20µM JSH-23 for 24 hours.  $p = 0.042$ .

Furthermore, prohibiting p65 translocation in human blood-derived monocytes, visibly decreased Vegf-c protein, visualized in a histogram of representative samples (**Figure 3.2.9 A**) and analyzed by the median Fluorescent Intensity (FI) of VEGF-C positive cells in flow cytometry (**Figure 3.2.9 B**).

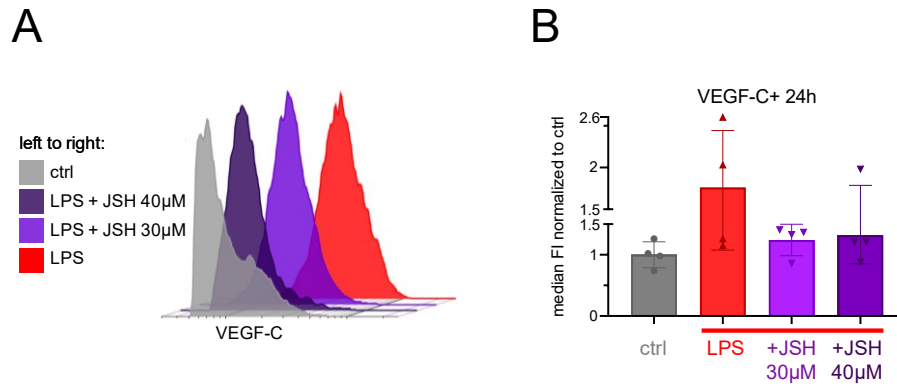


**Figure 3.2.9 Vegf-c Protein Levels in Human Blood Derived Monocytes.**

Protein levels were determined by flow cytometry with anti-VEGF-C antibody. Experiments, including two biological duplicates each, were repeated 2-3 independent times, leading to  $n = 4$  per condition in total. **(A)** Histogram of representative samples of VEGF-C values determined by flow cytometry **(B)** Quantification of VEGF-C in flow cytometry by median Fluorescent Intensity (FI) values of VEGF-C positive human blood-derived monocytes stimulated with  $1\mu\text{g/ml}$  LPS,  $1\mu\text{g/ml}$  LPS +  $30\mu\text{M}$  JSH-23 or  $1\mu\text{g/ml}$  LPS +  $40\mu\text{M}$  JSH-23 for 24 hours.

In total, online data analysis revealed regulatory potential and binding capability to the *Vegf-c* gene, while increased H3K4me3 peaks around the *Vegf-c* gene region indicated higher accessibility by LPS treatment. Inhibition of either both canonical and non-canonical or just the canonical NF- $\kappa$ B pathway in the cell line RAW264.7, primary BMDMs, as well as murine and human monocytes validated the positive regulation of *Vegf-c* by p65 upon LPS binding to TLR4. In addition, the same effect of p65 inhibition was detected for *Ccbe1* and *Adamts3* expression.

### 3.3 Negative Regulation of Pro-Lymphangiogenic Factors

As previous results repeatedly showed reduced expression of *Vegf-c* upon IFN $\gamma$  stimulation (e.g., **Figure 3.1.6 D**), I aimed to explore the downstream regulatory transcription factors. Therefore, the cistrome data browser toolkit was utilized to investigate the regulatory potential of STAT1 on *Vegf-c* expression. Analysis brought up several macrophage datasets, with a regulatory potential score of 0.38, 0.37, 0.2, and 0.16 (**Figure 3.3.1**) for Stat1 to regulate the *Vegf-c* gene within 10,000 kB of the transcription start site (TSS).

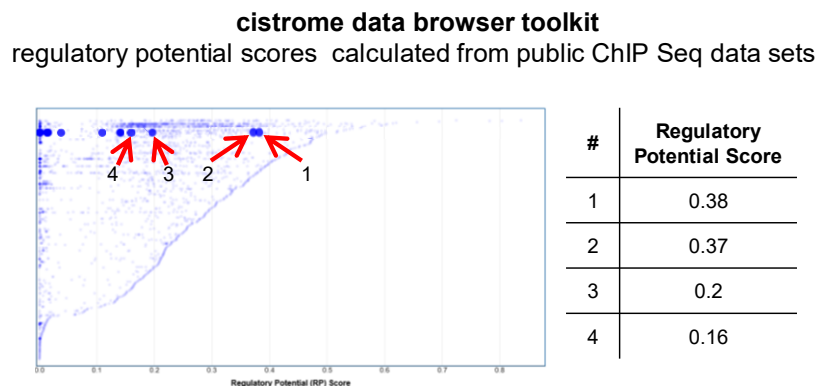


**Figure 3.3.1 Regulatory Potential of Stat1 to Regulate M $\Phi$  Vegf-c.**

The graphic depicting the dataset was downloaded from cistrome.org after adapting the settings according to the reference gene, biological source, and transcription factor. Dynamic plot display of STAT1 in macrophages samples.

Subsequently to the acquisition of online data about the regulatory potential score of STAT1, the regulatory potential of STAT1 on lymphangiogenic expression needed to be tested in vitro. Therefore, Fludarabine (Flu), which inhibits STAT1 activation and depletes Stat1 protein, was applied to RAW264.7 cells one hour before treatment with LPS and IFN $\gamma$  for 24 hours. Firstly, the Vegf-c protein was measured by flow cytometry (**Figure 3.3.2**) and quantified by mean Fluorescent Intensity (FI) (**Figure 3.3.2 B**) and representative samples displayed as histograms (**Figure 3.3.2 A**). As shown before (**Figure 3.1.3**) and replicated here (**Figure 3.3.2**), combined stimulation with LPS and IFN $\gamma$  led to a visibly reduced level of Vegf-c protein compared to LPS treatment alone. Adding 5  $\mu$ M or 20  $\mu$ M Fludarabine indeed rescued the LPS-induced increase concentration-dependent (**Figure 3.3.2 A, B**).

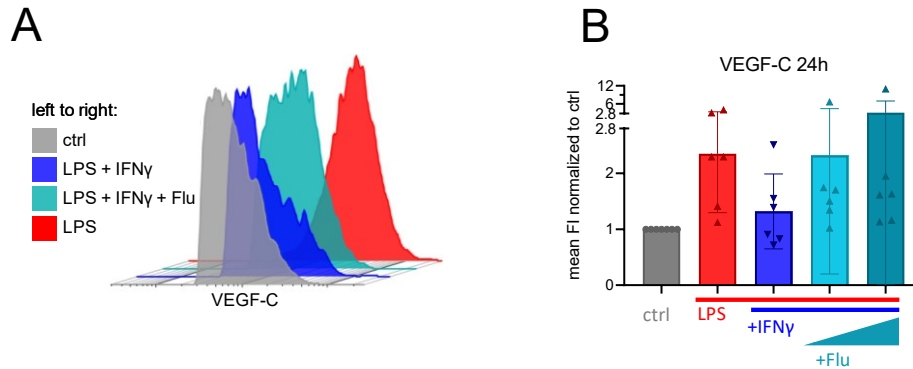


**Figure 3.3.2 Vegf-c Protein Levels in RAW264.7 Cells Determined by Flow Cytometry.**

Protein levels were determined by flow cytometry with anti-VEGF-C antibody. Experiments, including two biological duplicates each, were repeated 2-3 independent times (mean  $\pm$ SD). **(A)** representative Vegf-c protein levels in RAW264.7 cells determined by flow cytometry after 24 hours of stimulation with 1  $\mu$ g/ml LPS, 1  $\mu$ g/ml LPS + 20ng/ml IFN $\gamma$ , 1  $\mu$ g/ml LPS + 20ng/ml IFN $\gamma$  + 20  $\mu$ M Fludarabine, 1  $\mu$ g/ml LPS + 20ng/ml IFN $\gamma$  + 40  $\mu$ M Fludarabine. **(B)** Quantification of Vegf-c protein levels by measuring the mean Fluorescent Intensity (FI) of all cells represented in Fig. A.

To verify the result and the efficiency of Fludarabine, the same setup was repeated with murine BMDMs (**Figure 3.3.3**). Levels of Stat1 mRNA stayed relatively equal throughout all stimulations (**Supplementary Figure A 3.3.3**), which reflects that phosphorylation and overall protein levels, but not mRNA levels, are affected explicitly by Fludarabine treatment.

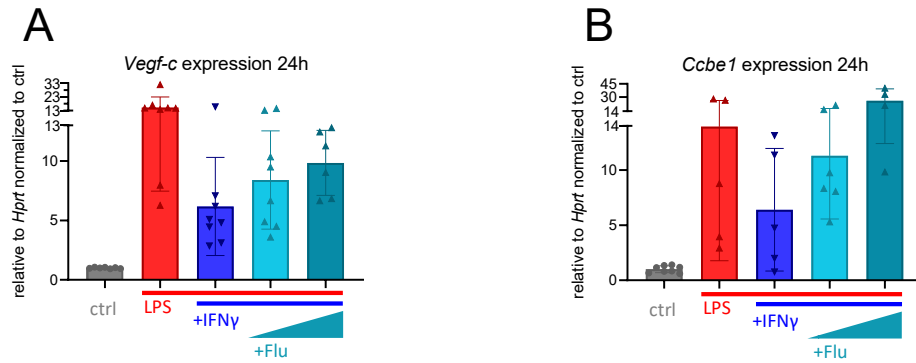


**Figure 3.3.3 Pro-Lymphangiogenic Expression in BMDMs.**

mRNA levels were determined by qPCR, including technical duplicates, and normalized to *Hprt1* as well as to untreated controls. Experiments, including two biological duplicates and two technical duplicates each, were repeated 1-3 independent times (mean  $\pm$ SD). **(A)** Relative mRNA levels of *Vegf-c* in BMDMs, differentiated with M-CSF and stimulated with 1  $\mu$ g/ml LPS, 1  $\mu$ g/ml LPS + 20ng/ml IFN $\gamma$ , 1  $\mu$ g/ml LPS + 20ng/ml IFN $\gamma$  + 5  $\mu$ M Fludarabine, 1  $\mu$ g/ml LPS + 20ng/ml IFN $\gamma$  + 20  $\mu$ M Fludarabine for 24 hours. **(B)** Relative mRNA levels of *Ccbe1* in BMDMs, differentiated with M-CSF and stimulated with 1  $\mu$ g/ml LPS, 1  $\mu$ g/ml LPS + 20ng/ml IFN $\gamma$ , 1  $\mu$ g/ml LPS + 20ng/ml IFN $\gamma$  + 5  $\mu$ M Fludarabine, 1  $\mu$ g/ml LPS + 20ng/ml IFN $\gamma$  + 20  $\mu$ M Fludarabine for 24 hours.

However, mRNA of *Irf1*, a direct downstream target of STAT1, was clearly upregulated with LPS + IFN $\gamma$  stimulation compared to LPS alone and by treatment with Fludarabine, reduced to the level of LPS stimulation in a concentration-dependent manner (**Supplementary Figure A 3.3.3**). *Vegf-c* expression, upregulated by LPS, was strongly reduced by LPS + IFN $\gamma$ , whereas in combination with increasing concentrations of Fludarabine, visibly leveled up *Vegf-c* expression again (**Figure 3.3.3 A**). Further, qPCR of *Ccbe1* revealed an even stronger expression rescue in the presence of Fludarabine compared to treatment with LPS and IFN $\gamma$  alone (**Figure 3.3.3 B**).

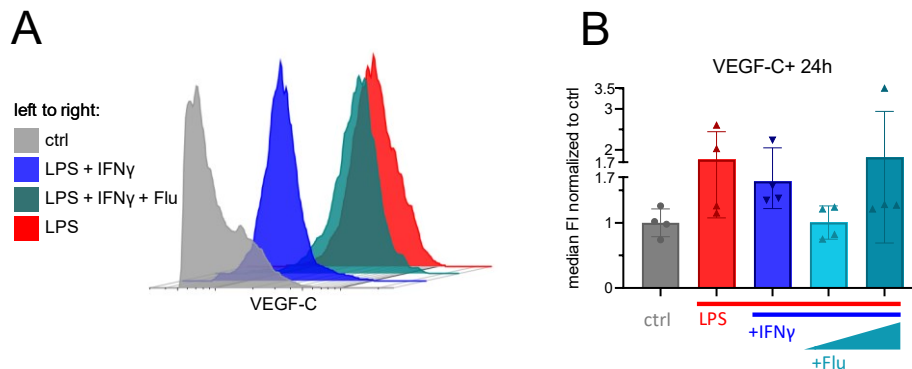


**Figure 3.3.4 VEGF-C Levels in Human Blood-Derived Monocytes Determined by Flow Cytometry.**

Experiments, including two biological duplicates each, were repeated two independent times. **(A)** representative *Vegf-c* protein levels in human blood-derived monocytes determined by flow cytometry after 24 hours of stimulated with 1  $\mu$ g/ml LPS, 1  $\mu$ g/ml LPS + 20ng/ml IFN $\gamma$ , 1  $\mu$ g/ml LPS + 20ng/ml IFN $\gamma$  + 20  $\mu$ M Fludarabine, 1  $\mu$ g/ml LPS + 20ng/ml IFN $\gamma$  + 40  $\mu$ M Fludarabine for 24 hours. **(B)** Quantification of *Vegf-c* protein levels by measuring median Fluorescent Intensity (FI) of VEGF-C positive cells.

Last, but not least, treatment with Fludarabine in combination with LPS and IFN $\gamma$  was done on human blood-derived monocytes (**Figure 3.3.4 A, B**). Again, a concentration-dependent rescue of *Vegf-c* protein was measured, proving the STAT1 dependency of its downregulation. **Figure 3.3.4 A** clearly visualizes representative samples of *Vegf-c* protein in a histogram of fluorescent intensity. Especially a concentration of 40ng/ml Fludarabine lifted the level of *Vegf-c* protein to

the condition of LPS treatment as quantified by median Fluorescent Intensity (FI) (**Figure 3.3.4 B**).

### 3.4 Treatment of SVEC4.10 Cells with Macrophage Conditioned Medium

As VEGF-C is a lymphatic endothelial growth factor, I wanted to use a VEGFR-3 positive endothelial cell line and thus utilized SVEC4.10 cells. With the cultivation and characterization of SVEC4.10 cells, the lymphatic marker PODOPLANIN (PDPN) was highly expressed, as shown in immunofluorescent cell staining (**Figure 3.4.1 A**) and flow cytometry (**Figure 3.4.1 C**). More specifically, Vegfr-3 surface protein was detected in SVEC4.10 cells by the very same method (**Figure 3.4.1 B**).

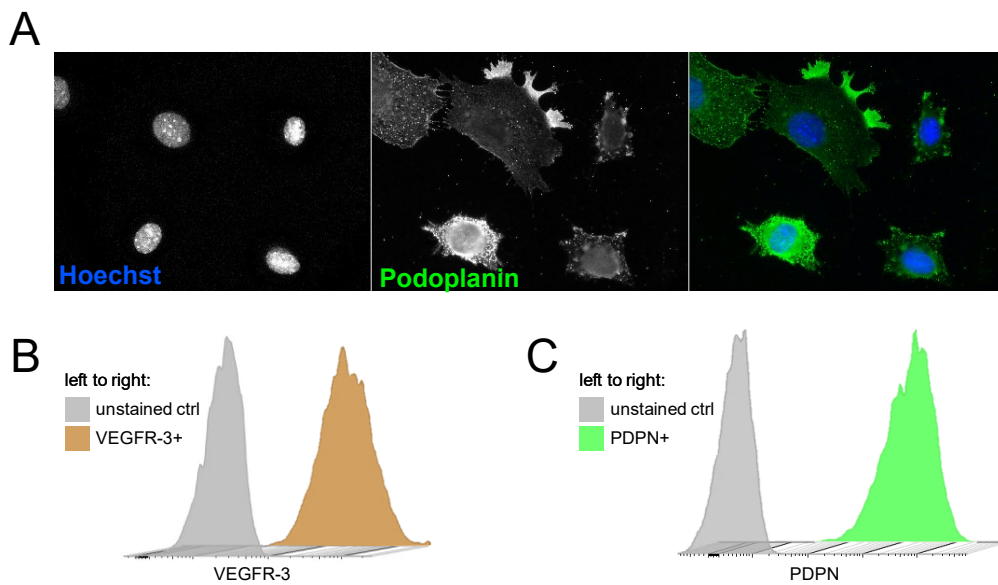


**Figure 3.4.1 PODOPLANIN and VEGFR-3 Expression In SVEC4.10 Cells.**

(**A**) Representative images of immunofluorescence cell staining with Hoechst-dye (blue) marking cell nuclei as well as an anti-PODOPLANIN antibody (green) of SVEC4.10 cells. (**B**) Histogram of VEGFR-3 fluorescent intensity in flow cytometry of SVEC4.10 cells. (**C**) Histogram of PODOPLANIN fluorescent Intensity (FI) in flow cytometry of SVEC4.10 cells.

To validate the presence of functional VEGFR-3 receptors on the surface of SVEC4.10 cells, immunoblotting of p44 and p42 phosphorylation, a standard method to measure activation of VEGF-C-VEGFR-3 signaling, was carried out.

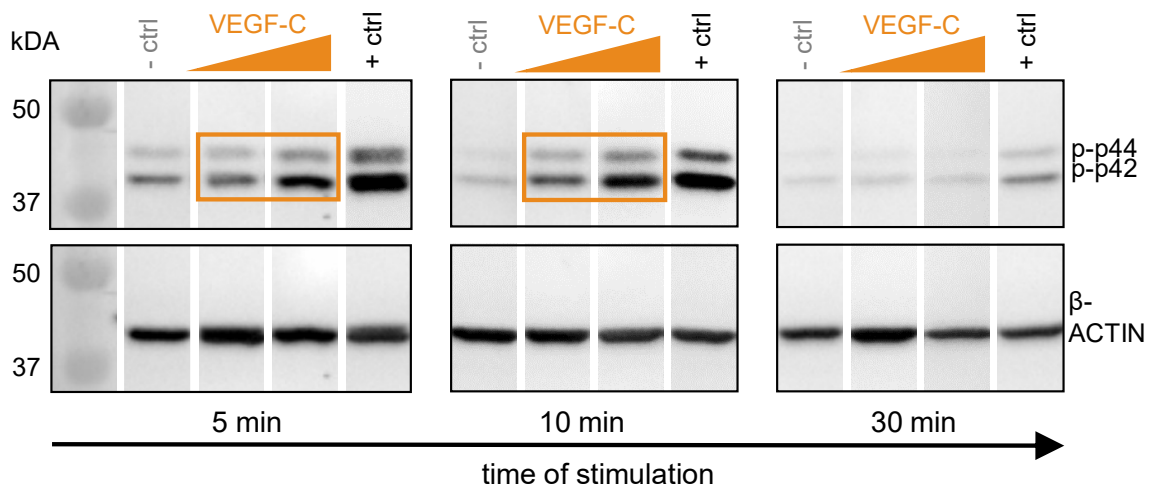


**Figure 3.4.2 p-p44/p42 Levels in rhVEGF-C156s Stimulated SVEC4.10 Cells.**

Protein levels were determined by immunoblotting and with anti-p-p44/p42 and  $\beta$ -ACTIN antibodies. Experiments included two biological duplicates. Representative samples of immunoblotting of SVEC4.10 total cell lysate with anti-p-p44/p42 antibody and anti- $\beta$ -ACTIN antibody after five, ten, and 30 minutes of stimulation with pure medium (- ctrl), 100ng/ml rhVEGF-C156s, 500ng/ml rhVEGF-C156s or 10% FCS-medium (+ ctrl) respectively.

SVEC4.10 cells were subjected to 100 or 500 ng/ml recombinant human (rh)VEGF-C156s for 5, 10, and 30 minutes before immunoblotting total cell lysate with anti-phospho-p44/p42 antibody, as well as anti- $\beta$ -ACTIN antibody as loading control for total protein. Analyzing bands of phospho-p44 at a size of 44 kDa as well as p-p42 at a size of 42 kDa, a rise in phosphorylation is clearly visible in all conditions after five and ten minutes of treatment, whereas p44/p42 phosphorylation of the negative control and rhVEGF-C156s stimulation after 30 minutes becomes rather faint compared to the positive control. Compared to the negative controls of five and ten-minute timepoints, treatment with rhVEGF-C156s clearly increased p44/p42 phosphorylation in a concentration-dependent manner, as expected. Herewith, I clearly show SVEC4.10 cells with high expression of PDPN as well as VEGFR-3 and increasing p44/p42 phosphorylation by rhVEGF-C156s treatment, proving activation of the VEGFR-3 - VEGF-C signaling pathway, which in summary composes lymphatic endothelial identity.

To investigate the functional effect of macrophage-derived VEGF-C on activation of VEGFR-3 signaling in lymphatic endothelium, I applied a conditioned medium, derived from unstimulated and LPS-stimulated RAW264.7 cells, respectively, on top of SVEC4.10 cells for five ten and 30 minutes (**Figure 3.4.4**), as done before with rhVEGF-C156s (**Figure 3.4.2**).

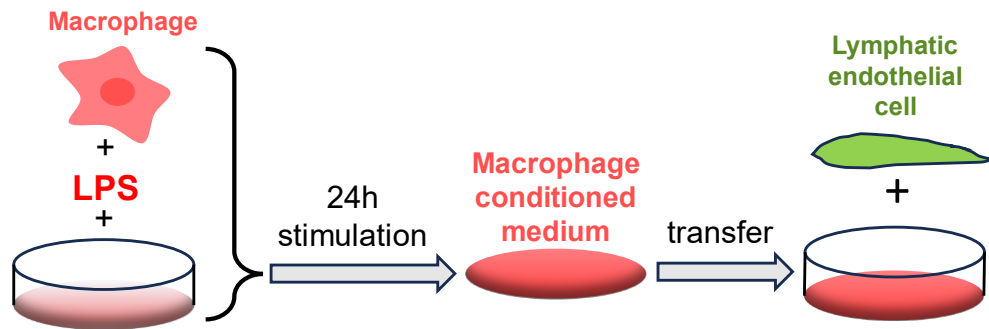


**Figure 3.4.3 Experimental Setup with LPS-Stimulated Macrophage Conditioned Medium.**

Macrophages were cultured in a standard growth medium supplemented with LPS for 24h. After 24h, the supernatant called conditioned medium, is removed, and applied on top of cultured SVEC4.10 cells for 5 – 10 minutes.

Since SVEC4.10 cells are insensitive to LPS, any LPS left from previous stimulation of RAW264.7 cells does not affect SVEC4.10 cells. To further rule out any TLR4-specific effect on SVEC4.10 cells, LPS was also included in the medium of the negative control. Treatment with the conditioned medium of unstimulated RAW264.7 cells for 5 minutes resulted in a visibly firmer p44 phosphorylation level than the negative control. Stimulation with the conditioned medium of LPS stimulated RAW264.7 cells further increased the levels of p-p44 and thus even surpassed p-p44 levels of the positive control (**Figure 3.4.4 A, B**). Whereas the difference between SVEC4.10 p-p44 of unstimulated versus LPS stimulated RAW264.7 medium increased, both further exceeded the positive control after 10 minutes of SVEC4.10 treatment (**Figure 3.4.4 A, C**). The most robust upregulation of p-p44 levels was detected after 30 minutes of treatment with conditioned medium LPS-stimulated RAW264.7 cells. The signal of that lane appeared so rapid and intense that more prolonged exposure for better visualization of negative and positive control bands would have exceeded the detection range in the LPS-stimulated RAW264.7 sample. Besides that, the positive control bands are still detectable (**Figure 3.4.4 A, D**).

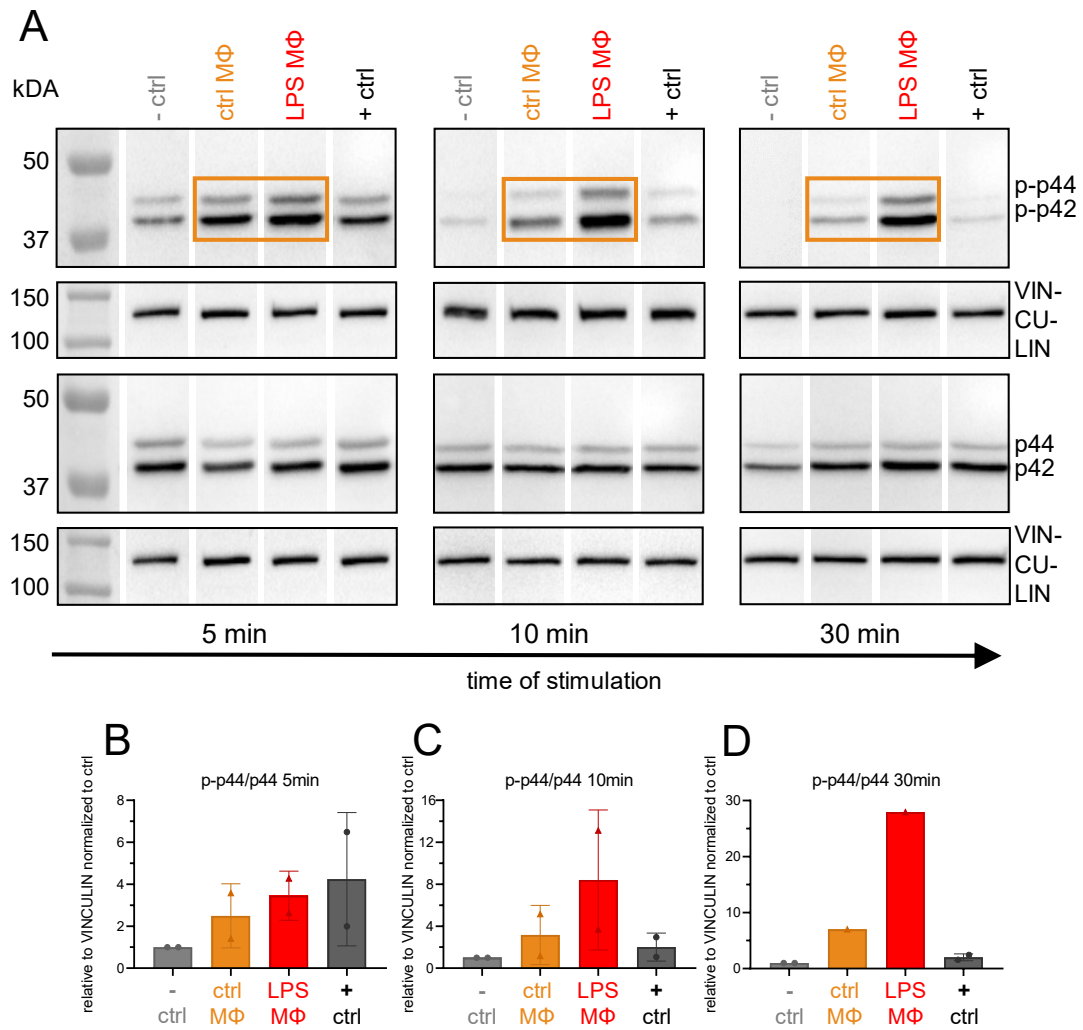


**Figure 3.4.4 p-p44/p42 Levels in SVEC4.10 Cells Treated by Macrophage Conditioned Medium.**

Protein levels were determined by immunoblotting and with anti-p-p44/p42, anti-p44/p42, and anti-VINCULIN antibodies. Experiments, including two biological duplicates each, were repeated two independent times. Quantification was done by normalizing each p-p44 and p44 band to the respective loading control (VINCULIN) of the same membrane before calculating the ratio of p-p44/p44 and normalizing these to the negative control of the respective time point. **(A)** representative samples of immunoblotting of SVEC4.10 total cell lysate with anti-phospho-p44/p42 antibody and anti-VINCULIN antibody after 5, 10, and 30 minutes of stimulation with pure medium (-ctrl), conditioned medium derived from 24-hour unstimulated RAW264.7 cells, conditioned medium from 24-hour LPS-stimulated RAW264.7 cells or 10% FCS-medium (+ ctrl). **(B)** Quantification of p44/p42 phosphorylation levels as shown in **Figure 3.4.4 A**, normalized to VINCULIN, total p44/p42 levels, and negative control of the 5-minute timepoint. **(C)** Quantification of p44/p42 phosphorylation levels as shown in **Figure 3.4.4 A**, normalized to VINCULIN, total p44/p42 levels, and negative control of the 10-minute timepoint. **(D)** Quantification of p44/p42 phosphorylation levels shown in **Figure 3.4.4 A**, normalized to VINCULIN, total p44/p42 levels and negative control of the 30-minute timepoint.

To further validate VEGFR-3 activation in SVEC4.10 cells by primary macrophage-derived VEGF-C, the conditioned medium of primary BMDMs was put on top of SVEC4.10 cells for 30 minutes (**Figure 3.4.5**). Total cell lysate of SVEC4.10 cells was immunoblotted with anti-p44/p42 phosphorylation antibody and anti-VINCULIN antibody (**Figure 3.4.6**).

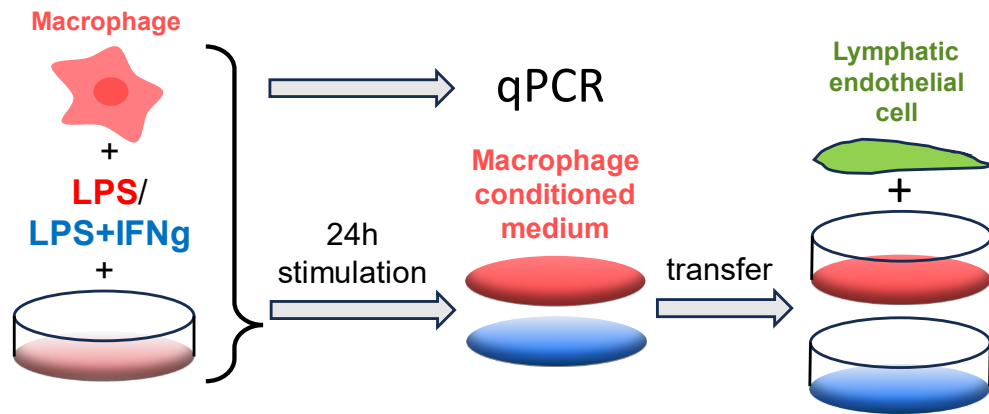


**Figure 3.4.5 Experimental Setup with LPS + IFN $\gamma$ -Stimulated Macrophage Conditioned Medium.**

Macrophages were cultured in a standard growth medium supplemented with LPS or LPS+ IFN $\gamma$ , respectively, for 24h. After 24h, the supernatant called conditioned medium, is removed, and applied on top of cultured SVEC4.10 cells for 5 – 10 minutes.

The conditioned medium of unstimulated BMDMs induced a low p44/p42 phosphorylation level. Medium of LPS-stimulated BMDMs resulted in an enormously increased band intensity of p-p44/p42. However, treatment with the medium of LPS + IFN $\gamma$  stimulated BMDMs displayed a visibly reduced level of p44/p42 phosphorylation compared to LPS-stimulated BMDMs (**Figure 3.4.6, Figure 3.4.7**).

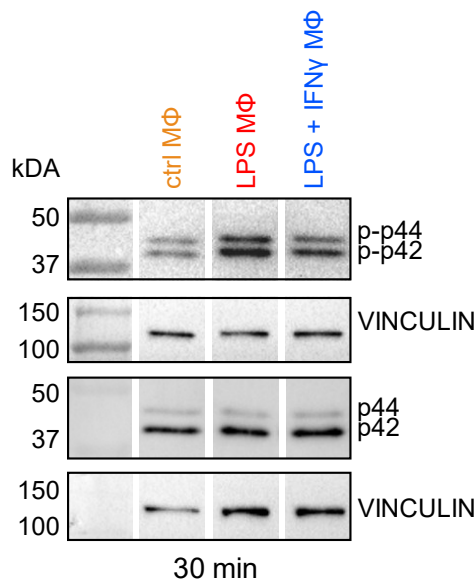


**Figure 3.4.6 SVEC4.10 Cells Treated with LPS/LPS +IFN $\gamma$ -Macrophage Conditioned Medium.**

Protein levels were determined by immunoblotting and with anti-p-p44/p42, anti-p44/p42 and anti-VINCULIN antibodies. Experiments, including two biological duplicates each, were repeated three independent times. Representative samples of immunoblotting SVEC4.10 total cell lysate with anti-phospho-p44/p42 antibody and anti- $\beta$ -ACTIN antibody following 30 minutes of stimulation with conditioned medium derived from BMDMs.

As shown in **Figure 3.4.5**, the *Vegf-c* expression of the medium-conditioning macrophages was determined by qPCR. Each datapoint of *Vegf-c* expression in BMDM cells displayed in **Figure 3.4.7 A** corresponds to one p-p44/p44 ratio measured in SVEC4.10 cells (**Figure 3.4.7 B**), treated with the respective conditioned medium.

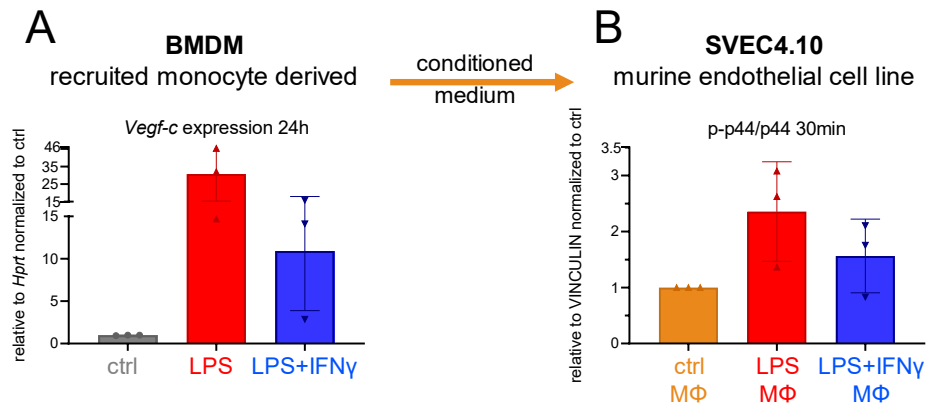


**Figure 3.4.7 Vegf-c Expression of BMDMs and Respective p-p44 Levels Induced in SVEC4.10 Cells.** mRNA levels were determined by qPCR, including technical duplicates, and normalized to *Hprt1* as well as to untreated controls. Experiments, including two biological duplicates and two technical duplicates each, were repeated 1-3 independent times (mean  $\pm$ SD). **(A)** Relative mRNA levels of *Vegf-c* in BMDMs differentiated with M-CSF and stimulated with 1 $\mu$ g/ml LPS or 1 $\mu$ g/ml LPS + 20ng/ml IFN $\gamma$  for 24 hours. **(B)** Quantification of three independent experiments, including the representative example from **Figure 3.4.6**. Quantification of band intensity was done by densitometry and normalizing each p-p44 as well as p44 band to the respective loading control (VINCULIN) of the same membrane before calculating the ratio of p-p44/p44 and normalizing these to the negative control of the respective time point.

In summary, levels of p44 phosphorylation (**Figure 3.4.6, Figure 3.4.7 B**), indicating VEGFR3 activation, were correlated to *Vegf-c* expression levels (**Figure 3.4.7 A**) of these BMDMs.

## 4. Discussion

### 4.1 *Vegf-c*, *Ccbe1* and *Adamts3* Expression is Upregulated In Pro-Inflammatory Macrophages and Monocytes

First, the macrophage cell line RAW264.7 (**Figure 3.1.1**, **Figure 3.1.2**, **Figure 3.1.3**), murine BMDMs (**Figure 3.1.6**), murine monocytes (**Figure 3.1.9**), as well as human blood-derived monocytes (**Figure 3.1.10**) were treated with either LPS, LPS + IFN $\gamma$ , IFN $\gamma$  or IL-4 to model the stimulatory environment after transplantation. In vivo, HMGB1 released during Ischemia-Reperfusion (Leventhal & Schroppe, 2012; Scaffidi et al., 2002) or LPS from post-transplant bacterial infection with *P. aeruginosa* (Botha et al., 2008), can bind to TLR4, which was shown to play a vital role in IRI and allograft rejection (Kastelijin et al., 2010; Merry et al., 2015; Shimamoto et al., 2006). Further, IFN $\gamma$  is associated with BOS development (Botha et al., 2008), and other post-transplantation conditions (Chang et al., 1991; Hodge et al., 2009; Hodge et al., 2012; Moudgil et al., 1999; Ross et al., 1999; Serrick et al., 1994). Since inflammation is a prevalent post-LTx phenomenon and macrophages were detected as potentially pro-lymphangiogenic cells, I hypothesized macrophages to express high levels of *Vegf-c* in pro-inflammatory conditions. In addition, I hypothesized *Ccbe1* and *Adamts3* to be expressed by the same cellular source. Experimentally, IL-4, was used as an anti-inflammatory stimulus compared to the pro-inflammatory conditions. My experiments have proven that macrophages and monocytes, whether from mice or humans, consistently express *Vegf-c* at both the mRNA and protein levels across all time intervals. These data align with previously published data on macrophages in inflammatory conditions expressing *Vegf-c* (Baluk et al., 2020; C. Cursiefen et al., 2004; Hwang et al., 2020; Hwang et al., 2019; Maruyama et al., 2005). More specifically, the pro-inflammatory stimulus LPS resulted in elevated *Vegf-c* expression compared to untreated controls. In support of this finding, CD11b+ VEGF-C+ cells in diaphragms of LPS-treated WT mice appeared in close proximity to lymphatic vessels, which were clearly reduced by macrophage depletion (Matsuda et al., 2021). Further confirming my data, 30 min of LPS treatment led to increased expression of VEGF-C in human blood-derived monocytes in vitro (Schoppmann et al., 2002). However, no specific research on spatial and temporal patterns of *Vegf-c* expression in human lung transplantation exists yet. As VEGF-C gets released in its unprocessed form, the expression of two common VEGF-C processing molecules, CCBE1 and ADAMTS3 (Janssen et al., 2016; Jeltsch et al., 2014), was accessed in murine macrophages and monocytes, too. Notably, *Ccbe1* expression, which was never seen in macrophages before, was visibly elevated by LPS stimulation.

Reduction of *Ccbe1* mRNA by LPS+ IFN $\gamma$ , compared to LPS treatment alone or IFN $\gamma$  treatment compared to untreated control, was discovered after six hours of treatment in RAW264.7 cells or BMDMs, respectively. Determining mRNA levels of *Adamts3*, formerly not known to be expressed by macrophages, brought up an apparent increase of expression in pro-inflammatory recruited monocyte-derived BMDMs compared to their untreated controls. These novel discoveries on *Ccbe1* and *Adamts3* emphasize the limited knowledge base in this field, indicating a clear need for further comprehensive research on their expression, regulation, and role in lung transplantation. All in all, pro-inflammatory macrophages and monocytes can be a rich source for all three lymphangiogenic factors.

## 4.2 LPS Upregulates *Vegf-c*, *Ccbe1* and *Adamts3* via the NF- $\kappa$ B Subunit p65

The LPS-induced increased expression of lymphangiogenic factors in macrophages and monocytes raises questions about the associated signaling pathways and transcription factors. As TLR4-signaling in myeloid cells is commonly known to be regulated via NF- $\kappa$ B signaling, I hypothesized this pathway to be involved in lymphangiogenesis. To address this, the online tool "cistrome data browser toolkit" (Zheng et al., 2019) was employed for predicting common transcription factors' regulatory potential for *Vegf-c* expression ("<http://dbtoolkit.cistrome.org/>"). Notably, high RP scores of p65 in macrophages suggested regulation of *Vegf-c*. This was supported by increased H3K4me3 peaks at the *Vegf-c* promoter region as well as increased p65 binding upon LPS stimulation in macrophages compared to controls in publicly available ChIPseq datasets. To validate this analysis, NF- $\kappa$ B signaling was chemically inhibited in RAW264.7 cells, BMDMs, murine BM-derived monocytes, and human blood-derived monocytes. Interestingly, specific inhibition of the canonical NF- $\kappa$ B pathway by p65 translocation was as efficient as inhibition of both the canonical and non-canonical NF- $\kappa$ B pathway in reducing the upregulation of *Vegf-c* expression by 6, 12, and 24-hour LPS stimulation of RAW264.7 cells and primary murine monocytes. Strongly reduced expression of *Vegf-c* upon specific inhibition of p65 translocation was further proven by qPCR in LPS-treated primary murine BMDMs and flow cytometry in primary human blood-derived monocytes.

In support of my findings, inhibition of both canonical and non-canonical NF- $\kappa$ B pathways in LPS-stimulated colorectal cancer cells leads to a decrease in *Vegf-c* protein compared to LPS alone (Zhu et al., 2016). In a study of mouse cornea, depleting corneal macrophages reduced IL-1 $\beta$ -induced lymphangiogenesis and *Vegf-c* mRNA by 50%. Blocking the translocation of NF- $\kappa$ B subunit p50, which can form a heterodimeric complex with p65, decreased *Vegf-c* expression and lymphangiogenesis in IL-1 $\beta$ -treated corneas (Watari et al., 2008). In one single in vitro experiment by Zhang et al., the knockdown of p65 in peritoneal exudate macrophages (PEM) significantly reduced an LPS-induced release of *Vegf-c* protein compared to LPS-stimulated WT PEMs (Y. Zhang et al., 2014). In summary, two studies affirm that p65 regulates *Vegf-c* expression. However, only one published in vitro experiment demonstrated the direct relationship between p65 and *Vegf-c* in macrophages. Therefore, the thorough exploration of p65 regulating *Vegf-c* in this thesis corroborates the data from Zhang et al. and further substantiates that knowledge by the detailed epigenetic, transcriptional, and translational analysis. Intriguingly, the same response to NF- $\kappa$ B inhibition in *Vegf-c* expression was observed for *Ccbe1* in my experiments. However, in contrast to the little existing knowledge about the regulation of *Vegf-c* expression, nothing is known about the regulation of *Ccbe1* expression so far. The experiments in this thesis thus extend the understanding of *Ccbe1* expression in the context of lymphangiogenesis. Astonishingly, my data revealed that even *Adamts3* is expressed by macrophages and monocytes, upregulated by LPS, and repressed by NF- $\kappa$ B inhibition in BMDMs and murine monocytes. Reviewing the existing body of literature, even less is known about *Adamts3* than *Ccbe1*. Herewith, the discovery of *Adamts3* expression in murine macrophages and monocytes and its regulation by LPS and p65 is a novel finding. Indeed, the same pathway of regulation for *Vegf-c*, *Ccbe1*, and *Adamts3* displays logical consistency as CCBE1 and ADAMTS3 are known to facilitate the proteolytic processing of VEGF-C (Jeltsch et al., 2014). Nonetheless, further research is needed to corroborate these findings of *Ccbe1* and *Adamts3* regulation in macrophages.

### 4.3 IFN $\gamma$ Induced Inhibition of *Vegf-C* and *Ccbe1* Expression Signals via a STAT1 Dependent Pathway

Certainly, apart from increased levels of *Vegf-c* upon LPS stimulation, the combined treatment with LPS as well as IFN $\gamma$  repeatedly led to a decline in the expression of *Vegf-c*, *Ccbe1*, and *Adamts3* compared to LPS alone in murine macrophages (**Figure 3.1.1**, **Figure 3.1.6**, **Figure 3.1.7**, **Figure 3.3.3**). Therefore, I hypothesized that the suppressive effect of IFN $\gamma$  after transplantation interferes with the enhancing effect of LPS binding to TLR4 via the TF STAT1. Hence, the question arises via which pathway or transcription factor the downregulating effect of IFN $\gamma$  takes place.

Using the cistrome data browser toolkit (Zheng et al., 2019) (see also "http://dbtoolkit.cistrome.org/"), STAT1 was identified as a transcription factor with a high potential to regulate *Vegf-c* expression (**Figure 3.3.1**). The homodimeric protein complex of STAT1 mediates signaling downstream of the IFN $\gamma$ R, which further induces the expression of *Irf1* (Lehtonen et al., 1997). Therefore, I explored the predicted regulatory potential of STAT1 on lymphangiogenic gene expression in vitro. Fludarabine, a selective inhibitor of STAT1 phosphorylation and depleting agent of Stat1 protein, was applied to RAW267.4 cells, BMDMs, as well as human blood-derived monocytes one hour prior to combined stimulation with LPS and IFN $\gamma$ . In comparison to stimulation with LPS and IFN $\gamma$ , blockage of STAT1 phosphorylation despite LPS + IFN $\gamma$  resulted in a clearly visible rise of *Vegf-c* protein in RAW264.7 cells (**Figure 3.3.2**) as well as *Vegf-c* and *Ccbe1* mRNA levels in BMDMs (**Figure 3.3.3**). Efficacy of the STAT1 phosphorylation inhibitor Fludarabine was proven by a reduction in gene expression of the direct downstream target of STAT1, *Irf1* in BMDMs (**Supplementary Figure A 3.3.3**). As levels of *Stat1* mRNA stayed relatively equal throughout all stimulations (**Supplementary Figure A 3.3.3**), this reflects that specifically phosphorylation of STAT1, but not mRNA levels are affected by Fludarabine treatment. Besides the clear rescue of *Vegf-c* expression in murine BMDMs, the same data were replicated in human blood-derived monocytes (**Figure 3.3.4**).

Reviewing the literature, most studies discuss the superinduction of genes by combined treatment with LPS + IFN $\gamma$  (Schroder et al., 2004; Schroder et al., 2006). Only a few studies explore the repression of LPS-induced genes by IFN $\gamma$  (Hoeksema et al., 2015; Kang et al., 2019). However, further investigating the interference of both TLR4 and IFN $\gamma$ R engagement might be vital in the setting of lung transplantation. It is well known that TLR4 plays an essential role in IRI and allograft rejection (Kastelijn et al., 2010; Merry et al., 2015; Shimamoto et al., 2006), while simultaneously IFN $\gamma$  levels are strongly increased post-IRI and allograft rejection, as proven by numerous studies (Chang et al., 1991; Hodge et al., 2009; Hodge et al., 2012; Moudgil et al., 1999; Ross et al., 1999; Serrick et al., 1994). Further, Cui et al. (Cui et al., 2015), as well as Baluk et al. (Baluk et al., 2020) have shown a need for additional VEGF-C to treat or prevent pathological mechanisms like rejection and fibrosis in mouse lungs, respectively. While my previous in vitro experiments delineate the positive regulation of lymphangiogenesis upon TLR4 engagement, my observations of STAT1-dependent downregulation of *Vegf-c* expression may explain the phenomenon of needed external VEGF-C. This suggests that the negative effect of IFN $\gamma$  on lymphangiogenic gene expression may outweigh the positive effect of LPS on lymphangiogenic gene expression. In line with my findings, previous work on lymph nodes of athymic mice presented increased *Vegf-c* mRNA and increased Lymphatic Vessel Density (LVD), which got significantly reduced by adoptive transfer of either T cells or IFN $\gamma$ . In the same study, LPS-induced inflammation massively increased LVD and *Vegf-c* mRNA. In contrast, Concanavalin-induced inflammation with a concurrent rise of IFN $\gamma$ + T cells neither displayed a

difference in LVD nor Vegf-c mRNA (Kataru et al., 2011). This strongly supports the mechanism of Vegf-c induction by LPS and repression by IFN $\gamma$  in an in vivo context.

While there is limited information regarding the connection between lymphangiogenesis and IFN $\gamma$ , there is scarcely any literature available concerning Stat1 and Vegf-c. In a study with CCR7 $^{++}$  expressing B16 melanoma, a significant reduction of Stat1 protein co-occurred with an increase of VEGF-C $^{+}$  CD45 $^{+}$  cells, increased *Ccl21* expression, as well as increased lymphangiogenesis in the tumor tissue (Takekoshi et al., 2012). This might potentially give a hint at the negative effects of STAT1-dependent signaling on *Vegf-c* expression. However, the discussed loose association of VEGF-C and STAT1 in melanoma cells should only be considered very cautiously and in light of a research gap concerning this mechanism. As mentioned before, only little research is done on the repression of LPS-induced genes by IFN $\gamma$ . Research done by Hoeksema et al. shows less p65 recruitment at enhancer or promoter sites of repressed genes due to IFN $\gamma$  induced epigenetic remodeling/silencing, which reduces chromatin accessibility. Further, in their experiments, priming with IFN $\gamma$  before LPS stimulation and the simultaneous presence of both ligands decreased the expression of LPS-induced genes. Also, they identified STAT1-binding motifs enriched in promoters of repressed genes (Hoeksema et al., 2015). Hoeksema et al.'s shown mechanism may perhaps also apply to lymphangiogenic genes like *Vegf-c* and *Ccbe1*. In another paper, Kang et al. identified a cluster of enhancers whose LPS-induced activation mark H3K27ac is blocked by IFN $\gamma$ . In addition, these enhancers exhibit enrichment of STAT1 binding motifs. However, it is mentioned that indirect mechanisms of gene repression (e.g., STAT1-induced expression of transcriptional or signaling inhibitors) are more likely (Kang et al., 2019). Therefore, both discussed mechanisms of Hoeksema and Kang remain a mere speculation for lymphangiogenic gene regulation and requires further research.

Contrary to my findings, in a recent study of corneal allograft rejection, blocking STAT1 activation by Tofacitinib significantly improved allograft survival alongside reduced M1 polarization, LVD, and Vegf-c mRNA in the graft. Additionally, in vitro application of Tofacitinib reduced RAW264.7 cell M1 polarization and Vegf-c mRNA levels (Yu et al., 2022). Even though, one might want to apply that result of improved corneal allograft survival to lung transplantation, it needs to be considered that VEGF-C had opposite effects on allograft survival in lung (Cui et al., 2015) and cornea (Claus Cursiefen et al., 2004).

In summary, the exact details of the STAT1-p65 intersection in lymphangiogenic gene regulation need further investigation following these first promising results adding to the knowledge base.

#### **4.4 Macrophage Derived VEGF-C Activates VEGFR-3 Signaling in Lymphatic Endothelial Cells**

Following the findings of increased lymphangiogenic expression upon LPS and abolition of the increase in combination with IFN $\gamma$ , I aimed to test the functional effects of macrophage VEGF-C on lymphatic endothelium in vitro. I hypothesized macrophage derived VEGF-C to activate lymphatic SVEC4.10 cells in this setting. Thus, the cell line SVEC4.10 was used. SVEC4.10 is a lymphatic endothelial cell line generated from a mouse lymph node in 1990 (O'Connell & Edidin, 1990). Wu and colleagues verified its lymphatic endothelial identity (Wu et al., 2014).

Cultivating and characterizing SVEC4.10 cells myself, the presence of PODOPLANIN, which is frequently used to characterize lymphatic endothelial cells (Broggi et al., 2014; Kang et al., 2009; Navarro et al., 2008; Pan & Yago, 2014; Pham et al., 2010; Watari et al., 2008; Xiong et

al., 2017), was confirmed by immunofluorescent cell staining in fixated SVEC4.10 cells as well as by flow cytometry of SVEC4.10 cells (**Figure 3.4.1**). Besides that, the presence of the receptor VEGFR-3, mainly present in lymphatic endothelial cells (Kaipainen et al., 1995) and substantial for VEGF-C signaling, was verified by flow cytometry (**Figure 3.4.1**). To validate the functionality of VEGFR-3 receptors on the surface of SVEC4.10 cells, immunoblotting of p44 and p42 phosphorylation, a standard method to measure activation of VEGF-C-VEGFR-3 signaling (Coso et al., 2011; Deng et al., 2015; Mäkinen et al., 2001) after rhVegf156s stimulation was carried out. Upon stimulation with rhVEGF-C156s, the phosphorylated levels of p44/p42 protein at the size of 44 and 42 kDa, respectively, increased visibly after 5 minutes, with a peak at 10 minutes before vanishing at 30 minutes (**Figure 3.4.2**). This is in line with previously published data of p44/p42 phosphorylation increasing between 10- and 60 minutes post-stimulation of LECs with either VEGF-C or rhVEGF-C156s (Coso et al., 2011; Deng et al., 2013; Deng et al., 2015; Mäkinen et al., 2001). Altogether, the presence of PDPN and VEGFR3 on the cell surface, as well as increasing p44/p42 phosphorylation by rhVEGF-C156s treatment, proving activation of the VEGFR-3 - VEGF-C signaling pathway, confirmed Lymphatic Endothelial Cell (LEC) identity of SVEC4.10 cells. Subsequently, supernatant of cultured RAW264.7 cells with or without LPS stimulation for 24 hours was saved as a conditioned medium and applied to SVEC4.10 cells for 5, 10, and 30 minutes before proceeding with protein isolation and immunoblotting p44/p42 phosphorylation levels. Since SVEC4.10 cells are derived from C3H/HeJ mice (O'Connell & Edidin, 1990), which have a genetic mutation in the TLR4 gene and thus a defective TLR4 receptor, SVEC4.10 cells are insensitive to LPS (Poltorak et al., 1998). This means any LPS left from the previous stimulation of RAW264.7 cells does not affect SVEC4.10 cells. To further rule out any TLR4-specific effect on SVEC4.10 cells, LPS was also included in the medium of the negative control. Compared to fresh medium alone, the conditioned medium of unstimulated RAW264.7 cells strongly induced p44/p42 phosphorylation in SVEC4.10 cells. The supernatant of LPS-treated RAW264.7 cells resulted in an even more substantial increase of p-p44/p-p42 levels. These data suggest that increased levels of functional VEGF-C, released by RAW264.7 cells, activated the VEGFR-3 signaling pathway in SVEC4.10 cells. In detail, the response to RAW264.7 derived VEGF-C by p-p44/p-p42 in SVEC4.10 cells remains at 30 minutes, whereas rhVEGF-C156s had induced a shorter and less intense p44/p42 phosphorylation. This difference in LEC activation is supported by literature, where rhVEGF-C156s stimulation in endothelial cells displayed a weaker and shortened signaling compared to VEGF-C (Coso et al., 2011; Mäkinen et al., 2001). My findings are in line with previous work done by Kang and colleagues. Their experiments involved intraperitoneal LPS injection in mice, resulting in increased LVD in the diaphragm. Removal of macrophages by clodronate liposomes abolished that lymphangiogenic effect. LPS injection in C3H/HeJ mice, which are defective in TLR4 signaling, did not change LVD at all (Kang et al., 2009). Another study found increased formation of tubule-like structures in Human Dermal LECs (HDLECs) upon stimulation with supernatant of LPS-treated colorectal cancer cells. Knockdown of *Vegf-c* or NF- $\kappa$ B inhibition in colorectal cancer cells abolished tubule formation of HDLECs (Zhu et al., 2016). Both publications underline the relevance of LPS-triggered VEGF-C release for lymphangiogenesis. In a nutshell, this study uncovered how *Vegf-c* expression is influenced by p65 and STAT1 in RAW264.7 cells. Released VEGF-C triggers p44/p42 phosphorylation downstream of the VEGFR-3 receptor in SVEC4.10 cells. Therefore, combining previous work with this study outlines the different mechanistic steps from stimulants to tissue remodeling by lymphangiogenesis.

Last, but not least, I intended to confirm the effect of macrophage-derived VEGF-C on LECs with primary cells (BMDMs) and extend the experiment by the conditioned medium of macrophages stimulated not only with LPS but also with LPS + IFN $\gamma$  (**Figure 3.4.6**). In this experi-

ment, the conditioned medium of LPS-stimulated BMDMs induced a high p44/p42 phosphorylation level in SVEC4.10 cells compared to the conditioned medium of unstimulated BMDMs. Additionally, the conditioned medium of BMDMs stimulated by LPS and IFN $\gamma$  simultaneously resulted in less p44/p42 phosphorylation than the conditioned medium of LPS-stimulated BMDMs. Notably, the gene expression of the corresponding BMDM cells of the used conditioned medium was previously measured by qPCR. Conditioned medium of BMDMs with increased *Vegf-c* expression induced more p44 phosphorylation in SVEC4.10 cells. The same pattern was observed by applying the conditioned medium of LPS + IFN $\gamma$  stimulated BMDMs, which had a dampened increase of *Vegf-c* expression compared to LPS alone on SVEC4.10 cells. Decreased *Vegf-c* mRNA in LPS + IFN $\gamma$  BMDM macrophages was associated with decreased p-p44 in the corresponding SVEC4.10 sample compared to the conditioned medium of LPS-stimulated BMDMs (**Figure 3.4.7**). Nevertheless, this experiment did not account for a potential direct impact of IFN $\gamma$  on p-p44/p-p42 in SVEC4.10 cells. On the other hand, it is still suggested that IFN $\gamma$  has a negative effect on lymphangiogenesis, as the negative impact of IFN $\gamma$  on lymphangiogenesis was observed by other researchers in the past (Kataru et al., 2011) and discussed in the previous chapter, too. Controversially to my findings with macrophages, the Conditioned Medium of Decidual Natural Killer Cells (dNK-CM) increased *Vegf-c* expression in Cytotrophoblasts (CT) by an IFN $\gamma$ -STAT1 dependent mechanism. This was demonstrated by both IFN $\gamma$ R blocking antibodies and isolated IFN $\gamma$  stimulation in CTs and the extravillous CT cell line mHTR8/SVneo. Moreover, dNK-CM and IFN $\gamma$  increased STAT1 Tyr701/Ser727 phosphorylation in HTR8/SVneo cells, and Stat1 siRNA resulted in reduced VEGF-C secretion compared to the control (Eastabrook et al., 2012). Similarly, human retinal pigment cells respond with increased VEGF-C secretion upon IFN $\gamma$  treatment (Kommineni et al., 2007). Whereas these two publications indicate a positive effect of IFN $\gamma$ -STAT1 signaling on VEGF-C release, IFN $\gamma$  treatment of the cancer cell line Hep-2 reduced *Vegf-c* mRNA and protein levels below baseline control levels (Chen et al., 2008). The difference in these studies underlines that regulation of *Vegf-c* expression by IFN $\gamma$  is specific to different cell types and must be interpreted carefully for different systems and medical conditions. In this study, negative regulation of *Vegf-c* expression by a STAT1-dependent pathway in macrophages and monocytes is an unknown finding that extends previous knowledge.

## 5. Conclusions, Limitations, and Future Directions

Studies involving the relationship between macrophage-derived VEGF-C and lymphangiogenesis are rare, and the given evidence mainly comprises unspecific measurements, as most experiments are done *in vivo*. Thus, this project meticulously studied the role of p65 and STAT1 in macrophage Vegf-c regulation and its effects on LECs for the first time *in vitro*.

All in all, this study has proven upregulation of Vegf-c, Ccbe1 as well as Adamts3 mRNA by TLR4 engagement in a p65-dependent manner in a macrophage cell line, as well as in primary murine macrophages and primary murine monocytes. VEGF-C protein was upregulated by LPS treatment in a macrophage cell line and human monocytes, and the regulatory effect of p65 on Vegf-c protein was also validated in primary human monocytes. Besides positive regulation of all three lymphangiogenic factors, negative regulation through a STAT1-dependent IFN $\gamma$ -signaling pathway was investigated by predicted regulatory potential scores and inhibition of STAT1 phosphorylation in *in vitro* experiments. IFN $\gamma$  stimulation reduced mRNA of Vegf-c and Ccbe1 in a macrophage cell line, primary mouse macrophages, and Vegf-C protein in primary human monocytes, and blockage of pSTAT1 rescued Vegf-c and Ccbe1 mRNA in primary mouse macrophages and rescued Vegf-c protein in a mouse macrophage cell line and human monocytes. Conditioned medium of cell line and primary murine macrophages repeatedly elevated p44/p42 phosphorylation downstream of the VEGFR-3 receptor of a tested endothelial cell line of lymphatic identity by released and functionally cleaved VEGF-C protein of cell line and primary murine macrophages. Notably, the observed p44/p42 phosphorylation in lymphatic endothelial cells mirrored macrophage Vegf-c mRNA, which IFN $\gamma$  reduces in a STAT1-dependent manner.

These novel discoveries on Vegf-c, Ccbe1, and Adamts3 emphasize the limited knowledge base in this field, indicating a clear need for further comprehensive research on their expression, regulation, and role in lung transplantation. All in all, pro-inflammatory macrophages and monocytes can be a rich source for all three lymphangiogenic factors regulated by an interplay of p65 and STAT1-dependent pathways. In summary, the current study solidifies previous work done in different *in vivo* studies of lymphatic research, extends the scarce knowledge base in the regulation of Vegf-c, Ccbe1, and Adamts3 expression in macrophages under the stimulatory environment of lung transplantation, and provides a prospect for future lymphatic research in lung transplantation.

Nonetheless, as a universal pattern in research, this study has its apparent limitations. Immunopathological mechanisms of post-transplant complications are very complex and, thus, still not fully understood. Especially in the field of lymphatic research and spatial and temporal patterns of Vegf-c expression, very little to nothing is known. Besides that, nothing is known about the proteolytic processing of VEGF-C by ADAMTS3 and CCBE1 in murine and human lungs, especially in lung transplantation. Therefore, analysis of Vegf-c, Ccbe1, and Adamts3 expression post-transplantation in murine and human lung tissue would be a valuable extension of knowledge. For example, analysis of RNAseq data of human lung tissue of stable versus acute and chronically rejected lung transplants could immensely enhance the knowledge base. Besides that, the inhibition and stimulation of VEGFR-3 signaling in LTx must be evaluated to determine the timing and a detailed risk-benefit analysis of lymphatic growth in lung allografts.

Further, mimicry of lung transplantation settings in an *in-vitro* system is challenging, and our model with LPS and IFN $\gamma$  displays a very distinct simplification to study isolated signaling pathways. Ideally, creating an immortal specific lymphatic cell line from human or murine lung lymphatics instead of lymph node-derived cells like SVEC4.10 would be a huge asset for future *in-*

vitro research. In addition, in this project, the release of VEGF-C could not be measured due to technical challenges. However, it should be included in future experiments, as well as CCBE1 and ADAMTS3, for which working antibodies and ELISA conditions did not exist. Also, appropriate controls for excluding direct inhibitory effects of fludarabine on p-p44/p42 in SVEC4.10 cells were missing. In a perfect setting, VEGFR3 blockage or measurements of VEGFR3 autophosphorylation would be included in experiments of macrophage-conditioned medium, too.

Regarding the limited literature on this thesis topic, comparison with current knowledge partially had to be based on research, which is not closely related to my results. Therefore, some comparisons to different disease models, organs, or cell types might potentially be far-fetched in a few cases. However, with a constantly growing field of lymphatic research, this should improve in the future.

For future research, a plethora of experiments could be envisioned and discussed. For example, since lymphatic endothelium collects immune cells from tissue and transports them towards draining lymph nodes, trans-lymphatic endothelial migration (Xiong et al., 2017) of immune cells and their involved cytokines would be exciting to further explore in the context of the alloimmune response. Finally, the knowledge gained from this project should be confirmed and applied in an in-vivo mouse lung transplantation model by using Food and Drug Administration (FDA)-approved STAT1 inhibitory drugs or specific knockouts of IFN $\gamma$  with subsequent analysis of allograft health. However, it needs to be evaluated and discussed whether and how STAT1 depletion directly affects LECs, how to specifically target lung macrophages only, and in which timeframe Vegf-c expression should be modulated. Interestingly, one study has shown that Ischemia-Reperfusion, or IFN $\gamma$ , increases STAT1 phosphorylation and thus leads to subsequent apoptosis (Stephanou et al., 2000). In a follow-up publication, Stephanou and Latchman therefore discussed STAT-1 inhibition as a potential therapeutic target for IRI-related cell death (Stephanou & Latchman, 2003). Further, a study performed on rat lung transplantation observed beneficial effects of treatment with JAK inhibitors six days after transplantation (Higuchi et al., 2005). Recently, Beeckmans et al. applied RNA sequencing and gene set variation analysis of the JAK/STAT Kyoto Encyclopedia of Genes and Genomes (KEGG) gene list, which revealed increased expression of JAK/STAT pathway genes in CLAD lungs compared to unused human donor lungs. Further, they discussed that JAK/STAT signaling might play a key role in the chronic inflammation and fibrosis process in CLAD, which suggests that JAK inhibitors could have therapeutic potential in treating and possibly preventing CLAD (Beeckmans et al., 2022). Few datasets exist from usage of the JAK-inhibitor Ruxolitinib, a drug approved for steroid-refractory Graft Versus Host Disease (GVHD), in patients with steroid-resistant BOS, which can also develop after Hematopoietic Stem Cell Transplantation (HSCT) (Meng et al., 2021; Schoettler et al., 2019; Streiler et al., 2020; Uygun et al., 2020). Excitingly, Fludarabine, the pSTAT1-inhibitory drug used in this project, was reported to be used in four pediatric cases of steroid-refractory, nonspecific inflammatory lung injury after HSCT. In three of these four patients, a positive response could be recorded. In addition, another patient with BO post LTx benefited from Fludarabine treatment (Raphael et al., 2013).

Altogether, my findings, in combination with published data, raise the question of the possible use of pSTAT1 inhibitors in a clinical setting of lung transplantation. If the temporal and spatial pattern of pro-lymphangiogenic gene expression and its function are figured out, cell-specific targeting of the involved signaling could be explored with an increasing pool of available biomedical techniques like liposome mRNA delivery.

## References

- Abraham, E., Arcaroli, J., Carmody, A., Wang, H., & Tracey, K. J. (2000). Cutting edge: HMG-1 as a mediator of acute lung inflammation. *The Journal of Immunology*, *165*(6), 2950-2954. <https://doi.org/10.4049/jimmunol.165.6.2950>
- Achen, M. G., Jeltsch, M., Kukk, E., Mäkinen, T., Vitali, A., Wilks, A. F., Alitalo, K., & Stacker, S. A. (1998). Vascular endothelial growth factor D (VEGF-D) is a ligand for the tyrosine kinases VEGF receptor 2 (Flk1) and VEGF receptor 3 (Flt4). *Proc Natl Acad Sci*, *95*(2), 548-553. <https://doi.org/10.1073/pnas.95.2.548>
- Alders, M., Hogan, B. M., Gjini, E., Salehi, F., Al-Gazali, L., Hennekam, E. A., Holmberg, E. E., Mannens, M. M., Mulder, M. F., & Offerhaus, G. J. A. (2009). Mutations in CCBE1 cause generalized lymph vessel dysplasia in humans. *Nature genetics*, *41*(12), 1272-1274. <https://doi.org/10.1038/ng.484>
- Alitalo, K. (2011). The lymphatic vasculature in disease. *Nat Med*, *17*(11), 1371-1380. <https://doi.org/10.1038/nm.2545>
- Andrade, C. F., Kaneda, H., Der, S., Tsang, M., Lodyga, M., Dos Santos, C. C., Keshavjee, S., & Liu, M. (2006). Toll-like receptor and cytokine gene expression in the early phase of human lung transplantation. *J Heart Lung Transplant*, *25*(11), 1317-1323. <https://doi.org/10.1016/j.healun.2006.09.017>
- Arjuna, A., Olson, M. T., Walia, R., Bremner, R. M., Smith, M. A., & Mohanakumar, T. (2021). An update on current treatment strategies for managing bronchiolitis obliterans syndrome after lung transplantation. *Expert Rev Respir Med*, *15*(3), 339-350. <https://doi.org/10.1080/17476348.2021.1835475>
- Arslan, F., Keogh, B., McGuirk, P., & Parker, A. (2010). TLR2 and TLR4 in ischemia reperfusion injury. *Mediators Inflamm.*, *2010*(1), 704202. <https://doi.org/10.1155/2010/704202>
- Baluk, P., Naikawadi, R. P., Kim, S., Rodriguez, F., Choi, D., Hong, Y. K., Wolters, P. J., & McDonald, D. M. (2020). Lymphatic Proliferation Ameliorates Pulmonary Fibrosis after Lung Injury. *Am J Pathol*, *190*(12), 2355-2375. <https://doi.org/10.1016/j.ajpath.2020.08.018>
- Baluk, P., Tammela, T., Ator, E., Lyubynska, N., Achen, M. G., Hicklin, D. J., Jeltsch, M., Petrova, T. V., Pytowski, B., Stacker, S. A., Yla-Herttuala, S., Jackson, D. G., Alitalo, K., & McDonald, D. M. (2005). Pathogenesis of persistent lymphatic vessel hyperplasia in chronic airway inflammation. *J Clin Invest*, *115*(2), 247-257. <https://doi.org/10.1172/JCI22037>
- Bando, K., Paradis, I. L., Komatsu, K., Konishi, H., Matsushima, M., Keenan, R. J., Hardesty, R. L., Armitage, J. M., & Griffith, B. P. (1995). Analysis of time-dependent risks for infection, rejection, and death after pulmonary transplantation. *The Journal of Thoracic and Cardiovascular Surgery*, *109*(1), 49-59. [https://doi.org/10.1016/s0022-5223\(95\)70419-1](https://doi.org/10.1016/s0022-5223(95)70419-1)
- Barker, A. F., Bergeron, A., Rom, W. N., & Hertz, M. I. (2014). Obliterative bronchiolitis. *N Engl J Med*, *370*(19), 1820-1828. <https://doi.org/10.1056/NEJMra1204664>
- Beeckmans, H., McDonough, J. E., De Sadeleer, L., Sacreas, A., Vanstapel, A., Kaes, J., Van Herck, A., Maes, K., Gayan-Ramirez, G., Janssens, W., Schoemans, H., Wauters, E., Neyrinck, A. P., Verleden, G. M., Dupont, L. J., Laurent, G., Ceulemans, L. J., Van Raemdonck, D. E., Vanaudenaerde, B. M., & Vos, R. (2022, 04 September 2022). *JAK-STAT pathway is upregulated in CLAD 08.02 - Transplantation*, Barcelona.
- Bergantini, L., d'Alessandro, M., De Vita, E., Perillo, F., Fossi, A., Luzzi, L., Paladini, P., Perrone, A., Rottoli, P., Sestini, P., Bargagli, E., & Bennett, D. (2021). Regulatory and Effector Cell Disequilibrium in Patients with Acute Cellular Rejection and Chronic Lung Allograft Dysfunction after Lung Transplantation: Comparison of Peripheral and Alveolar Distribution. *Cells*, *10*(4). <https://doi.org/10.3390/cells10040780>
- Bharat, A., Kuo, E., Steward, N., Aloush, A., Hachem, R., Trulock, E. P., Patterson, G. A., Meyers, B. F., & Mohanakumar, T. (2008). Immunological link between primary graft dysfunction and chronic lung allograft rejection. *The Annals of Thoracic Surgery*, *86*(1), 189-197. <https://doi.org/10.1016/j.athoracsur.2008.03.073>
- Bhat, M. Y., Solanki, H. S., Advani, J., Khan, A. A., Keshava Prasad, T., Gowda, H., Thiyagarajan, S., & Chatterjee, A. (2018). Comprehensive network map of interferon gamma signaling. *Journal of cell communication and signaling*, *12*, 745-751. <https://doi.org/10.1007/s12079-018-0486-y>
- Bittmann, I., Dose, T., Baretton, G. B., Müller, C., Schwaiblmair, M., Kur, F., & Löhrs, U. (2001). Cellular chimerism of the lung after transplantation: an interphase cytogenetic study. *Am J Clin Pathol*, *115*(4), 525-533. <https://doi.org/10.1309/gafn-5mpa-ly8e-dtpq>

- Blouin, C. M., Hamon, Y., Gonnord, P., Boularan, C., Kagan, J., de Leseqno, C. V., Ruez, R., Maiffert, S., Bertaux, N., & Loew, D. (2016). Glycosylation-dependent IFN- $\gamma$ R partitioning in lipid and actin nanodomains is critical for JAK activation. *Cell*, 166(4), 920-934. <https://doi.org/10.1016/j.cell.2016.07.003>
- Boehler, A., Kesten, S., Weder, W., & Speich, R. (1998). Bronchiolitis obliterans after lung transplantation: a review. *Chest*, 114(5), 1411-1426. <https://doi.org/10.1378/chest.114.5.1411>
- Botha, P., Archer, L., Anderson, R. L., Lordan, J., Dark, J. H., Corris, P. A., Gould, K., & Fisher, A. J. (2008). Pseudomonas aeruginosa colonization of the allograft after lung transplantation and the risk of bronchiolitis obliterans syndrome. *Transplantation*, 85(5), 771-774. <https://doi.org/10.1097/tp.0b013e31816651de>
- Broggi, M. A., Schmalzer, M., Lagarde, N., & Rossi, S. W. (2014). Isolation of murine lymph node stromal cells. *J Vis Exp*(90), e51803. <https://doi.org/10.3791/51803>
- Bui, H. M., Enis, D., Robciuc, M. R., Nurmi, H. J., Cohen, J., Chen, M., Yang, Y., Dhillon, V., Johnson, K., Zhang, H., Kirkpatrick, R., Traxler, E., Anisimov, A., Alitalo, K., & Kahn, M. L. (2016). Proteolytic activation defines distinct lymphangiogenic mechanisms for VEGFC and VEGFD. *J Clin Invest*, 126(6), 2167-2180. <https://doi.org/10.1172/JCI83967>
- Burton, C. M., Iversen, M., Carlsen, J., Mortensen, J., Andersen, C. B., Steinbrüchel, D., & Scheike, T. (2009). Acute cellular rejection is a risk factor for bronchiolitis obliterans syndrome independent of post-transplant baseline FEV1. *The Journal of Heart and Lung Transplantation*, 28(9), 888-893. <https://doi.org/10.1016/j.healun.2009.04.022>
- Byrne, A. J., Powell, J. E., O'Sullivan, B. J., Ogger, P. P., Hoffland, A., Cook, J., Bonner, K. L., Hewitt, R. J., Wolf, S., Ghai, P., Walker, S. A., Lukowski, S. W., Molyneaux, P. L., Saglani, S., Chambers, D. C., Maher, T. M., & Lloyd, C. M. (2020). Dynamics of human monocytes and airway macrophages during healthy aging and after transplant. *J Exp Med*, 217(3). <https://doi.org/10.1084/jem.20191236>
- Byrne, D., Nador, R. G., English, J. C., Yee, J., Levy, R., Bergeron, C., Swiston, J. R., Mets, O. M., Muller, N. L., & Bilawich, A.-M. (2021). Chronic lung allograft dysfunction: review of CT and pathologic findings. *Radiology: Cardiothoracic Imaging*, 3(1), e200314. <https://doi.org/10.1148/ryct.2021200314>
- Chambers, D. C., Cherikh, W. S., Harhay, M. O., Hayes, D., Jr., Hsich, E., Khush, K. K., Meiser, B., Potena, L., Rossano, J. W., Toll, A. E., Singh, T. P., Sadavarte, A., Zuckermann, A., Stehlik, J., International Society for, H., & Lung, T. (2019). The International Thoracic Organ Transplant Registry of the International Society for Heart and Lung Transplantation: Thirty-sixth adult lung and heart-lung transplantation Report-2019; Focus theme: Donor and recipient size match. *J Heart Lung Transplant*, 38(10), 1042-1055. <https://doi.org/10.1016/j.healun.2019.08.001>
- Chambers, D. C., Yusef, R. D., Cherikh, W. S., Goldfarb, S. B., Kucheryavaya, A. Y., Khusch, K., Levvey, B. J., Lund, L. H., Meiser, B., Rossano, J. W., Stehlik, J., International Society for, H., & Lung, T. (2017). The Registry of the International Society for Heart and Lung Transplantation: Thirty-fourth Adult Lung And Heart-Lung Transplantation Report-2017; Focus Theme: Allograft ischemic time. *J Heart Lung Transplant*, 36(10), 1047-1059. <https://doi.org/10.1016/j.healun.2017.07.016>
- Chang, S.-C., Hsu, H.-K., Perng, R.-P., Shiao, G.-M., & Lin, C.-Y. (1991). Significance of biochemical markers in early detection of canine lung allograft rejection. *Transplantation*, 51(3), 579-584. <https://doi.org/10.1097/00007890-199103000-00007>
- Chappier, A., Boisson-Dupuis, S., Jouanguy, E., Vogt, G., Feinberg, J., Prochnicka-Chalouf, A., Casrouge, A., Yang, K., Soudais, C., & Fieschi, C. (2006). Novel STAT1 alleles in otherwise healthy patients with mycobacterial disease. *PLoS genetics*, 2(8), e131. <https://doi.org/10.1371/journal.pgen.0020131>
- Chatterjee, S., Nieman, G. F., Christie, J. D., & Fisher, A. B. (2014). Shear stress-related mechanosignaling with lung ischemia: lessons from basic research can inform lung transplantation. *Am J Physiol Lung Cell Mol Physiol*, 307(9), L668-680. <https://doi.org/10.1152/ajplung.00198.2014>
- Chen, G. Y., & Nunez, G. (2010). Sterile inflammation: sensing and reacting to damage. *Nat Rev Immunol*, 10(12), 826-837. <https://doi.org/10.1038/nri2873>
- Chen, J., Zhou, J., & Wang, J. (2008). Effect of interferon-gamma on the expression of vascular endothelial growth factor C on Hep-2 laryngeal carcinoma cell lines. *Lin Chuang er bi yan hou tou jing wai ke za zhi= Journal of Clinical Otorhinolaryngology, Head, and Neck Surgery*, 22(3), 108-111.

- Chen, Y., Wermeling, F., Sundqvist, J., Jonsson, A. B., Tryggvason, K., Pikkarainen, T., & Karlsson, M. C. (2010). A regulatory role for macrophage class A scavenger receptors in TLR4-mediated LPS responses. *Eur J Immunol*, 40(5), 1451-1460. <https://doi.org/10.1002/eji.200939891>
- Chung, P. A., & Dilling, D. F. (2020). Immunosuppressive strategies in lung transplantation. *Annals of Translational Medicine*, 8(6). <https://doi.org/doi.org/10.21037/atm.2019.12.117>
- Coso, S., Zeng, Y., Sooraj, D., & Williams, E. D. (2011). Conserved signaling through vascular endothelial growth (VEGF) receptor family members in murine lymphatic endothelial cells. *Exp Cell Res*, 317(17), 2397-2407. <https://doi.org/10.1016/j.yexcr.2011.07.023>
- Cui, Y., Liu, K., Monzon-Medina, M. E., Padera, R. F., Wang, H., George, G., Toprak, D., Abdelnour, E., D'Agostino, E., Goldberg, H. J., Perrella, M. A., Forteza, R. M., Rosas, I. O., Visner, G., & El-Chemaly, S. (2015). Therapeutic lymphangiogenesis ameliorates established acute lung allograft rejection. *J Clin Invest*, 125(11), 4255-4268. <https://doi.org/10.1172/JCI79693>
- Cursiefen, C., Cao, J., Chen, L., Liu, Y., Maruyama, K., Jackson, D., Kruse, F. E., Wiegand, S. J., Dana, M. R., & Streilein, J. W. (2004). Inhibition of hemangiogenesis and lymphangiogenesis after normal-risk corneal transplantation by neutralizing VEGF promotes graft survival. *Invest Ophthalmol Vis Sci*, 45(8), 2666-2673. <https://doi.org/10.1167/iovs.03-1380>
- Cursiefen, C., Chen, L., Borges, L. P., Jackson, D., Cao, J., Radziejewski, C., D'Amore, P. A., Dana, M. R., Wiegand, S. J., & Streilein, J. W. (2004). VEGF-A stimulates lymphangiogenesis and hemangiogenesis in inflammatory neovascularization via macrophage recruitment. *J Clin Invest*, 113(7), 1040-1050. <https://doi.org/10.1172/JCI20465>
- D'Alessio, S., Correale, C., Tacconi, C., Gandelli, A., Pietrogrande, G., Vetrano, S., Genua, M., Arena, V., Spinelli, A., Peyrin-Biroulet, L., Fiocchi, C., & Danese, S. (2014). VEGF-C-dependent stimulation of lymphatic function ameliorates experimental inflammatory bowel disease. *J Clin Invest*, 124(9), 3863-3878. <https://doi.org/10.1172/JCI72189>
- Dashkevich, A., Raissadati, A., Syrjala, S. O., Zarkada, G., Keranen, M. A., Tuuminen, R., Krebs, R., Anisimov, A., Jeltsch, M., Leppanen, V. M., Alitalo, K., Nykanen, A. I., & Lemstrom, K. B. (2016). Ischemia-Reperfusion Injury Enhances Lymphatic Endothelial VEGFR3 and Rejection in Cardiac Allografts. *Am J Transplant*, 16(4), 1160-1172. <https://doi.org/10.1111/ajt.13564>
- de Perrot, M., Liu, M., Waddell, T. K., & Keshavjee, S. (2003). Ischemia-reperfusion-induced lung injury. *American journal of respiratory and critical care medicine*, 167(4), 490-511. <https://doi.org/10.1164/rccm.200207-670so>
- Decker, T., Kovarik, P., & Meinke, A. (1997). GAS elements: a few nucleotides with a major impact on cytokine-induced gene expression. *J Interferon Cytokine Res*, 17(3), 121-134. <https://doi.org/10.1089/jir.1997.17.121>
- den Hengst, W. A., Gielis, J. F., Lin, J. Y., Van Schil, P. E., De Windt, L. J., & Moens, A. L. (2010). Lung ischemia-reperfusion injury: a molecular and clinical view on a complex pathophysiological process. *Am J Physiol Heart Circ Physiol*, 299(5), H1283-1299. <https://doi.org/10.1152/ajpheart.00251.2010>
- Deng, Y., Atri, D., Eichmann, A., & Simons, M. (2013). Endothelial ERK signaling controls lymphatic fate specification. *J Clin Invest*, 123(3), 1202-1215. <https://doi.org/10.1172/JCI63034>
- Deng, Y., Zhang, X., & Simons, M. (2015). Molecular controls of lymphatic VEGFR3 signaling. *Arterioscler Thromb Vasc Biol*, 35(2), 421-429. <https://doi.org/10.1161/ATVBAHA.114.304881>
- Dupont, L., Joannes, L., Morfisse, F., Blacher, S., Monseur, C., Deroanne, C. F., Noël, A., & Colige, A. C. (2022). ADAMTS2 and ADAMTS14 can substitute for ADAMTS3 in adults for pro-VEGF-C activation and lymphatic homeostasis. *JCI Insight*, 7(8). <https://doi.org/10.1172/jci.insight.151509>
- Eastbrook, G. D., Hu, Y., Tan, R., Dutz, J. P., Maccalman, C. D., & von Dadelszen, P. (2012). Decidual NK cell-derived conditioned medium (dNK-CM) mediates VEGF-C secretion in extravillous cytotrophoblasts. *Am J Reprod Immunol*, 67(2), 101-111. <https://doi.org/10.1111/j.1600-0897.2011.01075.x>
- Epelman, S., Lavine, K. J., & Randolph, G. J. (2014). Origin and functions of tissue macrophages. *Immunity*, 41(1), 21-35. <https://doi.org/10.1016/j.immuni.2014.06.013>
- Estenne, M., & Hertz, M. I. (2002). Bronchiolitis obliterans after human lung transplantation. *Am J Respir Crit Care Med*, 166(4), 440-444. <https://doi.org/10.1164/rccm.200201-003pp>

- Fernandes, R. J., Hirohata, S., Engle, J. M., Colige, A., Cohn, D. H., Eyre, D. R., & Apte, S. S. (2001). Procollagen II amino propeptide processing by ADAMTS-3. Insights on dermatosparaxis. *J Biol Chem*, 276(34), 31502-31509. <https://doi.org/10.1074/jbc.M103466200>
- Ferrari, R. S., & Andrade, C. F. (2015). Oxidative Stress and Lung Ischemia-Reperfusion Injury. *Oxid Med Cell Longev*, 2015, 590987. <https://doi.org/10.1155/2015/590987>
- Fiser, S. M., Tribble, C. G., Long, S. M., Kaza, A. K., Kern, J. A., Jones, D. R., Robbins, M. K., & Kron, I. L. (2002). Ischemia-reperfusion injury after lung transplantation increases risk of late bronchiolitis obliterans syndrome. *The Annals of Thoracic Surgery*, 73(4), 1041-1048. [https://doi.org/10.1016/s0003-4975\(01\)03606-2](https://doi.org/10.1016/s0003-4975(01)03606-2)
- Gaudino, S. J., & Kumar, P. (2019). Cross-talk between antigen presenting cells and T cells impacts intestinal homeostasis, bacterial infections, and tumorigenesis. *Frontiers in Immunology*, 10, 360. <https://doi.org/10.3389/fimmu.2019.00360>
- Geissmann, F., Manz, M. G., Jung, S., Sieweke, M. H., Merad, M., & Ley, K. (2010). Development of monocytes, macrophages, and dendritic cells. *Science*, 327(5966), 656-661. <https://doi.org/10.1126/science.1178331>
- Gelman, A. E., Li, W., Richardson, S. B., Zinselmeyer, B. H., Lai, J., Okazaki, M., Kornfeld, C. G., Kreisel, F. H., Sugimoto, S., Tietjens, J. R., Dempster, J., Patterson, G. A., Krupnick, A. S., Miller, M. J., & Kreisel, D. (2009). Cutting edge: Acute lung allograft rejection is independent of secondary lymphoid organs. *J Immunol*, 182(7), 3969-3973. <https://doi.org/10.4049/jimmunol.0803514>
- Gelman, A. E., Okazaki, M., Sugimoto, S., Li, W., Kornfeld, C. G., Lai, J., Richardson, S. B., Kreisel, F. H., Huang, H. J., Tietjens, J. R., Zinselmeyer, B. H., Patterson, G. A., Miller, M. J., Krupnick, A. S., & Kreisel, D. (2010). CCR2 regulates monocyte recruitment as well as CD4 T1 allorecognition after lung transplantation. *Am J Transplant*, 10(5), 1189-1199. <https://doi.org/10.1111/j.1600-6143.2010.03101.x>
- Global Observatory on Donation and Transplantation*. World Health Organization and Organización Nacional de Trasplantes. Retrieved 10.11.2023 from <http://www.transplant-observatory.org/summary/>
- Hamilton, J. A. (2002). GM-CSF in inflammation and autoimmunity. *Trends in Immunology*, 23(8), 403-408. [https://doi.org/10.1016/s1471-4906\(02\)02260-3](https://doi.org/10.1016/s1471-4906(02)02260-3)
- Hamrah, P., Chen, L., Zhang, Q., & Dana, M. R. (2003). Novel Expression of Vascular Endothelial Growth Factor Receptor (VEGFR)-3 and VEGF-C on Corneal Dendritic Cells. *The American Journal of Pathology*, 163(1), 57-68. [https://doi.org/10.1016/s0002-9440\(10\)63630-9](https://doi.org/10.1016/s0002-9440(10)63630-9)
- Hanley, M. E., & Welsh, C. H. (2003). *CURRENT Diagnosis & Treatment in Pulmonary Medicine*. McGraw-Hill Companies, Incorporated. <https://books.google.de/books?id=ObTWEMrPehEC>
- Hasenauer, A., Bedat, B., Parapanov, R., Lugin, J., Debonneville, A., Abdelnour-Berchtold, E., Gonzalez, M., Perentes, J. Y., Piquilloud, L., Szabo, C., Krueger, T., & Liaudet, L. (2021). Effects of cold or warm ischemia and ex-vivo lung perfusion on the release of damage associated molecular patterns and inflammatory cytokines in experimental lung transplantation. *J Heart Lung Transplant*, 40(9), 905-916. <https://doi.org/10.1016/j.healun.2021.05.015>
- Hashimoto, D., Chow, A., Noizat, C., Teo, P., Beasley, M. B., Leboeuf, M., Becker, C. D., See, P., Price, J., & Lucas, D. (2013). Tissue-resident macrophages self-maintain locally throughout adult life with minimal contribution from circulating monocytes. *Immunity*, 38(4), 792-804. <https://doi.org/10.1016/j.immuni.2013.04.004>
- Higuchi, T., Shiraiishi, T., Shirakusa, T., Hirayama, S., Shibaguchi, H., Kuroki, M., Hiratuka, M., Yamamoto, S., Iwasaki, A., & Kuroki, M. (2005). Prevention of acute lung allograft rejection in rat by the janus kinase 3 inhibitor, tyrphostin AG490. *The Journal of Heart and Lung Transplantation*, 24(10), 1557-1564. <https://doi.org/10.1016/j.healun.2004.11.017>
- Hodge, G., Hodge, S., Chambers, D., Reynolds, P. N., & Holmes, M. (2009). Bronchiolitis obliterans syndrome is associated with absence of suppression of peripheral blood Th1 proinflammatory cytokines. *Transplantation*, 88(2), 211-218. <https://doi.org/10.1097/tp.0b013e3181ac170f>
- Hodge, G., Hodge, S., Chambers, D. C., Reynolds, P. N., & Holmes, M. (2012). Increased expression of graft intraepithelial T-cell pro-inflammatory cytokines compared with native lung during episodes of acute rejection. *J Heart Lung Transplant*, 31(5), 538-544. <https://doi.org/10.1016/j.healun.2012.02.004>

- Hoeksema, M. A., Scicluna, B. P., Boshuizen, M. C., van der Velden, S., Neele, A. E., Van den Bossche, J., Matlung, H. L., van den Berg, T. K., Goossens, P., & de Winther, M. P. (2015). IFN-gamma priming of macrophages represses a part of the inflammatory program and attenuates neutrophil recruitment. *J Immunol*, *194*(8), 3909-3916. <https://doi.org/10.4049/jimmunol.1402077>
- Hussell, T., & Bell, T. J. (2014). Alveolar macrophages: plasticity in a tissue-specific context. *Nature Reviews Immunology*, *14*(2), 81-93. <https://doi.org/doi.org/10.1038/nri3600>
- Hwang, I., Kim, J. W., Ylaja, K., Chung, E. J., Kitano, H., Perry, C., Hanaoka, J., Fukuoka, J., Chung, J. Y., & Hewitt, S. M. (2020). Tumor-associated macrophage, angiogenesis and lymphangiogenesis markers predict prognosis of non-small cell lung cancer patients. *J Transl Med*, *18*(1), 443. <https://doi.org/10.1186/s12967-020-02618-z>
- Hwang, S. D., Song, J. H., Kim, Y., Lim, J. H., Kim, M. Y., Kim, E. N., Hong, Y. A., Chung, S., Choi, B. S., Kim, Y. S., & Park, C. W. (2019). Inhibition of lymphatic proliferation by the selective VEGFR-3 inhibitor SAR131675 ameliorates diabetic neuropathy in db/db mice. *Cell Death Dis*, *10*(3), 219. <https://doi.org/10.1038/s41419-019-1436-1>
- Janssen, L., Dupont, L., Bekhouche, M., Noel, A., Leduc, C., Voz, M., Peers, B., Cataldo, D., Apte, S. S., Dubail, J., & Colige, A. (2016). ADAMTS3 activity is mandatory for embryonic lymphangiogenesis and regulates placental angiogenesis. *Angiogenesis*, *19*(1), 53-65. <https://doi.org/10.1007/s10456-015-9488-z>
- Jaramillo, A., Fernandez, F. G., Kuo, E. Y., Trulock, E. P., Patterson, G. A., & Mohanakumar, T. (2005). Immune mechanisms in the pathogenesis of bronchiolitis obliterans syndrome after lung transplantation. *Pediatr Transplant*, *9*(1), 84-93. <https://doi.org/10.1111/j.1399-3046.2004.00270.x>
- Jeltsch, M., Jha, S. K., Tvorogov, D., Anisimov, A., Leppanen, V. M., Holopainen, T., Kivela, R., Ortega, S., Karpanen, T., & Alitalo, K. (2014). CCBE1 enhances lymphangiogenesis via A disintegrin and metalloprotease with thrombospondin motifs-3-mediated vascular endothelial growth factor-C activation. *Circulation*, *129*(19), 1962-1971. <https://doi.org/10.1161/CIRCULATIONAHA.113.002779>
- Jha, S. K., Rauniyar, K., Karpanen, T., Leppänen, V.-M., Brouillard, P., Vikkula, M., Alitalo, K., & Jeltsch, M. (2017). Efficient activation of the lymphangiogenic growth factor VEGF-C requires the C-terminal domain of VEGF-C and the N-terminal domain of CCBE1. *Scientific reports*, *7*(1), 1-13. <https://doi.org/10.1038/s41598-017-04982-1>
- Joukov, V., Pajusola, K., Kaipainen, A., Chilov, D., Lahtinen, I., Kukk, E., Saksela, O., Kalkkinen, N., & Alitalo, K. (1996). A novel vascular endothelial growth factor, VEGF-C, is a ligand for the Flt4 (VEGFR-3) and KDR (VEGFR-2) receptor tyrosine kinases. *EMBO J*, *15*(2), 290-298. <https://doi.org/10.1002/j.1460-2075.1996.tb00359.x>
- Kaipainen, A., Korhonen, J., Mustonen, T., Van Hinsbergh, V., Fang, G.-H., Dumont, D., Breitman, M., & Alitalo, K. (1995). Expression of the fms-like tyrosine kinase 4 gene becomes restricted to lymphatic endothelium during development. *Proc Natl Acad Sci*, *92*(8), 3566-3570. <https://doi.org/10.1073/pnas.92.8.3566>
- Kang, K., Bachu, M., Park, S. H., Kang, K., Bae, S., Park-Min, K. H., & Ivashkiv, L. B. (2019). IFN-gamma selectively suppresses a subset of TLR4-activated genes and enhancers to potentiate macrophage activation. *Nat Commun*, *10*(1), 3320. <https://doi.org/10.1038/s41467-019-11147-3>
- Kang, S., Lee, S. P., Kim, K. E., Kim, H. Z., Memet, S., & Koh, G. Y. (2009). Toll-like receptor 4 in lymphatic endothelial cells contributes to LPS-induced lymphangiogenesis by chemotactic recruitment of macrophages. *Blood*, *113*(11), 2605-2613. <https://doi.org/10.1182/blood-2008-07-166934>
- Kastelijn, E. A., van Moorsel, C. H., Rijkers, G. T., Ruven, H. J., Karthaus, V., Kwakkel-van Erp, J. M., Van de Graaf, E., Zanen, P., van Kessel, D. A., & Grutters, J. C. (2010). Polymorphisms in innate immunity genes associated with development of bronchiolitis obliterans after lung transplantation. *The Journal of Heart and Lung Transplantation*, *29*(6), 665-671. <https://doi.org/10.1016/j.healun.2009.12.013>
- Kataru, R. P., Kim, H., Jang, C., Choi, D. K., Koh, B. I., Kim, M., Gollamudi, S., Kim, Y. K., Lee, S. H., & Koh, G. Y. (2011). T lymphocytes negatively regulate lymph node lymphatic vessel formation. *Immunity*, *34*(1), 96-107. <https://doi.org/10.1016/j.immuni.2010.12.016>
- Kennedy, C. C., & Razonable, R. R. (2017). Fungal infections after lung transplantation. *Clinics in chest medicine*, *38*(3), 511-520. <https://doi.org/10.1016/j.ccm.2017.04.011>
- Knoop, C., Haverich, A., & Fischer, S. (2004). Immunosuppressive therapy after human lung transplantation. *European Respiratory Journal*, *23*(1), 159-171. <https://doi.org/10.1183/09031936.03.00039203>

- Koch, S., Tugues, S., Li, X., Gualandi, L., & Claesson-Welsh, L. (2011). Signal transduction by vascular endothelial growth factor receptors. *Biochem J*, 437(2), 169-183. <https://doi.org/10.1042/BJ20110301>
- Kommineni, V. K., Nagineni, C. N., Detrick, B., & Hooks, J. J. (2007). Inflammatory Mediators Induce VEGF-A and VEGF-C secretion by Human Retinal Cells. *FASEB Journal*, A764-A764. <https://doi.org/10.1096/fasebj.21.6.a764-c>
- Kopecky, B. J., Frye, C., Terada, Y., Balsara, K. R., Kreisel, D., & Lavine, K. J. (2020). Role of donor macrophages after heart and lung transplantation. *Am J Transplant*, 20(5), 1225-1235. <https://doi.org/10.1111/ajt.15751>
- Krämer, O. H., Knauer, S. K., Greiner, G., Jandt, E., Reichardt, S., Gührs, K.-H., Stauber, R. H., Böhmer, F. D., & Heinzel, T. (2009). A phosphorylation-acetylation switch regulates STAT1 signaling. *Genes & Development*, 23(2), 223-235. <https://doi.org/10.1101/gad.479209>
- Kreisel, D., & Goldstein, D. R. (2013). Innate immunity and organ transplantation: focus on lung transplantation. *Transpl Int*, 26(1), 2-10. <https://doi.org/10.1111/j.1432-2277.2012.01549.x>
- Kreisel, D., Krupnick, A. S., Puri, V., Guthrie, T. J., Trulock, E. P., Meyers, B. F., & Patterson, G. A. (2011). Short-and long-term outcomes of 1000 adult lung transplant recipients at a single center. *The Journal of Thoracic and Cardiovascular Surgery*, 141(1), 215-222. <https://doi.org/10.1016/j.jtcvs.2010.09.009>
- Krupnick, A. S., Lin, X., Li, W., Higashikubo, R., Zinselmeyer, B. H., Hartzler, H., Toth, K., Ritter, J. H., Berezin, M. Y., Wang, S. T., Miller, M. J., Gelman, A. E., & Kreisel, D. (2014). Central memory CD8+ T lymphocytes mediate lung allograft acceptance. *J Clin Invest*, 124(3), 1130-1143. <https://doi.org/10.1172/JCI71359>
- Künnapuu, J., Bokharaie, H., & Jeltsch, M. (2021). Proteolytic Cleavages in the VEGF Family: Generating Diversity among Angiogenic VEGFs, Essential for the Activation of Lymphangiogenic VEGFs. *Biology (Basel)*, 10(2). <https://doi.org/10.3390/biology10020167>
- Laemmli, U. K. (1970). Cleavage of Structural Proteins during the Assembly of the Head of Bacteriophage T4. *Nature*, 227, 680. <https://doi.org/10.1038/227680a0>
- Laubach, V. E., & Sharma, A. K. (2016). Mechanisms of lung ischemia-reperfusion injury. *Curr Opin Organ Transplant*, 21(3), 246-252. <https://doi.org/10.1097/MOT.0000000000000304>
- Le Goff, C., Somerville, R. P., Kesteloot, F., Powell, K., Birk, D. E., Colige, A. C., & Apte, S. S. (2006). Regulation of procollagen amino-propeptide processing during mouse embryogenesis by specialization of homologous ADAMTS proteases: insights on collagen biosynthesis and dermatosparaxis. *Development*, 133(8), 1587-1596. <https://doi.org/10.1242/dev.02308>
- Lehtonen, A., Matikainen, S., & Julkunen, I. (1997). Interferons up-regulate STAT1, STAT2, and IRF family transcription factor gene expression in human peripheral blood mononuclear cells and macrophages. *Journal of immunology (Baltimore, Md.: 1950)*, 159(2), 794-803. <https://doi.org/10.4049/jimmunol.159.2.794>
- Leventhal, J. S., & Schroppel, B. (2012). Toll-like receptors in transplantation: sensing and reacting to injury. *Kidney Int*, 81(9), 826-832. <https://doi.org/10.1038/ki.2011.498>
- Ma, W., & Oliver, G. (2017). Lymphatic Endothelial Cell Plasticity in Development and Disease. *Physiology (Bethesda)*, 32(6), 444-452. <https://doi.org/10.1152/physiol.00015.2017>
- Mäkinen, T., Veikkola, T., Mustjoki, S., Karpanen, T., Catimel, B., Nice, E. C., Wise, L., Mercer, A., Kowalski, H., & Kerjaschki, D. (2001). Isolated lymphatic endothelial cells transduce growth, survival and migratory signals via the VEGF-C/D receptor VEGFR-3. *EMBO J*, 20(17), 4762-4773. <https://doi.org/10.1093/emboj/20.17.4762>
- Mamessier, E., Lorec, A.-M., Thomas, P., Badier, M., Magnan, A., & Reynaud-Gaubert, M. (2007). T regulatory cells in stable posttransplant bronchiolitis obliterans syndrome. *Transplantation*, 84(7), 908-916. <https://doi.org/10.1097/01.tp.0000281408.20686.cb>
- Mannon, R. B. (2012). Macrophages: contributors to allograft dysfunction, repair, or innocent bystanders? *Curr Opin Organ Transplant*, 17(1), 20-25. <https://doi.org/10.1097/MOT.0b013e32834ee5b6>
- Mantovani, A., Sica, A., Sozzani, S., Allavena, P., Vecchi, A., & Locati, M. (2004). The chemokine system in diverse forms of macrophage activation and polarization. *Trends in Immunology*, 25(12), 677-686. <https://doi.org/10.1016/j.it.2004.09.015>
- Martin, T. R., & Frevert, C. W. (2005). Innate immunity in the lungs. *Proceedings of the American Thoracic Society*, 2(5), 403-411. <https://doi.org/10.1513/pats.200508-090js>

- Martinu, T., Chen, D. F., & Palmer, S. M. (2009). Acute rejection and humoral sensitization in lung transplant recipients. *Proc Am Thorac Soc*, 6(1), 54-65. <https://doi.org/10.1513/pats.200808-080GO>
- Maruyama, K., Ii, M., Cursiefen, C., Jackson, D. G., Keino, H., Tomita, M., Van Rooijen, N., Takenaka, H., D'Amore, P. A., Stein-Streilein, J., Losordo, D. W., & Streilein, J. W. (2005). Inflammation-induced lymphangiogenesis in the cornea arises from CD11b-positive macrophages. *J Clin Invest*, 115(9), 2363-2372. <https://doi.org/10.1172/JCI23874>
- Matsuda, H., Ito, Y., Hosono, K., Tsuru, S., Inoue, T., Nakamoto, S., Kurashige, C., Hirashima, M., Narumiya, S., Okamoto, H., & Majima, M. (2021). Roles of Thromboxane Receptor Signaling in Enhancement of Lipopolysaccharide-Induced Lymphangiogenesis and Lymphatic Drainage Function in Diaphragm. *Arterioscler Thromb Vasc Biol*, 41(4), 1390-1407. <https://doi.org/10.1161/ATVBAHA.120.315507>
- Maus, U. A., Janzen, S., Wall, G., Srivastava, M., Blackwell, T. S., Christman, J. W., Seeger, W., Welte, T., & Lohmeyer, J. (2006). Resident alveolar macrophages are replaced by recruited monocytes in response to endotoxin-induced lung inflammation. *Am J Respir Cell Mol Biol*, 35(2), 227-235. <https://doi.org/10.1165/rcmb.2005-0241oc>
- Maus, U. A., Koay, M. A., Delbeck, T., Mack, M., Ermert, M., Ermert, L., Blackwell, T. S., Christman, J. W., Schlondorff, D., & Seeger, W. (2002). Role of resident alveolar macrophages in leukocyte traffic into the alveolar air space of intact mice. *American Journal of Physiology-Lung Cellular and Molecular Physiology*, 282(6), L1245-L1252. <https://doi.org/10.1152/ajplung.00453.2001>
- Maus, U. A., Waelsch, K., Kuziel, W. A., Delbeck, T., Mack, M., Blackwell, T. S., Christman, J. W., Schlondorff, D., Seeger, W., & Lohmeyer, J. (2003). Monocytes are potent facilitators of alveolar neutrophil emigration during lung inflammation: role of the CCL2-CCR2 axis. *J Immunol*, 170(6), 3273-3278. <https://doi.org/10.4049/jimmunol.170.6.3273>
- McLellan, T. (1982). Electrophoresis buffers for polyacrylamide gels at various pH. *Analytical Biochemistry*, 126(1), 94-99. [https://doi.org/10.1016/0003-2697\(82\)90113-0](https://doi.org/10.1016/0003-2697(82)90113-0)
- Medzhitov, R. (2001). Toll-like receptors and innate immunity. *Nature Reviews Immunology*, 1(2), 135-145. <https://doi.org/10.1038/35100529>
- Mei, S., Meyer, C. A., Zheng, R., Qin, Q., Wu, Q., Jiang, P., Li, B., Shi, X., Wang, B., & Fan, J. (2017). Cistrome cancer: a web resource for integrative gene regulation modeling in cancer. *Cancer research*, 77(21), e19-e22. <https://doi.org/10.1158/0008-5472.can-17-0327>
- Meng, G.-Q., Wang, Y.-N., Wang, J.-S., & Wang, Z. (2021). Ruxolitinib treatment for bronchiolitis obliterans syndrome following hematopoietic stem cell transplant in a patient with primary hemophagocytic lymphohistiocytosis. *Chinese Medical Journal*, 134(13), 1624-1625. <https://doi.org/10.1097/cm9.0000000000001324>
- Merry, H. E., Phelan, P., Doak, M. R., Zhao, M., Hwang, B., & Mulligan, M. S. (2015). Role of toll-like receptor-4 in lung ischemia-reperfusion injury. *Ann Thorac Surg*, 99(4), 1193-1199. <https://doi.org/10.1016/j.athoracsur.2014.12.062>
- Mills, C. D., Kincaid, K., Alt, J. M., Heilman, M. J., & Hill, A. M. (2000). M-1/M-2 macrophages and the Th1/Th2 paradigm. *The Journal of Immunology*, 164(12), 6166-6173. <https://doi.org/10.4049/jimmunol.164.12.6166>
- Moudgil, A., Bagga, A., Toyoda, M., Nicolaidou, E., Jordan, S., & Ross, D. (1999). Expression of  $\Gamma$ -IFN mRNA in bronchoalveolar lavage fluid correlates with early acute allograft rejection in lung transplant recipients. *Clin Transplant*, 13(2), 201-207. <https://doi.org/10.1034/j.1399-0012.1999.130208.x>
- Navarro, A., Perez, R. E., Rezaiekhalthigh, M., Mabry, S. M., & Ekekezie, I. I. (2008). T1 $\alpha$ /podoplanin is essential for capillary morphogenesis in lymphatic endothelial cells. *Am J Physiol Lung Cell Mol Physiol*, 295(4), L543-L551. <https://doi.org/10.1152/ajplung.90262.2008>
- Neuringer, I. P., Mannon, R. B., Coffman, T. M., Parsons, M., Burns, K., Yankaskas, J. R., & Aris, R. M. (1998). Immune cells in a mouse airway model of obliterative bronchiolitis. *American Journal of Respiratory Cell and Molecular Biology*, 19(3), 379-386. <https://doi.org/10.1165/ajrcmb.19.3.3023m>
- Nykanen, A. I., Sandelin, H., Krebs, R., Keranen, M. A., Tuuminen, R., Karpanen, T., Wu, Y., Pytowski, B., Koskinen, P. K., Yla-Herttuala, S., Alitalo, K., & Lemstrom, K. B. (2010). Targeting lymphatic vessel activation and CCL21 production by vascular endothelial growth factor receptor-3 inhibition has novel immunomodulatory and antiarteriosclerotic effects in cardiac allografts. *Circulation*, 121(12), 1413-1422. <https://doi.org/10.1161/CIRCULATIONAHA.109.910703>

- O'Connell, K. A., & Edidin, M. (1990). A mouse lymphoid endothelial cell line immortalized by simian virus 40 binds lymphocytes and retains functional characteristics of normal endothelial cells. *J Immun Balt*, *144*(2), 521-525. <https://doi.org/10.4049/jimmunol.144.2.521>
- Ogino, H., Hisanaga, A., Kohno, T., Kondo, Y., Okumura, K., Kamei, T., Sato, T., Asahara, H., Tsuiji, H., Fukata, M., & Hattori, M. (2017). Secreted Metalloproteinase ADAMTS-3 Inactivates Reelin. *J Neurosci*, *37*(12), 3181-3191. <https://doi.org/10.1523/JNEUROSCI.3632-16.2017>
- Ornstein, L. (1964). DISC ELECTROPHORESIS-I BACKGROUND AND THEORY\*. *Annals of the New York Academy of Sciences*, *121*(2), 321-349. <https://doi.org/doi:10.1111/j.1749-6632.1964.tb14207.x>
- Osawa, T., Tsuchida, R., Muramatsu, M., Shimamura, T., Wang, F., Suehiro, J.-i., Kanki, Y., Wada, Y., Yuasa, Y., & Aburatani, H. (2013). Inhibition of histone demethylase JMJD1A improves anti-angiogenic therapy and reduces tumor-associated macrophages. *Cancer research*, *73*(10), 3019-3028. <https://doi.org/10.1158/0008-5472.can-12-3231>
- Pan, Y., & Yago, T. (2014). Transcriptional regulation of podoplanin expression by Prox1 in lymphatic endothelial cells. *Microvasc Res*, *94*, 96-102. <https://doi.org/10.1016/j.mvr.2014.05.006>
- Pedersen, M. S., Muller, M., Rulicke, T., Leitner, N., Kain, R., Regele, H., Wang, S., Grone, H. J., Rong, S., Haller, H., Gueler, F., Rees, A. J., & Kerjaschki, D. (2020). Lymphangiogenesis in a mouse model of renal transplant rejection extends life span of the recipients. *Kidney Int*, *97*(1), 89-94. <https://doi.org/10.1016/j.kint.2019.07.027>
- Pham, T. H., Baluk, P., Xu, Y., Grigorova, I., Bankovich, A. J., Pappu, R., Coughlin, S. R., McDonald, D. M., Schwab, S. R., & Cyster, J. G. (2010). Lymphatic endothelial cell sphingosine kinase activity is required for lymphocyte egress and lymphatic patterning. *J Exp Med*, *207*(1), 17-27. <https://doi.org/10.1084/jem.20091619>
- Poltorak, A., He, X., Smirnova, I., Liu, M.-Y., Huffel, C. V., Du, X., Birdwell, D., Alejos, E., Silva, M., & Galanos, C. (1998). Defective LPS signaling in C3H/HeJ and C57BL/10ScCr mice: mutations in Tlr4 gene. *Science*, *282*(5396), 2085-2088. <https://doi.org/10.1126/science.282.5396.2085>
- Porteous, M. K., Diamond, J. M., & Christie, J. D. (2015). Primary graft dysfunction: lessons learned about the first 72 hours after lung transplantation. *Current opinion in organ transplantation*, *20*(5), 506. <https://doi.org/10.1097/mot.0000000000000232>
- Raphael, M. F., Rottier, B. L., & Boelens, J. J. (2013). Fludarabine in paediatric steroid-refractory inflammatory lung injury after stem cell transplantation. *European Respiratory Journal*, *41*(2), 479-483. <https://doi.org/10.1183/09031936.00029312>
- Ross, D. J., Moudgil, A., Bagga, A., Toyoda, M., Marchevsky, A. M., Kass, R. M., & Jordan, S. C. (1999). Lung allograft dysfunction correlates with  $\gamma$ -interferon gene expression in bronchoalveolar lavage. *J Heart Lung Transplant*, *18*(7), 627-636. [https://doi.org/10.1016/s1053-2498\(99\)00007-8](https://doi.org/10.1016/s1053-2498(99)00007-8)
- Ruggiero, R., Fietsam Jr, R., Thomas, G. A., Muz, J., Farris, R. H., Kowal, T. A., Myles, J. L., Stephenson, L. W., & Baciewicz Jr, F. A. (1994). Detection of canine allograft lung rejection by pulmonary lymphoscintigraphy. *J Thorac Cardiovasc Surg*, *108*(2), 253-258. [https://doi.org/10.1016/s0022-5223\(94\)70007-9](https://doi.org/10.1016/s0022-5223(94)70007-9)
- Salehi, S., & Reed, E. F. (2015). The divergent roles of macrophages in solid organ transplantation. *Current opinion in organ transplantation*, *20*(4), 446. <https://doi.org/10.1097/mot.0000000000000209>
- Sato, M. (2020). Bronchiolitis obliterans syndrome and restrictive allograft syndrome after lung transplantation: why are there two distinct forms of chronic lung allograft dysfunction? *Ann Transl Med*, *8*(6), 418. <https://doi.org/10.21037/atm.2020.02.159>
- Scaffidi, P., Misteli, T., & Bianchi, M. E. (2002). Release of chromatin protein HMGB1 by necrotic cells triggers inflammation. *Nature*, *418*(6894), 191-195. <https://doi.org/10.1038/nature00858>
- Schoettler, M., Duncan, C., Lehmann, L., Furutani, E., Subramaniam, M., & Margossian, S. (2019). Ruxolitinib is an effective steroid sparing agent in children with steroid refractory/dependent bronchiolitis obliterans syndrome after allogeneic hematopoietic cell transplantation. *Bone Marrow Transplantation*, *54*(7), 1158-1160. <https://doi.org/10.1016/j.imbio.2006.05.007>
- Schoppmann, S., Birner, P., Stöckl, J., Kalt, R., Ullrich, R., Caucig, C., Kriehuber, E., Nagy, K., Alitalo, K., & Kerjaschki, D. (2002). Tumor-Associated Macrophages Express Lymphatic Endothelial Growth Factors and Are Related to Peritumoral Lymphangiogenesis. *Am J Pathol*, *161*(3), 947-956. [https://doi.org/10.1016/s0002-9440\(10\)64255-1](https://doi.org/10.1016/s0002-9440(10)64255-1)

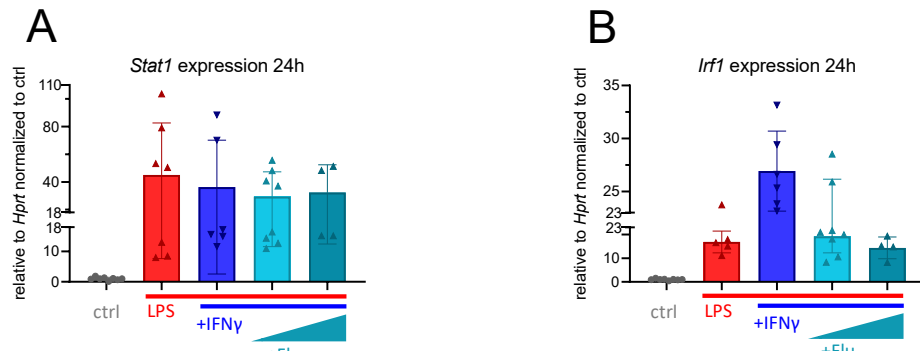
- Schreurs, I., Meek, B., Hijdra, D., van Moorsel, C. H. M., Luijk, H. D., Kwakkel-van Erp, J. M., Oudijk, E., van Kessel, D. A., & Grutters, J. C. (2020). Lung Transplantation Has a Strong Impact on the Distribution and Phenotype of Monocyte Subsets. *Transplant Proc*, 52(3), 958-966. <https://doi.org/10.1016/j.transproceed.2020.01.012>
- Schroder, K., Hertzog, P. J., Ravasi, T., & Hume, D. A. (2004). Interferon-gamma: an overview of signals, mechanisms and functions. *J Leukoc Biol*, 75(2), 163-189. <https://doi.org/10.1189/jlb.0603252>
- Schroder, K., Sweet, M. J., & Hume, D. A. (2006). Signal integration between IFN $\gamma$  and TLR signalling pathways in macrophages. *Immunobiology*, 211(6-8), 511-524. <https://doi.org/10.1016/j.imbio.2006.05.007>
- Serrick, C., Adoumie, R., Giaid, A., & Shennib, H. (1994). The early release of interleukin-2, tumor necrosis factor-alpha and interferon-gamma after ischemia reperfusion injury in the lung allograft. *Transplantation*, 58(11), 1158-1162. <https://doi.org/10.1097/00007890-199412150-00003>
- Sharma, A., LaPar, D., Stone, M., Zhao, Y., Kron, I., & Laubach, V. (2013). Receptor for advanced glycation end products (RAGE) on iNKT cells mediates lung ischemia-reperfusion injury. *Am J Transplant*, 13(9), 2255-2267. <https://doi.org/10.1097/00007890-199412150-00003>
- Sharma, A. K., LaPar, D. J., Stone, M. L., Zhao, Y., Mehta, C. K., Kron, I. L., & Laubach, V. E. (2016). NOX2 activation of natural killer T cells is blocked by the adenosine A2A receptor to inhibit lung ischemia-reperfusion injury. *American journal of respiratory and critical care medicine*, 193(9), 988-999. <https://doi.org/10.1164/rccm.201506-1253oc>
- Sharma, A. K., LaPar, D. J., Zhao, Y., Li, L., Lau, C. L., Kron, I. L., Iwakura, Y., Okusa, M. D., & Laubach, V. E. (2011). Natural killer T cell-derived IL-17 mediates lung ischemia-reperfusion injury. *Am J Respir Crit Care Med*, 183(11), 1539-1549. <https://doi.org/10.1164/rccm.201007-1173OC>
- Sharples, L. D., McNeil, K., Stewart, S., & Wallwork, J. (2002). Risk factors for bronchiolitis obliterans: a systematic review of recent publications. *The Journal of Heart and Lung Transplantation*, 21(2), 271-281. [https://doi.org/10.1016/s1053-2498\(01\)00360-6](https://doi.org/10.1016/s1053-2498(01)00360-6)
- Shimamoto, A., Pohlman, T. H., Shomura, S., Tarukawa, T., Takao, M., & Shimpō, H. (2006). Toll-like receptor 4 mediates lung ischemia-reperfusion injury. *Ann Thorac Surg*, 82(6), 2017-2023. <https://doi.org/10.1016/j.athoracsur.2006.06.079>
- Shin, H.-M., Kim, M.-H., Kim, B. H., Jung, S.-H., Kim, Y. S., Park, H. J., Hong, J. T., Min, K. R., & Kim, Y. (2004). Inhibitory action of novel aromatic diamine compound on lipopolysaccharide-induced nuclear translocation of NF- $\kappa$ B without affecting I $\kappa$ B degradation. *FEBS Lett*, 571(1-3), 50-54. <https://doi.org/10.1016/j.febslet.2004.06.056>
- Simons, M., Gordon, E., & Claesson-Welsh, L. (2016). Mechanisms and regulation of endothelial VEGF receptor signalling. *Nat Rev Mol Cell Biol*, 17(10), 611-625. <https://doi.org/10.1038/nrm.2016.87>
- Song, E., Mao, T., Dong, H., Boisserand, L. S. B., Antila, S., Bosenberg, M., Alitalo, K., Thomas, J. L., & Iwasaki, A. (2020). VEGF-C-driven lymphatic drainage enables immunosurveillance of brain tumours. *Nature*, 577(7792), 689-694. <https://doi.org/10.1038/s41586-019-1912-x>
- Song, J., Chen, W., Cui, X., Huang, Z., Wen, D., Yang, Y., Yu, W., Cui, L., & Liu, C.-Y. (2020). CCBE1 promotes tumor lymphangiogenesis and is negatively regulated by TGF $\beta$  signaling in colorectal cancer. *Theranostics*, 10(5), 2327. <https://doi.org/10.7150/thno.39740>
- Stanley, E., Lieschke, G. J., Grail, D., Metcalf, D., Hodgson, G., Gall, J., Maher, D. W., Cebon, J., Sinickas, V., & Dunn, A. R. (1994). Granulocyte/macrophage colony-stimulating factor-deficient mice show no major perturbation of hematopoiesis but develop a characteristic pulmonary pathology. *Proceedings of the National Academy of Sciences*, 91(12), 5592-5596. <https://doi.org/10.1073/pnas.91.12.5592>
- Stephanou, A., Brar, B. K., Scarabelli, T. M., Jonassen, A. K., Yellon, D. M., Marber, M. S., Knight, R. A., & Latchman, D. S. (2000). Ischemia-induced STAT-1 expression and activation play a critical role in cardiomyocyte apoptosis. *J Biol Chem*, 275(14), 10002-10008. <https://doi.org/10.1074/jbc.275.14.10002>
- Stephanou, A., & Latchman, D. S. (2003). STAT-1: a novel regulator of apoptosis. *Int J Exp Pathol*, 84(6), 239-244. <https://doi.org/10.1111/j.0959-9673.2003.00363.x>
- Streiler, C., Shaikh, F., Davis, C., Abhyankar, S., & Brownback, K. R. (2020). Ruxolitinib is an effective steroid sparing agent in bronchiolitis obliterans due to chronic graft-versus-host-disease. *Bone Marrow Transplantation*, 55(6), 1194-1196. <https://doi.org/10.1038/s41409-019-0662-6>

- Sweet, S. C. (2013). Induction therapy in lung transplantation. *Transplant International*, 26(7), 696-703. <https://doi.org/10.1111/tri.12115>
- Takahashi, M., Chen-Yoshikawa, T. F., Menju, T., Ohata, K., Kondo, T., Motoyama, H., Hijiya, K., Aoyama, A., & Date, H. (2016). Inhibition of Toll-like receptor 4 signaling ameliorates lung ischemia–reperfusion injury in acute hyperglycemic conditions. *J Heart Lung Transplant*, 35(6), 815-822. <https://doi.org/10.1016/j.healun.2015.12.032>
- Takamori, S., Shoji, F., Okamoto, T., Kozuma, Y., Matsubara, T., Haratake, N., Akamine, T., Katsura, M., Takada, K., & Toyokawa, G. (2019). HMGB1 blockade significantly improves luminal fibrous obliteration in a murine model of bronchiolitis obliterans syndrome. *Transpl Immunol*, 53, 13-20. <https://doi.org/10.1016/j.trim.2018.11.007>
- Takekoshi, T., Fang, L., Paragh, G., & Hwang, S. T. (2012). CCR7-expressing B16 melanoma cells downregulate interferon-gamma-mediated inflammation and increase lymphangiogenesis in the tumor microenvironment. *Oncogenesis*, 1, e9. <https://doi.org/10.1038/oncsis.2012.9>
- Talaie, T., DiChiacchio, L., Prasad, N. K., Pasirija, C., Julliard, W., Kaczorowski, D. J., Zhao, Y., & Lau, C. L. (2021). Ischemia-reperfusion injury in the transplanted lung: a literature review. *Transplantation direct*, 7(2). <https://doi.org/10.1097/txd.0000000000001104>
- Tatham, K. C., O'Dea, K. P., Romano, R., Donaldson, H. E., Wakabayashi, K., Patel, B. V., Thakuria, L., Simon, A. R., Sarathchandra, P., Harefield, P. i., Marczin, N., & Takata, M. (2018). Intravascular donor monocytes play a central role in lung transplant ischaemia-reperfusion injury. *Thorax*, 73(4), 350-360. <https://doi.org/10.1136/thoraxjnl-2016-208977>
- Tissot, A., Danger, R., Claustre, J., Magnan, A., & Brouard, S. (2019). Early Identification of Chronic Lung Allograft Dysfunction: The Need of Biomarkers. *Front Immunol*, 10, 1681. <https://doi.org/10.3389/fimmu.2019.01681>
- Todd, J. L., Wang, X., Sugimoto, S., Kennedy, V. E., Zhang, H. L., Pavlisko, E. N., Kelly, F. L., Huang, H., Kreisel, D., Palmer, S. M., & Gelman, A. E. (2014). Hyaluronan contributes to bronchiolitis obliterans syndrome and stimulates lung allograft rejection through activation of innate immunity. *Am J Respir Crit Care Med*, 189(5), 556-566. <https://doi.org/10.1164/rccm.201308-1481OC>
- Uygun, V., Karasu, G., Daloğlu, H., Öztürkmen, S., Kılıç, S. Ç., Yalçın, K., Celen, S. S., Hazar, V., & Yeşilipek, A. (2020). Ruxolitinib salvage therapy is effective for steroid-refractory graft-versus-host disease in children: a single-center experience. *Pediatric Blood & Cancer*, 67(4), e28190. <https://doi.org/10.1002/pbc.28190>
- Veikkola, T., Jussila, L., Makinen, T., Karpanen, T., Jeltsch, M., Petrova, T. V., Kubo, H., Thurston, G., McDonald, D. M., Achen, M. G., Stacker, S. A., & Alitalo, K. (2001). Signalling via vascular endothelial growth factor receptor-3 is sufficient for lymphangiogenesis in transgenic mice. *EMBO J*, 20(6), 1223-1231. <https://doi.org/10.1093/emboj/20.6.1223>
- Verleden, G. M., Raghu, G., Meyer, K. C., Glanville, A. R., & Corris, P. (2014). A new classification system for chronic lung allograft dysfunction. In (Vol. 33, pp. 127-133): Elsevier.
- Vimalraj, S., Hariprabu, K. N. G., Rahaman, M., Govindasami, P., Perumal, K., Sekaran, S., & Ganapathy, D. (2023). Vascular endothelial growth factor-C and its receptor-3 signaling in tumorigenesis. *3 Biotech*, 13(10), 326. <https://doi.org/10.1007/s13205-023-03719-4>
- Walker, J. M. (1994). The Bicinchoninic Acid (BCA) Assay for Protein Quantitation. In J. M. Walker (Ed.), *Basic Protein and Peptide Protocols* (pp. 5-8). Humana Press. <https://doi.org/10.1385/0-89603-268-x:5>
- Wang, G., Muhl, L., Padberg, Y., Dupont, L., Peterson-Maduro, J., Stehling, M., le Noble, F., Colige, A., Betsholtz, C., & Schulte-Merker, S. (2020). Specific fibroblast subpopulations and neuronal structures provide local sources of Vegfc-processing components during zebrafish lymphangiogenesis. *Nature Communications*, 11(1), 2724. <https://doi.org/10.1038/s41467-020-16552-7>
- Wang, S., Sun, H., Ma, J., Zang, C., Wang, C., Wang, J., Tang, Q., Meyer, C. A., Zhang, Y., & Liu, X. S. (2013). Target analysis by integration of transcriptome and ChIP-seq data with BETA. *Nature protocols*, 8(12), 2502-2515. <https://doi.org/10.1038/nprot.2013.150>
- Wang, X.-L., Zhao, J., Qin, L., & Cao, J.-L. (2016). VEGFR-3 blocking deteriorates inflammation with impaired lymphatic function and different changes in lymphatic vessels in acute and chronic colitis. *American journal of translational research*, 8(2), 827.
- Watari, K., Nakao, S., Fotovati, A., Basaki, Y., Hosoi, F., Bereczky, B., Higuchi, R., Miyamoto, T., Kuwano, M., & Ono, M. (2008). Role of macrophages in inflammatory lymphangiogenesis: Enhanced production of vascular endothelial growth factor C and D

- through NF-kappaB activation. *Biochem Biophys Res Commun*, 377(3), 826-831. <https://doi.org/10.1016/j.bbrc.2008.10.077>
- Weyker, P. D., Webb, C. A., Kiamanesh, D., & Flynn, B. C. (2013). Lung ischemia reperfusion injury: a bench-to bedside review. *Seminars in cardiothoracic and vascular anesthesia*, Witt, C. A., Puri, V., Gelman, A. E., Krupnick, A. S., & Kreisel, D. (2014). Lung transplant immunosuppression—time for a new approach? *Expert Rev Clin Immunol*, 10(11), 1419-1421. <https://doi.org/10.1586/1744666x.2014.959499>
- Wood, K. J., & Goto, R. (2012). Mechanisms of rejection: current perspectives. *Transplantation*, 93(1), 1-10. <https://doi.org/10.1097/tp.0b013e31823cab44>
- Wu, H., Chen, G., Wyburn, K. R., Yin, J., Bertolino, P., Eris, J. M., Alexander, S. I., Sharland, A. F., & Chadban, S. J. (2007). TLR4 activation mediates kidney ischemia/reperfusion injury. *J Clin Invest*, 117(10), 2847-2859. <https://doi.org/10.1172/JCI31008>
- Wu, H., Ma, J., Wang, P., Corpuz, T. M., Panchapakesan, U., Wyburn, K. R., & Chadban, S. J. (2010). HMGB1 contributes to kidney ischemia reperfusion injury. *Journal of the American Society of Nephrology: JASN*, 21(11), 1878. <https://doi.org/10.1681/asn.2009101048>
- Wu, M., Du, Y., Liu, Y., He, Y., Yang, C., Wang, W., & Gao, F. (2014). Low molecular weight hyaluronan induces lymphangiogenesis through LYVE-1-mediated signaling pathways. *PLoS One*, 9(3), e92857. <https://doi.org/10.1371/journal.pone.0092857>
- Xiong, Y., Brinkman, C. C., Famulski, K. S., Mongodin, E. F., Lord, C. J., Hippen, K. L., Blazar, B. R., & Bromberg, J. S. (2017). A robust in vitro model for trans-lymphatic endothelial migration. *Sci Rep*, 7(1), 1633. <https://doi.org/10.1038/s41598-017-01575-w>
- Xue, J., Schmidt, S. V., Sander, J., Draffehn, A., Krebs, W., Quester, I., De Nardo, D., Gohel, T. D., Emde, M., & Schmidleithner, L. (2014). Transcriptome-based network analysis reveals a spectrum model of human macrophage activation. *Immunity*, 40(2), 274-288. <https://doi.org/10.1016/j.immuni.2014.01.006>
- Yang, H., Hreggvidsdottir, H. S., Palmblad, K., Wang, H., Ochani, M., Li, J., Lu, B., Chavan, S., Rosas-Ballina, M., & Al-Abed, Y. (2010). A critical cysteine is required for HMGB1 binding to Toll-like receptor 4 and activation of macrophage cytokine release. *Proc Natl Acad Sci*, 107(26), 11942-11947. <https://doi.org/10.1073/pnas.1003893107>
- Yang, H., & Tracey, K. J. (2010). Targeting HMGB1 in inflammation. *BBA-Gene Regul Mech*, 1799(1-2), 149-156. <https://doi.org/10.1016/j.bbagr.2009.11.019>
- Yoshiyasu, N., & Sato, M. (2020). Chronic lung allograft dysfunction post-lung transplantation: The era of bronchiolitis obliterans syndrome and restrictive allograft syndrome. *World J Transplant*, 10(5), 104-116. <https://doi.org/10.5500/wjt.v10.i5.104>
- Yousem, S. A., Berry, G. J., Cagle, P. T., Chamberlain, D., Husain, A. N., Hruban, R. H., Marchevsky, A., Otori, N. P., Ritter, J., & Stewart, S. (1996). Revision of the 1990 working formulation for the classification of pulmonary allograft rejection: Lung Rejection Study Group. *The Journal of heart and lung transplantation: the official publication of the International Society for Heart Transplantation*, 15(1 Pt 1), 1-15.
- Yu, H., Lin, L., Zhang, Z., Zhang, H., & Hu, H. (2020). Targeting NF-kB pathway for the therapy of diseases: mechanism and clinical study. *Signal Transduct Target Ther*, 5(1), 209. <https://doi.org/10.1038/s41392-020-00312-6>
- Yu, J., Li, P., Li, Z., Li, Y., Luo, J., Su, W., & Liang, D. (2022). Topical administration of 0.3% tofacitinib suppresses M1 macrophage polarization and allograft corneal rejection by blocking STAT1 activation in the rat cornea. *Transl vis sci technol*, 11(3), 34-34. <https://doi.org/10.1167/tvst.11.3.34>
- Zanotti, G., Casiraghi, M., Abano, J. B., Tatreau, J. R., Sevala, M., Berlin, H., Smyth, S., Funkhouser, W. K., Burrige, K., & Randell, S. H. (2009). Novel critical role of Toll-like receptor 4 in lung ischemia-reperfusion injury and edema. *Am J Physiol Lung Cell Mol Physiol*, 297(1), L52-L63. <https://doi.org/10.1152/ajplung.90406.2008>
- Zawieja, D. (2005). Lymphatic biology and the microcirculation: past, present and future. *Microcirculation*, 12(1), 141-150. <https://doi.org/10.1080/10739680590900003>
- Zhang, W., Tian, J., & Hao, Q. (2014). HMGB1 combining with tumor-associated macrophages enhanced lymphangiogenesis in human epithelial ovarian cancer. *Tumor Biol*, 35, 2175-2186. <https://doi.org/10.1007/s13277-013-1288-8>
- Zhang, Y., Lu, Y., Ma, L., Cao, X., Xiao, J., Chen, J., Jiao, S., Gao, Y., Liu, C., Duan, Z., Li, D., He, Y., Wei, B., & Wang, H. (2014). Activation of vascular endothelial growth factor receptor-3 in macrophages restrains TLR4-NF-kappaB signaling and protects against endotoxin shock. *Immunity*, 40(4), 501-514. <https://doi.org/10.1016/j.immuni.2014.01.013>

- Zhao, M., Fernandez, L. G., Doctor, A., Sharma, A. K., Zarbock, A., Tribble, C. G., Kron, I. L., & Laubach, V. E. (2006). Alveolar macrophage activation is a key initiation signal for acute lung ischemia-reperfusion injury. *Am J Physiol Lung Cell Mol Physiol*, 291(5), L1018-L1026. <https://doi.org/10.1152/ajplung.00086.2006>
- Zhao, Y.-R., Liu, H., Xiao, L.-M., Jin, C.-G., Zhang, Z.-P., & Yang, C.-G. (2018). The clinical significance of CCBE1 expression in human colorectal cancer. *Cancer Management and Research*, 10, 6581. <https://doi.org/10.2147/cmar.s181770>
- Zheng, R., Wan, C., Mei, S., Qin, Q., Wu, Q., Sun, H., Chen, C.-H., Brown, M., Zhang, X., & Meyer, C. A. (2019). Cistrome Data Browser: expanded datasets and new tools for gene regulatory analysis. *Nucleic acids research*, 47(D1), D729-D735. <https://doi.org/10.1093/nar/gky1094>
- Zhu, G., Huang, Q., Huang, Y., Zheng, W., Hua, J., Yang, S., Zhuang, J., Wang, J., & Ye, J. (2016). Lipopolysaccharide increases the release of VEGF-C that enhances cell motility and promotes lymphangiogenesis and lymphatic metastasis through the TLR4-NF- $\kappa$ B/JNK pathways in colorectal cancer. *Oncotarget*, 7(45), 73711. <https://doi.org/10.18632/oncotarget.12449>

## Appendix A:

Supplementary Figure A.3.3.3 *Stat1* and *Irf1* Expression After Fludarabine Treatment.

## Acknowledgements

As I reflect on the completion of this academic journey, I am grateful to those who have been instrumental in shaping and supporting my research endeavors. Every contribution, no matter how small, has played a pivotal role in helping me successfully complete this thesis.

My sincere appreciation goes to my direct supervisor, Prof. Dr. med. vet. Ali Önder Yildirim, who believed in my capabilities and gave me the opportunity to start this exciting journey. Your guidance, open-door policy, and scientific ambitions have shaped my research trajectory and contributed significantly to the successful completion of this thesis.

I express my sincere gratitude to my external supervisor, PD. Dr. med. Alexey Dashkevich, PhD., for his unwavering commitment to our countless meetings and feedback sessions. Your support, diplomatic mediation in interpersonal challenges, and encouragement of my plans have been pivotal in overcoming obstacles and progressing in the right direction.

Prof. Dr. med. Sebastian Michel, Ph.D., the valuable first member of the Thesis Advisory Committee (TAC), deserves my sincere gratitude. Your support has been substantial.

Dr. Aicha Jeridi deserves special mention for her exceptional support, feedback, ideas, and positive vibes. Your motivation, guidance, and unwavering assistance, even amidst a busy schedule, have been indispensable to the success of this project.

Zeynep, your uplifting spirit, support, and creativity have significantly enriched my research experience. I appreciate the positive impact you have had on both the work environment and the overall journey.

Christine, your help, and motivation, both within and outside the lab, have been genuinely appreciated. Your contributions, often behind the scenes, have not gone unnoticed and have greatly influenced the overall success of this endeavor.

I am thankful for Miriam and her continuous support, insightful comments, and assistance throughout this academic journey. Your vibes have been uplifting, making our efforts both enjoyable and fruitful.

To all my friends and countless supporters, your encouragement and belief in my capabilities have been vital for successfully completing this challenging project. Each of you has contributed uniquely, creating a supportive network that has made this journey memorable and fruitful.

Finally, a whimsical but heartfelt acknowledgment goes to Pippilotta Viktualia Rollgardina Pfefferminza Efraimstochter, the cutest cat on earth, whose presence added a touch of joy to this journey's challenging moments.

## Affidavit

	LUDWIG- MAXIMILIANS- UNIVERSITÄT MÜNCHEN	Promotionsbüro Medizinische Fakultät		
<b>Affidavit</b>				

Schulte-Döinghaus, Sarah

\_\_\_\_\_  
Surname, first name

\_\_\_\_\_  
Street

\_\_\_\_\_  
Zip code, town, country

I hereby declare, that the submitted thesis entitled:

Regulation of pro-lymphangiogenic factors in post-lung transplant settings

.....

is my own work. I have only used the sources indicated and have not made unauthorised use of services of a third party. Where the work of others has been quoted or reproduced, the source is always given.

I further declare that the dissertation presented here has not been submitted in the same or similar form to any other institution for the purpose of obtaining an academic degree.

Munich, 17.07.2024

\_\_\_\_\_  
place, date

Sarah Schulte-Döinghaus

\_\_\_\_\_  
Signature doctoral candidate

## Confirmation of Congruency

	LUDWIG- MAXIMILIANS- UNIVERSITÄT MÜNCHEN	Promotionsbüro Medizinische Fakultät		
<b>Confirmation of congruency between printed and electronic version of the doctoral thesis</b>				

Schulte-Döinghaus, Sarah

\_\_\_\_\_  
Surname, first name

\_\_\_\_\_  
Street

\_\_\_\_\_  
Zip code, town, country

I hereby declare, that the submitted thesis entitled:

Regulation of pro-lymphangiogenic factors in post-lung transplant settings

.....

is congruent with the printed version both in content and format.

Munich, 17.07.2024

\_\_\_\_\_  
place, date

Sarah Schulte-Döinghaus

\_\_\_\_\_  
Signature doctoral candidate

## List of Publications

Ghislandi, P. G., Pekár, S., Matzke, M., **Schulte-Döinghaus, S.**, Bilde, T., & Tunì, C. (2018). Resource availability, mating opportunity and sexual selection intensity influence the expression of male alternative reproductive tactics. *Journal of evolutionary biology*, 31(7), 1035-1046.

### **Abstracts**

Liu, H., Zistler, K., Jeridi, A., Morrone, C., **Schulte-Döinghaus, S.**, Hagl, C., ... & Dashkevich, A. (2020). Rapid Activation of Pro-Lymphangiogenic Phenotype and Consequent Increase of Lymphatic Density Occurs during the Development of Chronic Lung Allograft Dysfunction. *The Journal of Heart and Lung Transplantation*, 39(4), S22.

**Schulte-Döinghaus, S.**, Liu, H., Michel, S., Hagl, C., Yildirim, A. O., & Dashkevich, A. (2022). The Role of VEGF-C Precursors in the Macrophage-Mediated Activation of VEGFR3 Signaling in Lymphatic Endothelium In Vitro. *The Thoracic and Cardiovascular Surgeon*, 70, S1-S61.